The Texas Medical Center Library

DigitalCommons@TMC

The University of Texas MD Anderson Cancer Center UTHealth Graduate School of Biomedical Sciences Dissertations and Theses (Open Access)

The University of Texas MD Anderson Cancer Center UTHealth Graduate School of Biomedical Sciences

5-2016

INSIGHTS INTO DETERMINANTS THAT CONTRIBUTE TO COLONIZATION, VIRULENCE AND ANTIBIOTIC RESISTANCE IN ENTEROCOCCI

Maria Camila Montealegre

Follow this and additional works at: https://digitalcommons.library.tmc.edu/utgsbs_dissertations

 Part of the Bacteriology Commons, Laboratory and Basic Science Research Commons, Medicine and Health Sciences Commons, and the Pathogenic Microbiology Commons

Recommended Citation

Montealegre, Maria Camila, "INSIGHTS INTO DETERMINANTS THAT CONTRIBUTE TO COLONIZATION, VIRULENCE AND ANTIBIOTIC RESISTANCE IN ENTEROCOCCI" (2016). *The University of Texas MD Anderson Cancer Center UTHealth Graduate School of Biomedical Sciences Dissertations and Theses (Open Access)*. 649.
https://digitalcommons.library.tmc.edu/utgsbs_dissertations/649

This Dissertation (PhD) is brought to you for free and open access by the The University of Texas MD Anderson Cancer Center UTHealth Graduate School of Biomedical Sciences at DigitalCommons@TMC. It has been accepted for inclusion in The University of Texas MD Anderson Cancer Center UTHealth Graduate School of Biomedical Sciences Dissertations and Theses (Open Access) by an authorized administrator of DigitalCommons@TMC. For more information, please contact digitalcommons@library.tmc.edu.

INSIGHTS INTO DETERMINANTS THAT CONTRIBUTE TO COLONIZATION, VIRULENCE AND ANTIBIOTIC RESISTANCE IN ENTEROCOCCI

by

Maria Camila Montealegre, MS.

APPROVED:

_____
Barbara E. Murray, MD.
Advisory Professor

_____
Ambro van Hoof, PhD.

_____
Barrett R. Harvey, PhD.

_____
Danielle A. Garsin, PhD.

_____
Hung Ton-That, PhD.

_____
Jeffrey K. Actor, PhD.

APPROVED

_____
Dean, The University of Texas
Graduate School of Biomedical Sciences at Houston

INSIGHTS INTO DETERMINANTS THAT CONTRIBUTE TO COLONIZATION, VIRULENCE AND ANTIBIOTIC RESISTANCE IN ENTEROCOCCI

A

DISSERTATION

Presented to the Faculty of

The University of Texas

Health Science Center at Houston

and

The University of Texas

MD Anderson Cancer Center

Graduate School of Biomedical Sciences

in Partial Fulfillment

of the Requirements

for the Degree of

DOCTOR OF PHILOSOPHY

by

Maria Camila Montealegre, MS.

Houston, Texas

May, 2016

DEDICATION

I dedicate my Doctor of Philosophy Dissertation to Armero and to all that it represents to my family and me. I also dedicate this work to my parents, Melva Ortiz Santos and Gustavo Montealegre Lynett, who in their own very different ways have supported me along this journey. Thank you dad for being an example of a great scholar and thank you mom for being an example of strength, courage, and more importantly love.

ACKNOWLEDGEMENTS

I would first like to acknowledge my advisor Dr. Barbara E. Murray, whose mentorship, and support have been instrumental throughout my graduate career. She has positively impacted my life at so many different levels that I feel very fortunate to have her as a mentor. Her knowledge, expertise, and scientific accuracy have been crucial to my growth as a scientist. She provided me with the independence to work on projects and ideas of interest to me, but she also pushed me to my limits, which helped me accomplish my goals. I owe much of my success as a Ph.D. student to the time she took to help me become a better writer. In addition to being a role model in my career, I would also want to thank her for the support she has given me outside of work; she has become an unconditional friend. Furthermore, she has been an inspiration for me to get back into an athletic life style.

I am also grateful to all my committee members, Dr. van Hoof, Dr. Harvey, Dr. Garsin, Dr. Ton-That, and Dr. Actor, for their valuable feedback that helped me undertake my projects. I am especially grateful to Dr. van Hoof, who literally always had an open door for my questions. I would also want to extend a special gratitude to Dr. Actor for his constant support for all my scholarship applications. I would also like to express my deepest gratitude to Dr. Kavindra Singh in Dr. Murray's laboratory; his mentorship has strengthened my scientific abilities and enhanced my skills. He was always available to answer my "small questions" and put my mind at ease.

I would also like to thank everyone who has been a part of the Murray laboratory during the past 5 years, in particular all the people who worked and contributed to the projects included in this dissertation. A special thanks to Dr. Singh and Karen Jaques-

Palaz for all their hard work related to the animal experiments presented in this document. I would like to especially acknowledge Dr. Sabina Leanti La Rosa, who in addition to her valuable scientific contributions became an amazing friend. In addition, I would also like to thank Dr. Jung Hyeob Roh for his contributions. I also want to extend my gratitude to Dr. Chungyu (Julie) Chang in Dr. Ton-That's laboratory, Emily Stinemetz in Dr. Harvey's laboratory, Dr. Milya Davlieva in Dr. Shamoo's laboratory, Dr. Sruti Debroy in Dr. Garsin's laboratory, and to Dr. Arias and to all members of his laboratory for their contributions and support.

Lastly, I would like to give a special thanks to my family and friends, in Colombia, here in Houston and in many other places around the world (it would take a whole dissertation to name Y'ALL) for all the love, support and great times during this journey.

INSIGHTS INTO DETERMINANTS THAT CONTRIBUTE TO COLONIZATION, VIRULENCE AND ANTIBIOTIC RESISTANCE IN ENTEROCOCCI

Maria Camila Montealegre, MS.

Advisory Professor: Barbara E. Murray, MD.

Enterococcus faecalis and *Enterococcus faecium* are increasingly common as causative agents of human infections, many of which are very difficult to treat due to multi-drug resistance. The work presented in the first part of this dissertation elucidates a mechanism for the regulation of pilus expression. I showed that ATT is the initiation codon of *ebpA*, the first gene of an operon that codes for the *e*ndocarditis and *b*iofilm-associated *p*ili (Ebp), a recognized virulence factor in *E. faecalis.* The presence of this rare start codon downregulates EbpA translation and protein levels, diminishing biofilm and binding abilities of *E. faecalis*, as compared to an engineered ATG codon. My studies also extended to the ortholog of Ebp in *E. faecium*, known as the *E. faecium p*ili (Emp), where the role of each Emp subunit in biofilm formation, adherence and experimental infection was demonstrated. This study highlighted the relevance of the tip subunit, EmpA, in pilus biogenesis and pilus-associated functions. Due to the rising clinical importance of *E. faecium* and the fact that enterococcal infections are commonly preceded by intestinal colonization, the second part of this dissertation focused on the dynamics of gastrointestinal tract (GIT) colonization of the three known *E. faecium* clades. This work found that clade B, composed of strains that are part of the normal human microbiota, outcompeted most of the clade A strains, which include strains linked to human infections or associated with animals, when present together in a mouse model of GIT colonization. Last, I demonstrated that the *pbp5* gene, part of the *E. faecium* core genome that shows sequence variation between the clades and encodes a

penicillin binding protein important for β-lactam resistance, is differentially expressed between strains, with higher PBP5 protein levels in clade A ampicillin-resistant strains as compared to clade B and subclade A2 ampicillin-susceptible strains. Furthermore, I found evidence that there are extensive differences within the region upstream of *pbp5* among the clades that correlate with the differential abundance of PBP5 and ampicillin resistance. Together these studies provide further insight into determinants that contribute to colonization, virulence and resistance in enterococci.

TABLE OF CONTENTS

LIST OF ILLUSTRATIONS

LIST OF TABLES

CHAPTER 1. BACKGROUND

1.1. Scope of this chapter

The information presented in this chapter **(Chapter 1**. **Background)** is focused on certain aspects of the biology of *Enterococcus faecalis* and *E. faecium* that provide a framework to understand the content of this dissertation. This dissertation is divided into two parts:

Insights into enterococcal pili and their association with virulence - includes two chapters, **Chapter 2** and **Chapter 3.** These chapters are focused on the study of one class of virulence determinants, named the *e*ndocarditis- and *b*iofilm-associated *p*ilus (Ebp) in *E. faecalis* and the corresponding *Enterococcus faecium p*ilus (Emp).

Defining the contribution of *E. faecium* clade types to gastrointestinal tract (GIT) colonization and ampicillin resistance - includes two chapters, **Chapter 4** and **Chapter 5**. These chapters are centered on studying the GIT colonization dynamics of the different *E. faecium* lineages and the contribution of penicillin-binding protein 5 (PBP5) levels to ampicillin resistance.

1.2. The genus *Enterococcus*

The genus *Enterococcus*, initially classified as part of the genus *Streptococcus* (1) and now composed of over 50 species (2), consist of Gram-positive, low GC, non-spore forming facultative anaerobes (3-5). Species from this genus are found in a variety of environments including soil, water, plants and the gastrointestinal tracts (GITs) of mammals, insects and nematodes (3). In addition, certain enterococcal strains have been widely used in the food industry and as probiotics, extending further their

distribution (6). Enterococci have been proven to survive and grow in harsh conditions, including a wide range of pHs, temperatures and salt concentrations (3, 5).

1.3. Epidemiology and antibiotic resistance

Enterococcus species, common commensal bacteria, were recognized as occasional causes of infections in the past; however, over the past few decades, the number of infections attributed to members of this genus has increased (5) and nowadays enterococci rank as important pathogens in the healthcare setting (7). *E. faecalis* and *E. faecium* are the enterococcal species most frequently found in the GIT of humans and are also the most relevant species at the clinical level (8). In the USA, enterococci began to emerge as a common cause of infection in hospitals during the 1970s; at that time, *E. faecalis* caused 90 to 95% of enterococcal infections (4, 5). Since the 1990s, the species *E. faecium* has partially displaced *E. faecalis,* and now accounts for approximately 38% of all the enterococcal infections (4, 5, 7).

Enterococci are well known for their intrinsic resistance to different antibiotics such as cephalosporins and aminoglycosides (4, 9). In addition, some enterococci have acquired other clinically important resistances via mutation of preexisting genetic elements; this appears to be the case of high-level ampicillin resistance in *E. faecium*, which is associated with mutations in the gene that encodes the low-affinity PBP5 (discussed later) (9). Enterococci have also acquired resistance determinants by means of horizontal gene transfer, a particularly common phenomenon in this genus. An example is the acquisition of the vancomycin resistance gene clusters (10). Vancomycin resistance was first reported in *E. faecium* in two European countries in 1986 (11, 12) and, although it occurs also in *E. faecalis* and other enterococcal species, the vast

majority of vancomycin resistant enterococci (VRE) are *E. faecium* (9). Within *E. faecium,* it appears that vancomycin resistance initially emerged in different lineages in the USA and in Europe. In the USA, VRE were and continue to be prevalent in hospitals (7) and the *van* resistance determinants mainly spread in *E. faecium* lineages that are highly resistant to ampicillin and remarkably adapted to the hospital environment (13, 14). In contrast, in Europe, VRE was first prevalent in farm animals and healthy individuals in an ampicillin-susceptible background (13, 14). However, Europe has also seen a rise in VRE infections since the early 2000s (14). Furthermore, resistance to newer antibiotic therapies, including linezolid and daptomycin, has been reported in some enterococcal strains, compromising further the ability to treat these already multidrug-resistant pathogens (5).

1.4. Colonization and infections caused by enterococci

Colonization of the GIT is usually recognized as the first step towards infection with many antibiotic resistant bacteria, including VRE (15, 16). Indeed, in patients with compromised immune systems due to pre-bone marrow transplant regimens, bloodstream infections by VRE are usually preceded by domination of the microbiota by *Enterococcus* (15, 16). Different studies, using mouse models of GIT colonization, have demonstrated that antibiotic treatment alters the gut microbiota diversity and allows VRE to displace the normal microbiota of the small and large intestine (15, 17, 18). In fact, depletion of Gram-negative bacteria by antibiotic treatment was shown to cause a decrease in the production of antimicrobial peptides, such as Reg3γ, by Paneth and epithelial cells of the mouse small intestine (19). Reg3γ is a C-type lectin that selectively targets Gram-positive bacteria; therefore, decreased production of this factor serves to facilitate VRE colonization and overgrowth in mice (19-21). These results, together with

evidence of the effect of antibiotic treatment on the intestinal microbiota in humans, underscore the role of intestinal homeostasis in promoting the health of the host (5).

Infections caused by *Enterococcus* species, initially considered to be only of endogenous origin, are often caused by certain genotypes that are highly adapted to the hospital setting (22). One of most common enterococcal infections is of the urinary tract (urinary tract infection, UTI) (7), which is often associated with the presence of catheters (catheter-associated urinary tract infection, CAUTI) (23). Enterococci are also common causes of intra-abdominal and pelvic infections, bacteremias and endocarditis (4), the later representing one of the most serious infections caused by *Enterococcus,* due to limited therapeutics options that have bactericidal activity against some of these bacteria (24).

1.5. Insights into enterococcal pili and its association with virulence

Adherence to host tissues is thought to be important in the pathogenesis of enterococcal infections such as UTIs and endocarditis (5, 25). The enterococcal genome encodes a number of factors, including members of the “microbial surface components recognizing adhesive matrix molecules” (MSCRAMM) family, that have been shown to play a role in adherence and to contribute to the pathogenesis of enterococci in experimental models of infections (5, 26). The enterococcal pili, like the pili of other Gram-positive organisms, are multimeric structures formed by LPxTG surface proteins that are part of the family of MSCRAMMs (26); these pili extend from the surface of the bacteria and are polymerized and anchored to the peptidoglycan cell wall by transpeptidase enzymes known as sortases (27, 28).

In *E. faecalis*, two pilus gene clusters (PGCs) have been described, the *ebp* (29) and the *bee* (*b*iofilm *e*nhancer in *e*nterococci) loci (30). The *ebp* locus is considered part of the core genome of *E. faecalis,* as it was reported present in 99.8 % of *E. faecalis* isolates (31). The *bee* locus, in contrast, was carried by only 1.2 % of the isolates studied (31) and it was demonstrated to be encoded on a conjugative plasmid (30). The Ebp pili of *E. faecalis* have been extensively investigated; studies have shown the contribution of each pilus subunit, EbpA, EbpB and EbpC, to pilus structure (32, 33), and the role of Ebp and/or its subunits in adherence to components of the host extracellular matrix (ECM) (34, 35), adherence to human platelets (31), biofilm formation (29, 32) and in experimental animal models of UTI (32, 36), CAUTI (37) and endocarditis (29). The roles of the pilus specific sortase, Bps, and the housekeeping sortase, SrtA, in pilus biogenesis have also been established, with the former catalyzing pilin polymerization and the later anchoring the polymerized pilus to the cell wall (32). Furthermore, regulators of Ebp expression have been described (38, 39), as well as the role played by environmental signals in inducing pili production (29, 40). **Chapter 2** of this dissertation elucidates an additional mechanism of Ebp regulation based on the presence of a rare initiation codon, ATT, as the translational start of the tip subunit of the pili, EbpA.

On the other hand, *E. faecium* can encode up to four PGCs, called PGC-1 to PGC-4, but the presence of these gene clusters is variable between *E. faecium* strains, as some of these clusters are present in plasmids that show predominance in isolates of clinical origin (41-44). In spite of the high relevance of *E. faecium* in the clinical setting, studies of *E. faecium* pili have been scarcer, with only two PGCs partially characterized, PGC-1 and PGC-3, the later also known as the *empABC* operon (previously, *ebpABC*$_{fm}$) (43, 45-47). Only one study has addressed the role of one of these type of pili, the Emp, in an experimental model of infection (47). **Chapter 3** of this dissertation serves to

provide further insight into the Emp pili; in particular, it contributes to the understanding of the role of each of the Emp subunits to pilus fiber structure, biofilm formation, adherence to ECM proteins and experimental infection.

1.6. Defining the contribution of *E. faecium* clade types to GIT colonization and ampicillin resistance.

The recent emergence of *E. faecium* in the healthcare setting is a reason of high concern for clinicians, as this species shows higher rates of antibiotic resistance, compared to *E. faecalis,* against antibiotics commonly used to treat enterococcal infections, including vancomycin and ampicillin (5, 7). Currently, the percentage of *E. faecium* isolates in US hospitals resistant to vancomycin is approximately 80% and an even higher percentage is resistant to ampicillin (5, 7, 48).

Multi-locus sequence typing (MLST), a technique that interrogates the sequence of internal regions of multiple housekeeping genes, usually seven, has been widely used to study the population structure of *E. faecalis* and *E. faecium* (8, 49, 50). Whole genome sequence comparisons have provided further insight into the evolutionary trajectories of these two enterococcal species (51). In this next section, I will summarize the most important findings on the population biology and comparative genomics of *E. faecium.*

Early population biology studies of *E. faecium*, using MLST and the eBURST algorithm, initially indicated that a certain lineage, named clonal complex 17 (CC17), was associated with the majority of hospital-acquired *E. faecium* infections and outbreaks (52). This clonal complex was characterized by high-level resistance to ampicillin, vancomycin and quinolones, and was also often associated with the presence of mobile

genetic elements such as IS*16* (53) and putative virulence factors, including *hylEfm* (encoding a protein with homology to glycosyltransferases), *espEfm* (*e*nterococcal *s*urface *p*rotein), and MSCRAMMs (5, 54). The use of a more suitable algorithm to analyze the MLST data from species with high rates of recombination as *E. faecium* (53), and the use of genomic analyses, initially whole-genome microarray (55) and pyrosequencing (56), subsequently indicated that the isolates of the "CC17" were not strictly clonal, meaning that hospital-acquired *E. faecium* evolved from more than one founder (53). Nevertheless, these analyses confirmed the profound differences between the strains isolated from hospitals, causing infections and outbreaks, and the strains commonly found colonizing the GIT of healthy individuals in the community (56).

More recent whole genome comparisons, by Galloway-Peña et al. and Palmer et al., found a deep evolutionary bifurcation between two *E. faecium* clades, the hospital-associated (HA) clade or clade A and the community-associated (CA) clade or clade B (51, 57). The core gene sequences of these two clades differ by 3.5 to 10%, revealing that the differences between them are not only in the accessory genome, as was initially suggested, but also at the core genomic level (57, 58). Furthermore, pairwise comparisons that quantitated the relationship of strains in the two clades spanned from 93.9 to 95.6% average nucleotide identity (ANI), which overlaps with the percentage that delineates a different species (51). In addition, molecular clock calculations indicated that this bifurcation occurred long before the antibiotic era, indicating that the emergence of *E. faecium* in the hospital setting is not a consequence of a recent evolution of a lineage from the commensal clade (57).

In 2013, Lebreton et al. sequenced and analyzed the genome of 51 strains that belong to different sequence types (STs) and were isolated from diverse sources at

different time points, and compared these strains along with the 22 previous analyzed genomes that at the time were publicly available in NCBI (59). The results of this analysis confirmed the previously described ancient phylogenetic split between the clades but, more importantly, it provided evidence of a more recent bifurcation within the clade A into subclade A1 (associated with infections in the hospital) and subclade A2 (associated primarily with animals but also reported in human infections) (59). It was estimated that this later split occurred around the time antibiotic use was instituted in clinical settings and animal agriculture practices (59).

Among many differences, strains of the *E. faecium* clades differ in genome size, with larger overall as well a core genomes found in subclade A1 strains compared to clade B and subclade A2 strains; however, subclade A2 strains have larger pan-genomes (59). Enrichment of mobile genetic elements including plasmids, prophages, genomic islands and insertion sequences was observed in subclade A1 strains (59). Furthermore, antibiotic resistance genes were more frequently found in clade A strains than in clade B strains, with some resistance determinants, including the *vanA* and *vanB* genes that confer resistance to vancomycin, completely absent from clade B strains (59). Clade A strains were also characterized by higher recombination and mutation rates compared to clade B strains (59, 60). In addition, differential presence of genes and gene clusters with predicted functions in carbohydrate metabolism was observed between the *E. faecium* clades (59). It has been suggested that the ability to utilize different carbohydrates by the *E. faecium* clades is one of the main driving forces for the divergent evolution of the clades (3, 59). Although these studies have established substantial sequence divergence in the core genome and differences in the gene content between the *E. faecium* clades, the determinants that favor clade B predominance in the GIT of healthy individuals but subclade A1 prevalence in individuals

in the healthcare setting are far from being understood (53, 55, 56, 59). In **Chapter 4**, using a murine model of GIT colonization, differences in colonization dynamics by the distinct *E. faecium* clades are investigated.

As described above, there are extensive differences between the *E. faecium* clades; one important core-intrinsic difference of prominent clinical relevance is the *pbp5* gene, which encodes a high molecular weight class B PBP, PBP5 (57, 58). PBPs are part of the penicilloyl serine transferase family of enzymes, which are involved in the final stages of peptidoglycan synthesis (61); these reactions include transglycosylation and transpeptidation (62). The genome of *E. faecium* encodes six different high molecular weight PBPs, three genes (*ponA*, *pbpF* and *pbpZ*) encoding class A PBPs, which are multifunctional enzymes with a glycosyltransferase (GTase) domain and a transpeptidase (TPase) domain and three genes (*pbp5*, *pbpA* and *pbpB*) encoding mono-functional class B TPases (63). β-lactam antibiotics exhibit structural analogy with the D-Ala-D-Ala carboxy terminus of the peptidoglycan pentapeptide; thus, these drugs irreversibly inactivate PBPs by forming an ester bond with the active site serine of the enzyme (64).

PBP5 is considered the main determinant of ampicillin resistance in *E. faecium* (65), which is attributed to its intrinsic low affinity for β-lactam antibiotics (66, 67). In **Chapter 5,** we further our previously published findings on the role that the different *pbp5* variants play in ampicillin resistance (58, 68) and evaluate the contribution of the *E. faecium* clade backgrounds to differential PBP5 protein levels.

CHAPTER 2. ATTenuation Starts with ATT.

This chapter is based upon work published in the journal mBio entitled "The Enterococcus faecalis EbpA Pilus Protein: Attenuation of Expression, Biofilm Formation, and Adherence to Fibrinogen Start with the Rare Initiation Codon ATT. mBio. ***2015****: 6: e00467-15. I am the first author of this publication (****Montealegre MC****, La Rosa SL, Roh JH, Harvey BR, Murray BE) and I was responsible for preparing the original manuscript and conducted the majority of experiments described. Copyright of all material published in mBio remains with the authors.*

For additional information about ASM's permission policies associated with commercial reuse of mBio content, see http://mbio.asm.org/site/misc/reprints.xhtml

2.1. INTRODUCTION

Ebp are considered important contributors to the pathogenicity of *E. faecalis* (29, 32, 36, 37). Our lab have previously shown that Ebp are important for adherence of *E. faecalis* OG1RF to host ECM proteins, including fibrinogen and collagen, a process that is considered crucial in the initial steps of infection (34, 35). Furthermore, it was demonstrated that Ebp pili play a role in biofilm formation (29, 32) and in experimental animal models of endocarditis (29) and ascending UTIs (36). The role of Ebp has also been established in a model of CAUTI (37). The *ebp* locus consists of an operon of three genes, *ebpA*, *ebpB* and *ebpC*, that encode the pilus subunits, or pilins, and *bps,* encoding a class C sortase (29, 32). The three pilin genes and the downstream sortase are co-transcribed, but a second promoter controls the independent expression of *bps* (32). Regulation of pilus expression has been shown to occur through the action of two positive regulators, EbpR and *rnjB* (38, 39) while the *fsr* system was shown to be a weak repressor (40). Furthermore, environmental conditions, including bicarbonate (40) and the presence of serum (29), positively affect Ebp pilus production.

Several reports have shown that EbpC forms the backbone polymer, while EbpA and EbpB are present at the tip and at the base of the pilus fiber, respectively (29, 32, 33, 37). In addition, our electron microscopy studies indicated that the majority of the EbpA protein is found on the surface of *E. faecalis* OG1RF cells (32) and analyses of the contribution of each structural subunit of the Ebp pili revealed the importance of EbpA to pilus biogenesis (32, 33, 37). We previously reported that deletion of *ebpA* resulted in the formation of fewer but extremely long pili compared to wild-type OG1RF, which suggested a role for EbpA in the initiation as well as termination of pilus polymerization (32). We corroborated the role of EbpA as a factor that influences the length of pili by controlled overexpression of EbpA from a nisin-inducible promoter in a Δ*ebpA* mutant,

which led to a gradual decrease in pilus length as the concentration of nisin was increased (32). Deletion of *ebpA* also affected the overall levels of the other Ebp pilin subunits, without altering the transcript levels of the downstream genes (32). EbpA has been demonstrated to play a crucial role in biofilm formation and in a model of UTI, with the *ebpA* deletion mutant attenuated approximately to the same level as observed with the *ebpABC* operon deletion (32). In addition, Nielsen et al. showed the contribution of EbpA in the colonization of bladders and intrabladder implants in CAUTIs, and revealed that the metal ion-dependent adhesion site (MIDAS) motif present in EbpA's von Willebrand factor A (VWA) domain is important for pilus function (37). More recently, this group demonstrated that immunization with EbpA inhibits binding of *E. faecalis* to fibrinogen and provides protection in catheter-associated bladder infection in mice (69). Additionally, we showed that a monoclonal antibody targeting the shaft of the pili, EbpC, prevents endocarditis in rats (70).

We previously predicted that the most likely translational start codon of EbpA in *E. faecalis* OG1RF is the very rarely used triplet ATT (AUU in the corresponding mRNA), which is located 9 bp downstream of a suitable ribosomal binding site (RBS) and 120 bp upstream of the current genome database annotation of an ATG start codon (Figure 2.1) (29). In the majority of mRNAs, translation initiates from the codon AUG that in prokaryotes codes for formylmethionine; nevertheless, other NUG codons are occasionally found as translational starts (71, 72).

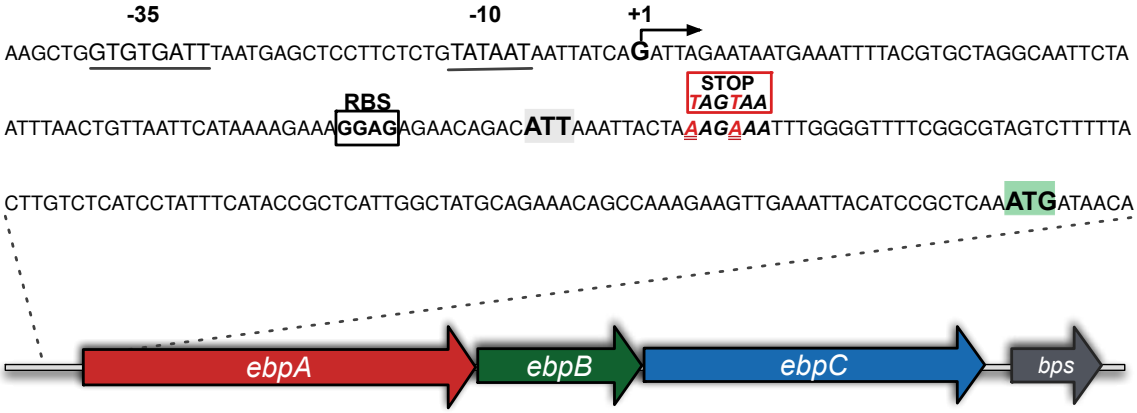

Figure 2.1. Schematic representation of the *ebpABC-bps* operon of *E. faecalis* OG1RF.

The locus consists of three genes *ebpA*, *ebpB* and *ebpC*, encoding the pilin subunits, and *bps* encoding a class C sortase. The putative promoter region (with the -35 and -10 promoter boxes), the predicted transcriptional start (+1), the predicted ribosome-binding site (RBS), the ATT postulated start codon and the ATG annotated start codon are shown. The position of the two successive stop codons introduced to generate strain TX5751 is also denoted.

In only very few instances has the AUU codon been reported as the translational start for protein synthesis in bacteria (73, 74). The rarity of AUU as a start codon is attributed to the fact that the initiation factor 3 (IF3) discriminates against non-canonical start codons (72). As observed in other prokaryotic species, in *E. faecalis* OG1RF, the use of AUU as the initiation of protein synthesis is very rare, and there is no evidence indicating that other *E. faecalis* proteins, besides EbpA, start translation with this codon. In addition, when our search of other several sequenced *E. faecalis* strains found conservation of this codon, we postulated that this codon participates in regulation of EbpA expression. To test this hypothesis and our prediction of AUU as the start codon of EbpA protein synthesis, we first used site-directed mutagenesis to introduce, in *E. faecalis* OG1RF, two successive stop codons between the ATT predicted initiation codon and the currently annotated ATG start codon, to experimentally show that the ATT indeed determines the start of EbpA protein synthesis. Then, we constructed a derivative of OG1RF in which the ATT codon of *ebpA* was replaced with ATG, and investigated the effect of this change on translation, EbpA and EbpC surface display, biofilm formation and adherence to fibrinogen.

2.2. MATERIALS AND METHODS

Bacterial strains, plasmids, and routine growth conditions

Bacterial strains and plasmids used in this chapter and their relevant characteristics are listed in Table 2-1. *E. faecalis* strains were routinely grown at 37°C using brain heart infusion (BHI) (Becton, Dickinson (BD), Franklin Lakes, NJ) broth or agar. Tryptic soy broth (BD) supplemented with 0.25% glucose v/v (TSB-G) and BHI broth supplemented with 40% horse serum (Sigma-Aldrich, Saint Louis, MO) v/v (BHI-S) were used for some experiments. *Escherichia coli* strains used for cloning experiments were grown at 37°C Luria-Bertani (LB) (BD) broth or agar. Growth characteristics of OG1RF and its derivatives were assessed in BHI broth based on the optical density at 600 nm (OD_{600}). In addition, samples were taken at 0, 3, 6, 8 and 24 hours for CFU determination on BHI agar, as previously described (47).

Construction of mutants

Specific point mutations were generated by modifying a previously described methodology (75), based on the pHOU1 vector (76) that carries the *pheS** allele that confers susceptibility to *p*-chloro-phenylalanine (*p*-Cl-Phe). Strains TX5751 and TX5731 were constructed using *E. faecalis* OG1RF as the parental strain, while a revertant strain, named TX5732, was generated by placing back the $ebpA_{ATT}$ start codon into the TX5731 strain background (Table 2-1). In brief, two external primers *ebpA*-Ext-F-BamHI and *ebpA*-Ext-R-PstI containing the BamHI and PstI restriction sites, respectively, and two internal complementary primers containing the desired change were designed (Table 2-2).

Table 2-1. Bacterial strains and plasmids used in chapter 2

Strain or Plasmid	Relevant Characteristic(s)	Reference
Strains		
E. faecalis		
OG1RF	Laboratory strain; RIF^R, FUS^R	(77)
TX5751	OG1RF with two point mutations at nucleotides 13 and 16 after the putative *ebpA* ATT initiation codon that changed two lysine residues (AAG and AAA) to two stop codons (TAG and TAA, respectively) ($ebpA_{STOP}$).	This study
TX5731	OG1RF with a point mutation that changed the *ebpA* putative ATT start codon ATT to ATG ($ebpA_{ATG}$).	This study
TX5732	Restored OG1RF $ebpA_{ATT}$. The mutated $ebpA_{ATG}$ codon was restored to wild-type $ebpA_{ATT}$.	This study
TX5608	OG1RFΔ*ebpABC*; *ebpABC* operon deletion mutant	(39)
TX5620	OG1RFΔ*ebpA*; *ebpA* deletion mutant	(32)
E. coli		
TG1	*E coli* host strain used for routine cloning	
EC1000	*E coli* host strain for cloning of RepA-dependent plasmids	(78)
Plasmids		
pGEM-T Easy	Plasmid used for initial cloning of PCR fragments; AMP^R.	Promega
pHOU1	Conjugative donor plasmid used for the introduction of point mutations into *E. faecalis*; confers GEN^R and carries the counterselectable *pheS** gene.	(76)
pSD2	Plasmid used to construct the translational *lacZ* fusions. The *lacZ* gene lacks a promoter, a RBS and a start codon; confers AMP^R and ERY^R.	(79)
pTEX5749	pSD2 plasmid containing a fragment from -261 bp upstream to 31 bp downstream of the ATT start codon of the *ebpA* gene of *E. faecalis* OG1RF (pSD2-$ebpA_{ATT}$::*lacZ*).	This study
pTEX5750	pSD2 plasmid containing a fragment from -261 bp upstream to 31 bp downstream of the mutated ATG start codon of the *ebpA* gene of *E. faecalis* TX5731 (pSD2-$ebpA_{ATG}$::*lacZ*).	This study

AMP, ampicillin; ERY, erythromycin: FUS, fusidic acid; GEN, gentamicin; RIF, rifampicin. Superscript "R" designates resistance.

Table 2-2. Oligonucleotides used in chapter 2

Primer Name	Sequence 5′- 3′	Relevant Characteristics
Mutant Construction		
***ebpA*-Ext-F-BamHI**	CGGGATCCTCGTTGACGTTTTTGCCATA	External forward; BamHI site underlined.
***ebpA*-Ext-R-PstI**	TTCTGCAGTGGGCACCACCATCTTTATT	External reverse; PstI site underlined.
***ebpA*-Stop-F**	ATTAAATTCTATAGTAATTTGGGGTTTTC	Internal forward; this primer creates two point mutations (underlined) that change two lysine residues (AAG and AAA) to two stop codons (TAG and TAA, respectively).
***ebpA*-Stop-R**	GAAAACCCCAAATTACTATAGTAATTTAAT	Internal reverse; this primer creates two point mutations (underlined) that change two lysine residues (AAG and AAA) to two stop codons (TAG and TAA, respectively).
***ebpA*-Ini-ATG-F**	GGAGAGAACAGACATGAAATTACTAAAGAAA	Internal forward; this primer creates a point mutation (underlined) that changes EbpA ATT predicted start codon of OG1RF to ATG.
***ebpA*-Ini-ATG-R**	TTTCTTTAGTAATTTCATGTCTGTTCTCTCC	Internal reverse; this primer creates a point mutation (underlined) that changes EbpA ATT predicted start codon of OG1RF to ATG.
***ebpA*-Ini-ATT-F**	GGAGAGAACAGACATTAAATTACTAAAGAAA	Internal forward; this primer creates a point mutation (underlined) that reverts the ATG mutated start codon of TX5731 back to ATT.
***ebpA*-Ini-ATT-R**	TTTCTTTAGTAATTTAAATGTCTGTTCTCTCC	Internal reverse; this primer creates a point mutation (underlined) that reverts the ATG mutated start codon of TX5731 back to ATT.
β-gal fusions		
***ebpA*-Fus-F-SalI**	GCGCGCGTCGACGACACGAATGATTTCTTCCA	Forward for the construction of *lacZ* fusions in the pSD2 vector; SalI site underlined.
***ebpA*-Fus-R-BamHI**	GCGCGCGGATCCCGAAAACCCCAAATTTCTTTAG	Reverse for the construction of *lacZ* fusions in the pSD2 vector; BamHI site underlined.

First, two independent PCR reactions using the respective external and internal primers were carried out. Then, the two PCR amplicons were joined together by a cross-over PCR and the generated fragments, now containing the desired mutations (confirmed by sequencing), were cloned into the pGEM vector and then subcloned into pHOU1 (76) using the BamHI and PstI sites. The recombinant pHOU1 plasmids were propagated in *E. coli* EC1000 and then electroporated into *E. faecalis* CK111 (Table 2-1) (75). Subsequently, the recombinant pHOU1 plasmids were transferred into *E. faecalis* OG1RF (or TX5731) by filter mating with CK111, followed by culturing the gentamicin-resistant colonies that integrated the plasmid on MM9-yeast extract glucose (MM9YEG) medium supplemented with 10 mM *p*-Cl-Phe as described in (75, 76), to select for the colonies from which the plasmid had excised. Sequencing and pulsed field gel electrophoresis (PFGE) were performed to detect the mutations in the correct background.

Construction of translational *lacZ* fusion vectors and β-galactosidase assay

The region extending from 261 bp upstream to 31 bp downstream of the postulated *ebpA* ATT translational start codon was PCR amplified from *E. faecalis* OG1RF and its *ebpA*$_{ATG}$ mutant, TX5731, digested with SalI and BamHI and cloned into the pSD2 vector (Table 2-1) (79). The reporter gene of pSD2, *lacZ,* lacks a promoter, a RBS and a start codon. Constructs, harboring either the native (pTEX5749) or the mutated (pTEX5750) form of the *ebpA* start codon, were propagated in *E. coli* TG1 before electroporation into *E. faecalis* OG1RF, TX5731 and TX5732. β-galactosidase activity was assayed in TSB-G or BHI-S, as previously described (80).

Flow cytometry

Flow cytometry analysis of *E. faecalis* strains was performed as previously described (39) with minor modifications. Cells grown in TSB-G to mid-logarithmic phase were collected by centrifugation and washed twice with 2% bovine serum albumin (BSA) in PBS. The bacterial cells were resuspended in 100 µl of the previously described affinity-purified polyclonal antibodies against EbpA (29) (1µg/ml), and incubated for 30 min at room temperature (RT). After a washing step, secondary labeling was performed with 1:100 of phycoerythrin-conjugated goat anti-rabbit IgG for 30 min, and cells were washed and fixed with 1% of paraformaldehyde for analysis using a BD FACS Calibur flow cytometer (BD Biosciences, San Jose, CA).

Whole-cell ELISA (WC ELISA)

EbpA and EbpC surface display by OG1RF and the panel of mutants was evaluated as previously described, with minor modifications (32). Briefly, bacteria grown overnight in TSB-G were diluted in the same medium to an OD_{600} of 0.1 and incubated until they reached mid-logarithmic phase. Cells were collected by centrifugation and washed twice with PBS before they were resuspended in 50 mM carbonate-bicarbonate buffer, pH 9.6, to an OD_{600} of 1.0. Immulon 1B plate wells (Thermo Fisher Scientific, Waltham, MA) were coated for 1 h with *E. faecalis* cells, followed by two washes with PBS containing 0.05% Tween 20 (PBS-T). The wells were then blocked for 1 h with 2% bovine serum albumin (BSA), followed by a 1 h incubation with affinity-purified polyclonal antibodies against EbpA and EbpC, respectively (1:5,000 dilution of 1 mg/ml) (29). After three washes with PBS-T to remove the unbound antibodies, goat anti-rabbit $F(ab')_2$ fragment conjugated to alkaline phosphatase (AP) (Jackson ImmunoResearch Laboratories, West Grove, PA) (1:5,000 dilution) was added and incubated for 1 h. Next, the wells were washed twice with PBS-T and once with PBS, followed by the addition of AP substrate

solution. The absorbance at 405 nm was measured with a microplate reader (Thermo Fisher Scientific).

Biofilm formation assay

Biofilm density was measured as previously described (81), with some modifications. In brief, *E. faecalis* strains from overnight cultures in TSB-G broth were diluted in the same medium to an OD_{600} of 0.1 and grown statically for 3 h or 24 h at 37°C in 96-well polystyrene plates (BD). The plates were gently washed with PBS, and then the cells were fixed with Bouin's solution (Sigma-Aldrich) for 30 min. After two washes with PBS, bacterial cells were stained with a 1% crystal violet solution (Sigma-Aldrich) for 30 min. Excess crystal violet was removed by rinsing thoroughly with distilled water followed by the addition of ethanol-acetone (80:20) to solubilize the dye and dissolve the biofilms. The absorbance at 570 nm was measured with a microplate reader (Thermo Fisher Scientific). Two independent experiments were performed in duplicate (8 wells per strain each in duplicate).

Fibrinogen binding assay

E. faecalis adherence to immobilized fibrinogen was assayed using the CytoSelect cell adhesion assay kit (Cell Biolabs, San Diego, CA). First, *E. faecalis* OG1RF and its derivatives from overnight cultures grown at 37°C in BHI-S were normalized to an OD_{600} of 0.05 and cultured to mid-log phase. Bacterial cells were collected by centrifugation, washed three times with PBS, and resuspended in 0.5% BSA to an OD_{600} of 1.0. A volume of 150 µl of the cell suspension was added to the fibrinogen-precoated wells and incubated for 1 h at 37°C. The unbound bacteria were removed by gently washing each well two times with PBS. Next, 200 µl of the cell stain solution was added to each well and incubated for 10 min at RT, followed by two washes with deionized water. After air-

drying the wells, 200 µl of extraction solution was added per well. The plate was incubated for 10 min on a shaker, and then 150 µl from each extracted sample was transferred to a 96-well microtiter plate (BD). The absorbance at 570 nm was measured with a microplate reader (Thermo Fisher Scientific).

Statistical analyses

Analysis of variance (ANOVA) with Bonferroni's multiple comparison post-test was used to compare the results. GraphPad Prism version 4.00 (GraphPad Software, San Diego, CA) was used for the statistical analyses.

2.3. RESULTS

Introduction of stop codons indicate that ATT (AUU) is the start codon of EbpA protein synthesis

The *ebpA* gene is the first gene of the *ebpABC* operon that encodes the *E. faecalis* Ebp pili (Figure 2.1). The current genome annotation of the *E. faecalis* strain V583 indicates that EbpA is an 1103-residue protein with a VWA domain; however, closer examination of the operon sequence revealed that no recognizable RBS is present upstream of the *ebpA* annotated start codon, ATG (29). In addition, no recognizable signal peptide or cleavage site was found downstream of the ATG annotated as the start codon of the predicted 1103-residue EbpA protein (EbpA-1103) (Figure 2.2-A). We predicted that the most likely, but very unusual, start codon of *ebpA* is the triplet ATT, located 9 bp downstream of a recognizable RBS and 120 bp upstream of the currently annotated ATG start codon (Figure 2.1). Using the SignalP 4.1 server (http://www.cbs.dtu.dk/services/SignalP/), we found a potential cleavage site at position 30 after the ATT codon (EbpA-1143) (Figure 2.2-B). In addition, the other two proteins encoded by the *ebpABC* operon, EbpB and EbpC, have well-defined signal sequences as well as cleavage sites (Figure 2.2-C-D). Furthermore, protein alignments of EbpA-1103 and EbpA-1143 with EmpA (EbpA homolog in *E. faecium*) supports the ATT start for EbpA protein synthesis (data not shown). To experimentally confirm that the designated ATG (located 120 bp downstream of our predicted ATT start) is not the start codon for EbpA protein synthesis, we used site-directed oligonucleotide mutagenesis to generate the strain TX5751 in which two lysine residues, AAG and AAA at positions five and six after the ATT, respectively, were changed to two stop codons, TAG (amber) and TAA (ocher) (Figure 2.1 & Table 2-1).

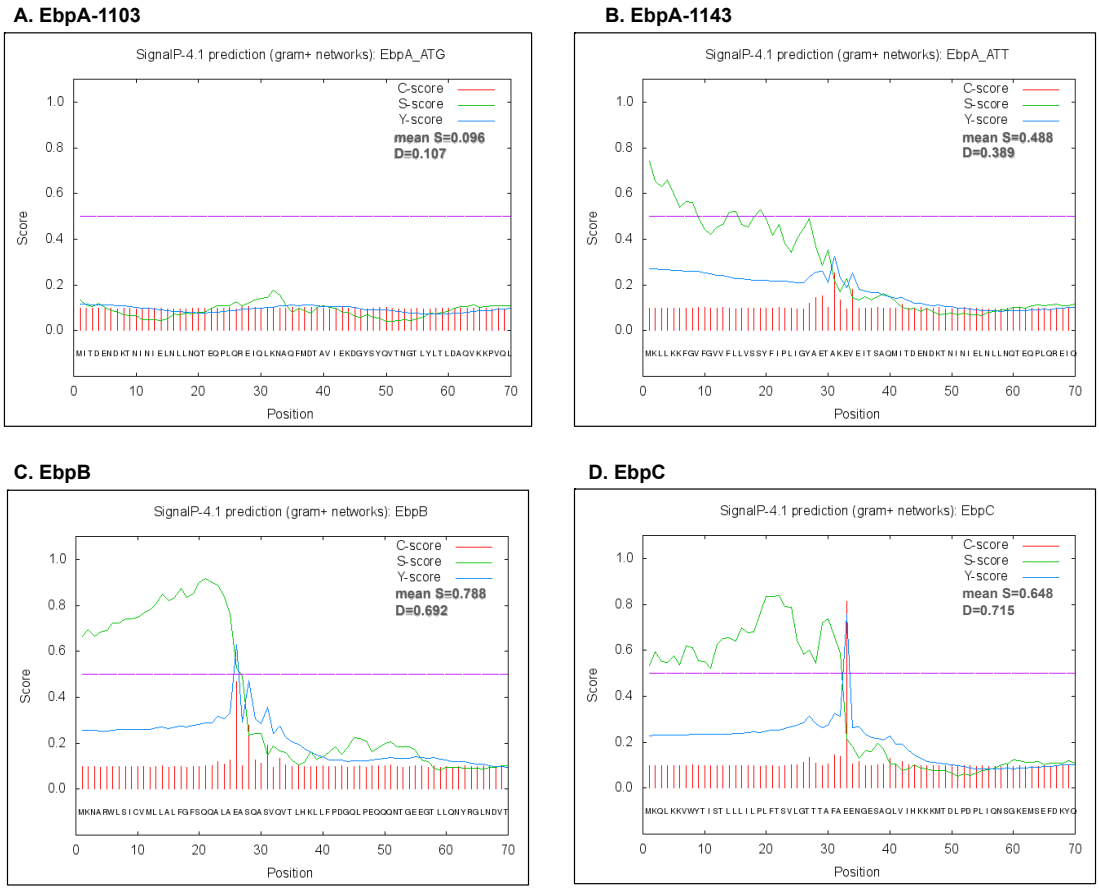

Figure 2.2. Prediction of signal peptides and cleavage sites of the proteins encoded by the *ebpABC* operon.

The presence and location of signal peptides and cleavage sites were predicted using the SignalP 4.1 server from the amino acid sequence of the annotated 1103-residue EbpA protein (EbpA-1103) **(A)**, the 1143-residue EbpA protein (EbpA-1143) **(B)**, EbpB **(C)** and EbpC **(D)**. The C-score (raw cleavage site score), S-score (signal peptide score) and Y-score (combined cleavage site score) are shown for each sequence. In addition, the average S-score (mean S) of the possible signal peptide (from position 1 to the position immediately before the maximal Y-score (combined cleavage site score)) and the D-score (discrimination score), used to discriminate signal peptides from not signal peptides, are indicated. The D-cutoff value used was 0.4.

Our rationale was that, if translation starts from ATT, the introduction of a stop codon would signal termination of translation and no EbpA protein would be produced; for this purpose, we introduced two stop codons in order to avoid read through, as was reported when only one stop codon was inserted at the 5' end of a chromosomal copy of a *gfp* reporter gene in *Bacillus subtilis* (82). In contrast, if the currently annotated ATG is the start of EbpA synthesis, the introduction of the stop codons before this ATG would not affect EbpA translation. As we predicted, flow cytometry showed that *E. faecalis* OG1RF displayed a strong EbpA signal (Figure 2.3-A), while strain TX5751 was negative for EbpA surface display (Figure 2.3-B). Next, we investigated the conservation of this unusual codon as the start of EbpA protein synthesis and found 100% conservation of the ATT codon in the 347 *E. faecalis* strains with available genome sequences in NCBI (data not shown). In addition, we interrogated the genome annotation for EbpA homologs in other enterococcal species including *E. faecium, Enterococcus hirae, Enterococcus casseliflavus, Enterococcus mundtti* and *Enterococcus gallinarum* and found that in all but *E. gallinarum,* ATG was annotated as start codon of these EbpA homologs (Figure 2.4). Furthermore, a recognizable RBS was present appropriately upstream of these *ebpA*-like genes' ATG annotated start codons. Interestingly, no recognizable RBS was observed upstream of the annotated *ebpA* ATC start codon in *E. gallinarum* (Figure 2.4), raising the possibility of an alternative start for EbpA protein synthesis in this enterococcal species.

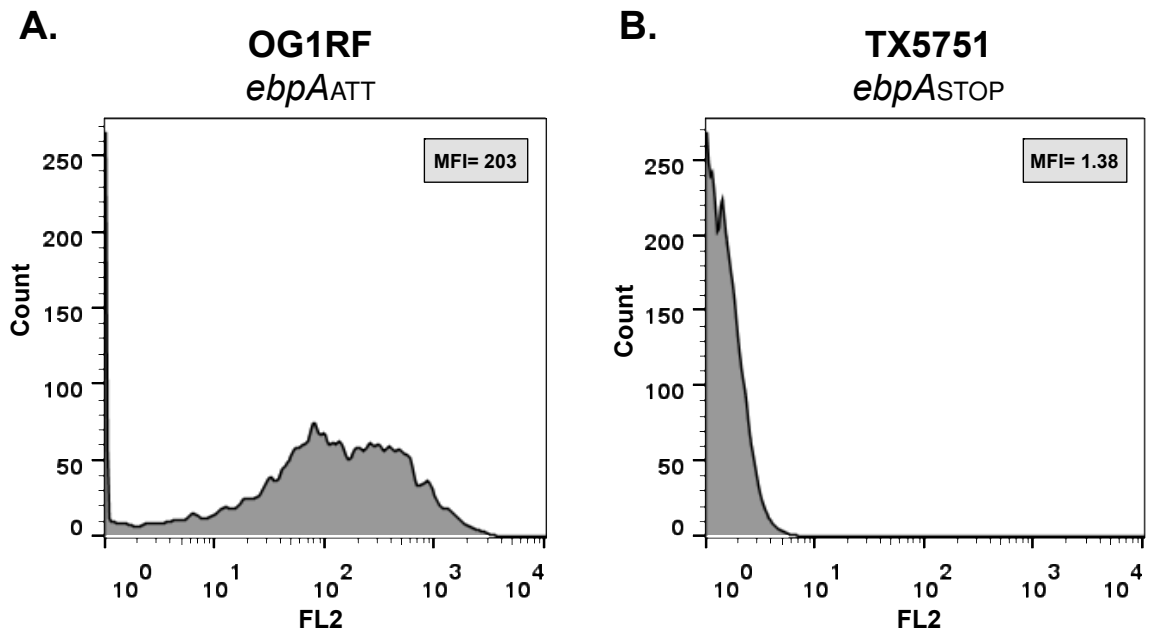

Figure 2.3. Flow cytometry analysis of EbpA surface display by wild-type *E. faecalis* OG1RF and TX5751.

Flow cytometry profile of **(A)** *E. faecalis* OG1RF ($ebpA_{ATT}$) and **(B)** TX5751 ($ebpA_{STOP}$), each grown in TSB-G to exponential phase and labeled with anti-rEbpA antibody. The mean fluorescence intensity (MFI) is indicated.

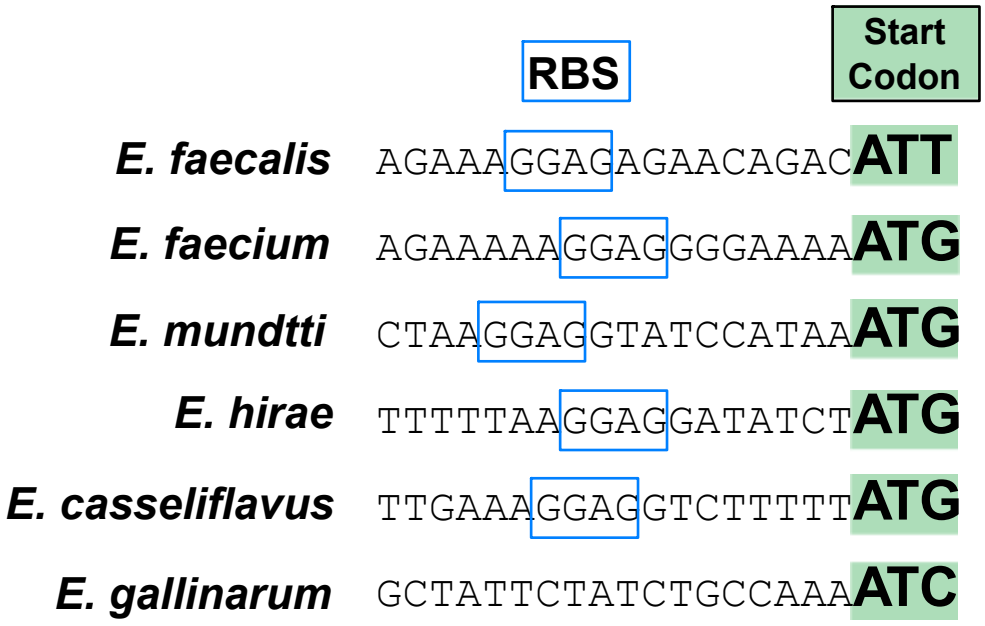

Figure 2.4. DNA sequence alignment of 18 nucleotides upstream of the annotated initiation codon of *E. faecalis ebpA* and its homologs in five enterococcal species. The annotated start codons and predicted RBSs are indicated for *E. faecalis ebpA* and its homologs in *E. faecium* (TX16), *E. hirae* (ATCC 9790), *E. casseliflavus* (EC20), *E. mundtti* (QU25) and *E. gallinarum* (A6981).

The start codon ATT affects EbpA surface display

The use of a rare start codon as the translational start of EbpA, along with its conservation in all published *E. faecalis* genomes, led us to the hypothesis that this codon may play a role in the regulation of Ebp pilus expression. To investigate this, we constructed a single nucleotide variant, named TX5731 in which the *ebpA* ATT triplet of *E. faecalis* OG1RF was replaced with ATG ($ebpA_{ATG}$), and then explored the effect of this initiation codon change on the levels of EbpA surface display. WC ELISA using anti-rEbpA, performed after growing the cells to exponential phase in TSB-G medium, revealed that strain TX5731 carrying ATG as the initiation codon of *ebpA* had significantly increased amounts of EbpA on the surface compared to OG1RF ($p < 0.001$; Figure 2.5). To confirm that the differences observed between the parental strain, OG1RF, and its $ebpA_{ATG}$ mutant (TX5731) were due to the mutation in the *ebpA* start codon, we generated a revertant strain (TX5732), by replacing the ATG of TX5731 with the original *ebpA* start codon ATT ($ebpA_{ATT}$), in the native location. TX5732 displayed similar EbpA levels on the surface to that observed on OG1RF, demonstrating the role of the initiation codon in the regulation of EbpA protein levels (Figure 2.5). In addition, WC ELISA did not show any EbpA on the surface of the strain carrying the two consecutive stop codons after the ATT initiation codon, TX5751, nor on the *ebpA* deletion mutant, TX5620 (Figure 2.5). EbpC surface display was also investigated under the same growth conditions and the results revealed a small but non-significant increase in EbpC on the surface of TX5731 compared to OG1RF and TX5732 (Figure 2.6). As expected, no surface display of either EbpA or EbpC was observed on the surface of TX5608, the *ebpABC* operon deletion mutant (Figure 2.5 & Figure 2.6). Similarly, when the cells were grown in BHI-S the $ebpA_{ATG}$ mutant, TX5731, also showed a significant increase surface

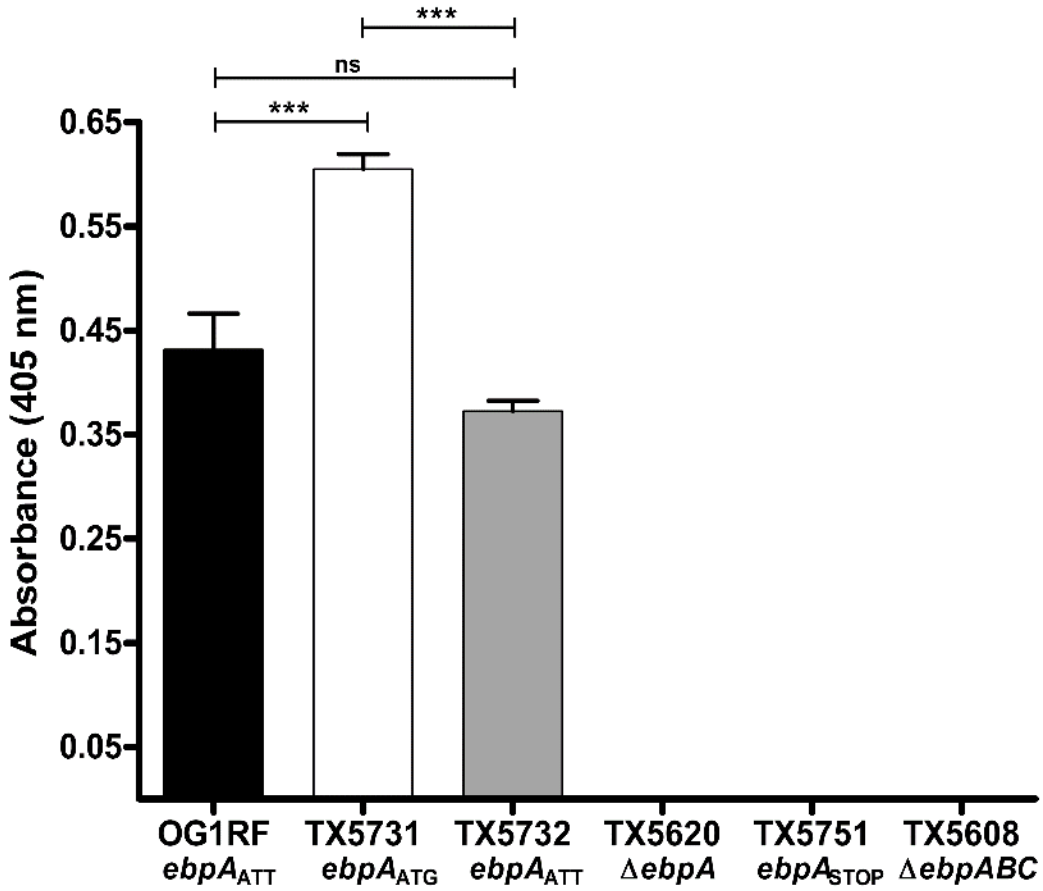

Figure 2.5. Effect of the *ebpA* initiation codon on EbpA surface display measured by WC ELISA.

EbpA surface display was detected using anti-rEbpA. Bars represent the means of absorbance measured at 405 nm ± standard deviations from two independent experiments representing six wells per strain. The mean absorbance values were compared using ANOVA with Bonferroni's post-test (***, $p \leq 0.001$; ns, $p > 0.05$).

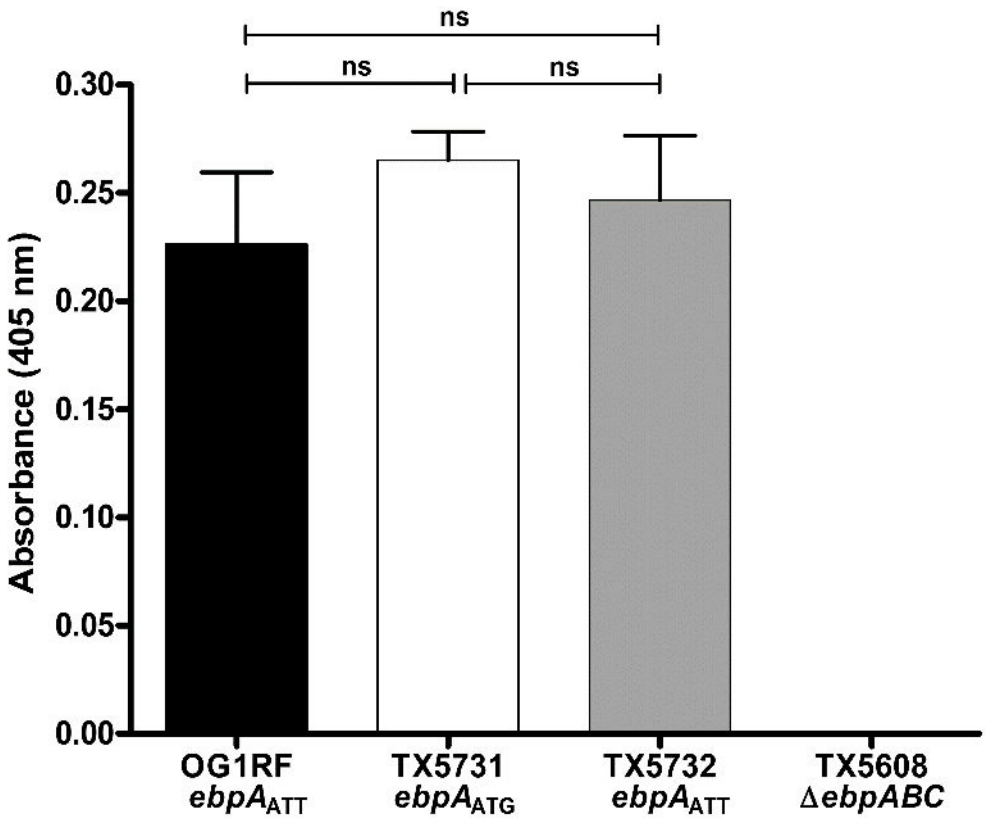

Figure 2.6. EbpC surface display measured by WC ELISA.

EbpC surface display was detected using affinity-purified polyclonal antibodies against EbpC. Bars represent the means of absorbance measured at 405 nm ± standard deviations from two independent experiments representing six wells per strain. The mean absorbance values were compared using ANOVA with Bonferroni's post-test (ns, $p > 0.05$).

display of EbpA compared to the *ebpA*$_{ATT}$ counterparts, OG1RF and TX5732 ($p < 0.001$; data not shown). Quantitation of surface-localized EbpA protein was also performed by flow cytometry. The mutant strain TX5731, with ATG, showed increased levels of EbpA on the cell surface, compared to OG1RF and TX5732, corroborating the results obtained with whole-cell ELISA (data not shown).

β-galactosidase production is reduced by the presence of ATT as the start codon of an *ebpA-lacZ* fusion

To explore the direct contribution of the EbpA initiation codon to translational efficiency, two translational reporter fusions, pTEX5749 and pTEX5750, were generated by amplifying an 292 bp fragment from -261, including the promoter region of *ebpA,* to 31 bp downstream of the translational start codon from *E. faecalis* OG1RF and TX5731, respectively (Figure 2.7). These fragments were fused to the reporter gene *lacZ* (Figure 2.7), and after electroporation of the fusion constructs into *E. faecalis* OG1RF, TX5731 and TX5732, β-galactosidase activity was assayed following growth in TSB-G (Figure 2.8) and BHI-S (Figure 2.9). Under both growth conditions and in each of the strain backgrounds, β-galactosidase activity from cells carrying the reporter fusion pTEX5750 with ATG as the start codon was significantly greater compared to cells carrying the reporter fusion pTEX5749 with the triplet ATT as the initiation codon of translation ($p < 0.001$) (Figure 2.8 & Figure 2.9). It is interesting to note that strain TX5731 carrying either pTEX5749 or pTEX5750 expressed significantly higher levels of the reporter protein compared to OG1RF and TX5732 carrying the corresponding reporter fusions ($p < 0.001$), which could suggest a positive-feedback loop controlling EbpA expression.

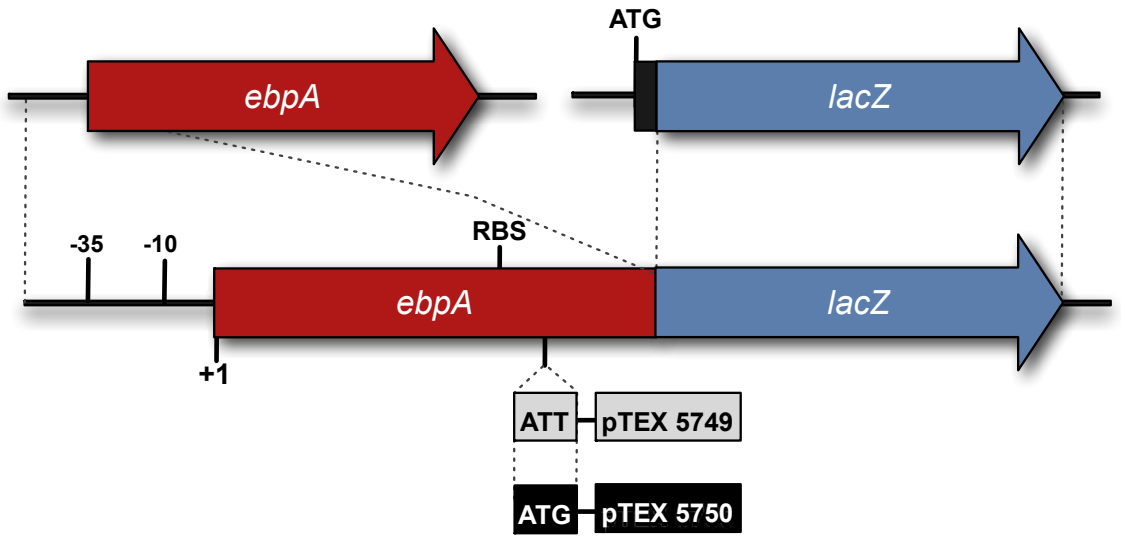

Figure 2.7. *ebpA*::*lacZ* tranlational fusions.

Schematic representation of the *ebpA::lacZ* fusions pTEX5749 (pSD2-$ebpA_{ATT}$::*lacZ*) and pTEX5750 (pSD2-$ebpA_{ATG}$::*lacZ*) carrying ATT and ATG as the start of EbpA::LacZ fusion protein synthesis, respectively.

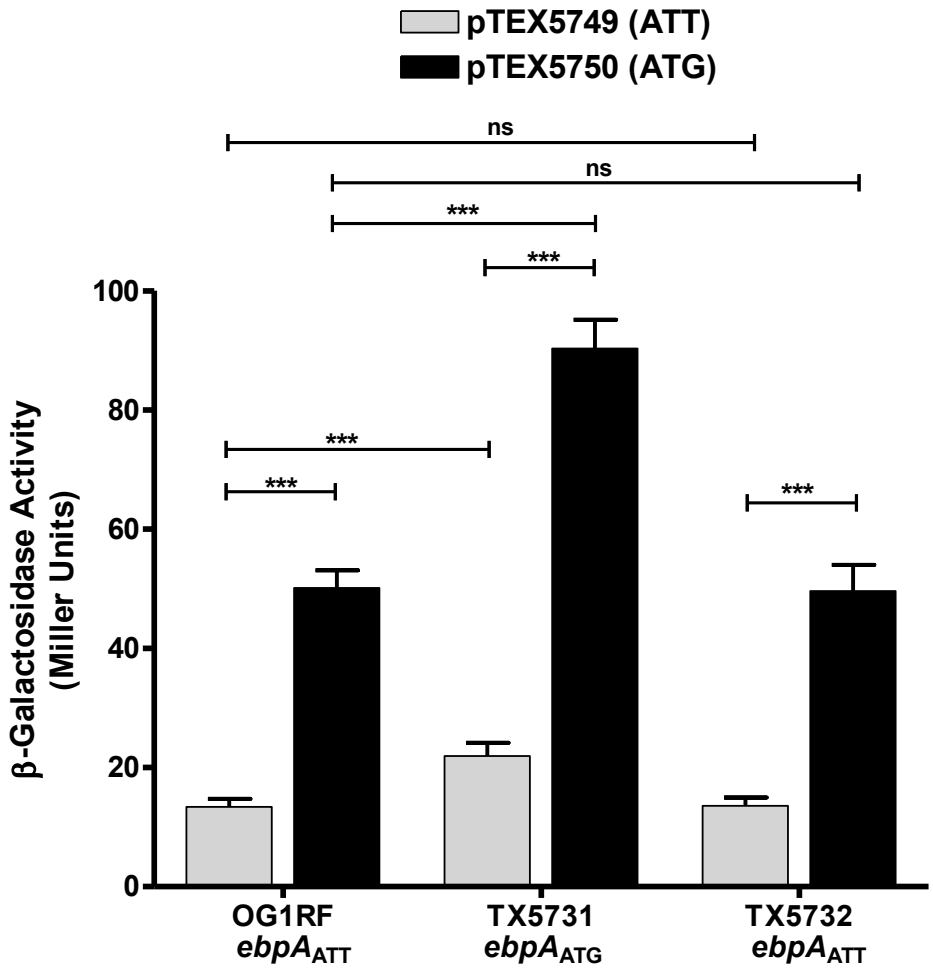

Figure 2.8. Beta-galactosidase expression from *ebpA::lacZ* tranlational fusions in TSB-G.

β-galactosidase activity in *E. faecalis* OG1RF and its *ebpA* start codon derivatives, TX5731 and TX5732 containing either pTEX5749 (gray bars) or pTEX5750 (black bars) after grown to mid-log phase in TSB-G. Bars represent the means ± standard deviations of four independent assays each with 2 duplicates. The mean values were compared using ANOVA with Bonferroni's post-test (***, p≤0.001; ns, p > 0.05). *Dr. Sabina Leanti La Rosa contributed to the β-galactosidase assay.*

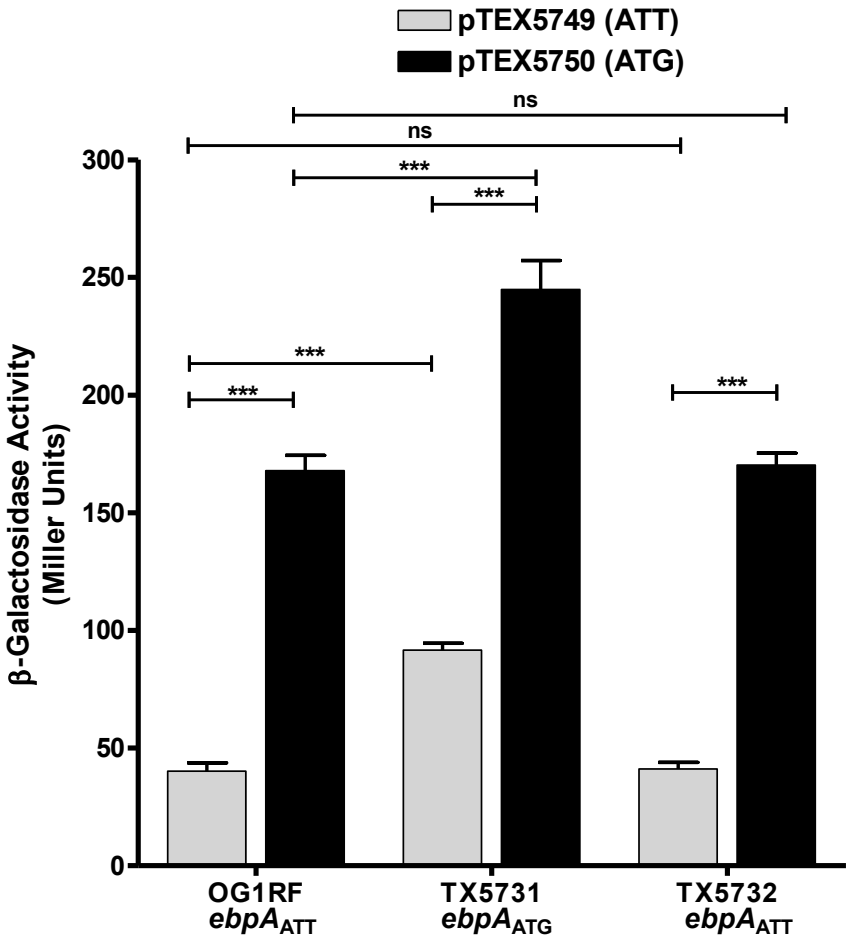

Figure 2.9. Beta-galactosidase expression from *ebpA::lacZ* translational fusions in BHI-S.

β-galactosidase activity in *E. faecalis* OG1RF and its *ebpA* start codon derivatives, TX5731 and TX5732 containing either pTEX5749 (gray bars) or pTEX5750 (black bars) after grown to mid-log phase in BHI-S. Bars represent the means ± standard deviations of four independent assays each with 2 duplicates. The mean values were compared using ANOVA with Bonferroni's post-test (***, p≤0.001; ns, p > 0.05). *Dr. Sabina Leanti La Rosa contributed to the β-galactosidase assay.*

In contrast, no differences in β-galactosidase activity were observed between OG1RF and TX5732 (Figure 2.8 & Figure 2.9). In addition, we observed that in BHI-S, β-galactosidase activity was increased approximately 3-fold compared to TSB-G grown cells in both the ATT (pTEX5749) and ATG (pTEX5750) constructs, but the relationship of β-galactosidase from the ATT and the ATG start codon was still maintained (Figure 2.8 & Figure 2.9). Importantly, the differences in β-galactosidase activity are not a consequence of differences in growth rate, as OG1RF and its derivatives carrying the two plasmids, pTEX5749 and pTEX5750, exhibited equivalent growth kinetics (data not shown).

ATT as the initiation codon of *ebpA* translation correlates with less biofilm formation

Previous studies showed that deletion of *ebpA* had a marked effect on the ability of *E. faecalis* OG1RF to form biofilm (32). We therefore investigated the impact of the *ebpA* initiation codon on early biofilm development (3 hours) and on mature biofilm (24 hours). When we scored biofilm after 3 hours of static incubation, the strain carrying ATG as the initiation codon of EbpA, TX5731, showed a significant increase in biofilm density compared to the strains carrying ATT, OG1RF and the revertant TX5732 (median for TX5731, 0.68 versus 0.58 and 0.57 for OG1RF and for TX5732, respectively; $p < 0.001$) (Figure 2.10-A). A smaller but still significant increase was observed in biofilm density after 24 hours of static incubation the $ebpA_{ATG}$ mutant, TX5731, compared to OG1RF and TX5732 ($p < 0.001$; Figure 2.10-B). Consistent with previous findings (29, 32, 38, 39), a marked reduction in biofilm formation was observed when the *ebpABC* operon (TX5608) or *ebpA* (TX5620) had been deleted ($p < 0.001$; Figure 2.10).

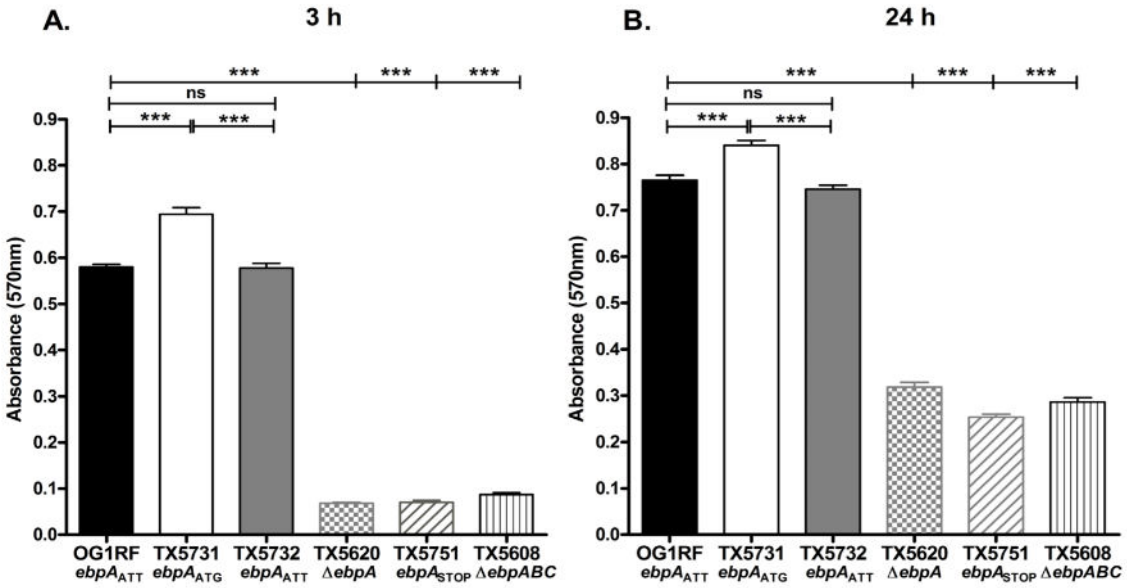

Figure 2.10. Effect of *ebpA* initiation codon on biofilm formation.

Bacterial cells grown 3 h **(A)** or 24 h **(B)** in TSB-G were analyzed for biofilm formation using a crystal violet based assay. Bars represent the means of absorbance at 570 nm ± standard deviations from four independent assays (forty wells per strain). ANOVA with Bonferroni's post-test was used to compare biofilm density values (***, p≤0.001; ns, p > 0.05).

In addition, TX5751, the strain in which two successive stop codons were introduced after the ATT EbpA start codon showed reduction in biofilm density comparable to these two deletion mutants, corroborating the role played by EbpA in biofilm formation. The greater difference in biofilm density observed at the earlier time point compared to 24 hours between the strain carrying ATG as the start codon of EbpA (TX5731) versus the strains carrying ATT (OG1RF and TX5732) may be related to the data of Bourgogne and colleagues who demonstrated that *ebpA* expression peaked at log phase, followed by a decline during stationary phase (40). Hence, our results corroborate the importance of EbpA in biofilm production and demonstrate that the levels of EbpA protein on the surface of the cells are important for *E. faecalis* biofilm formation, in particular during its initial stages.

ATT as the initiation codon of *ebpA* translation correlates with less binding to fibrinogen

Nallapareddy et al. demonstrated that Ebp pilus-deficient mutants of *E. faecalis* OG1RF showed reduced binding to fibrinogen and to collagen type I (34); in addition, Flores-Mireles et al. confirmed that EbpA mediates attachment of *E. faecalis* to host fibrinogen (69). Therefore, we investigated the ability of OG1RF, its $ebpA_{ATG}$ initiation codon mutant (TX5731) and the revertant strain $ebpA_{ATT}$ (TX5732), to bind to fibrinogen. A slight but significant increase in binding to fibrinogen was observed when the initiation codon of *ebpA* was changed to ATG (TX5731) compared to OG1RF and TX5732 with the ATT initiation codon ($p \leq 0.05$ and $p \leq 0.01$, respectively; Figure 2.11). This result therefore indicates that the ATT initiation codon of EbpA also affects *E. faecalis* adherence to fibrinogen.

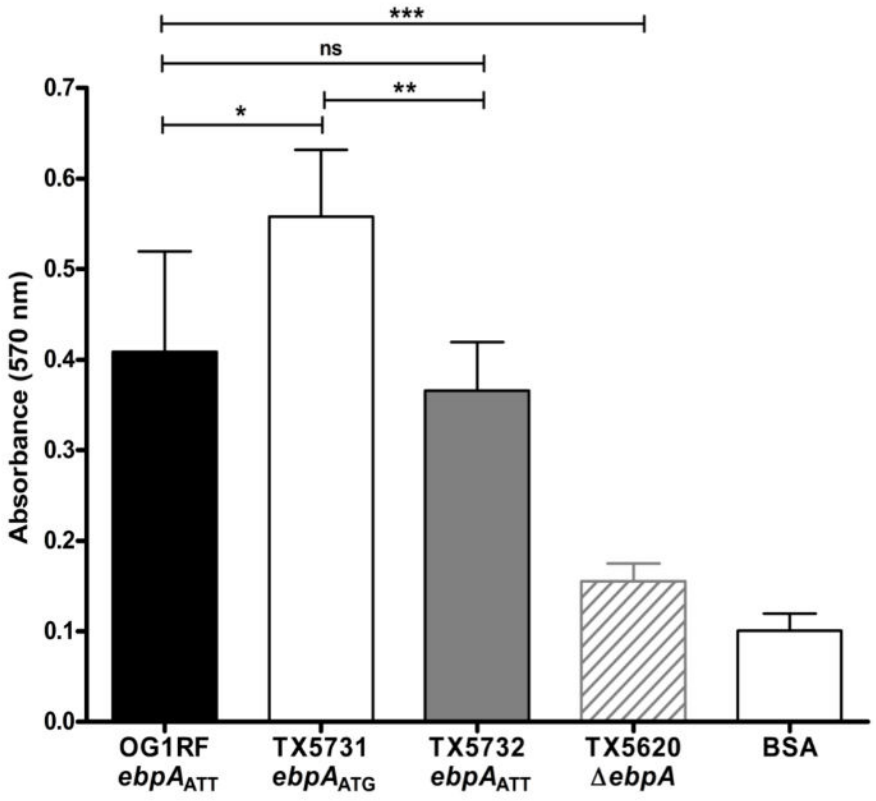

Figure 2.11. Effect of the *ebpA* initiation codon on the adherence of *E. faecalis* to immobilized fibrinogen.

Bars represent means ± standard deviations of absorbance measured at 570 nm (for 4 wells per strains). The mean values between *E. faecalis* OG1RF and its derivatives were analyzed using ANOVA with Bonferroni's post-test (***, $p \leq 0.001$; **, $p \leq 0.01$; *, $p \leq 0.05$; ns, $p > 0.05$).

2.4. DISCUSSION

In bacteria, the most frequently used translational start codon is AUG (90% of the *E. coli* mRNAs); however, alternative initiation codons including GUG (8%) and UUG (1%) are occasionally found (71, 72). In contrast, the triplet AUU has been reported in only two instances in *E. coli*, namely, the *pcnB* gene encoding poly(A) polymerase (PAPI) (73) and the *infC* gene encoding translation initiation factor IF3 (74). In both instances, expression of the corresponding proteins was limited by the presence of AUU as the translational initiation codon (73, 74, 83). We analyzed the genome of *E. faecalis* OG1RF and determined that in 81.5% of the open reading frames (ORFs), AUG is annotated to be the initiation codon, while in 10% and 8.5% of the instances, the codons GUG and UUG are predicted to initiate protein synthesis, respectively. However, we observed that the most likely translational start codon of EbpA in *E. faecalis* OG1RF is the rare triplet AUU (corresponding to ATT in the DNA) (Figure 2.1), while the *E. faecalis* *infC* gene, encoding IF3, is annotated to start with the canonical ATG. The presence of a rare start codon as the most likely start of EbpA protein synthesis and its conservation in all sequenced *E. faecalis* strains led us to the hypothesis that this codon plays a role in the translational regulation of EbpA expression. First, we experimentally confirmed that ATG is not the start of EbpA translation by introducing two successive stop codons in between the ATT we predicted is the initiation codon and the currently annotated ATG start codon of *ebpA*; as we expected, these stop codons abolished EbpA surface display (Figure 2.1 & Figure 2.3). Then, we constructed a derivative of OG1RF in which we replaced, in its native location, the ATT start codon of *ebpA* with ATG (TX5731) and then reverted this ATG to ATT (TX5732) and demonstrated that *E. faecalis* OG1RF and TX5732, carrying ATT as the start of EbpA protein synthesis, had reduced levels of EbpA on their surfaces compared to the strain TX5731, carrying ATG as the translational start (Figure 2.5). We previously demonstrated that EbpA levels influence the length and

number of pilus fibers, which led us to propose that EbpA is important for initiation as well as termination of pilus polymerization (32). Although it could be suggested that increased levels of EbpA protein observed on the surface of TX5731 carrying ATG as the initiation codon of ebpA (Figure 2.5) may result in a small increase in the number of pilus fibers but decreased pilus length, consistent with a small (albeit non-significant) increase in EbpC surface display (Figure 2.6), we postulate that the main effect of the ATT start codon is on EbpA levels exposed on *E. faecalis* cells, as the majority of EbpA appears as monomers on the cell surface (32).

We inferred that the reduced levels of EbpA on the surface of *E. faecalis* OG1RF and TX5732 are a consequence of reduced rates of translation when ATT is present as the start of EbpA protein synthesis. Our results using translational reporter fusions to *lacZ* also indicate that, in *E. faecalis,* ATG is a more efficient start codon for the initiation of EbpA translation than ATT (Figure 2.8 & Figure 2.9), which is in accordance with the hierarchy of start codon efficiencies proposed in *E. coli* (84). Although other signals and factors play a role in the rate of translation initiation (84), including the Shine-Dalgarno (SD) sequence and the initiation factors IF1, IF2 and IF3 (85), evidence in *E. coli* indicates that, in the presence of an ATT start codon, IF3 increases the dissociation of the initiation complex, which includes the 30S ribosomal subunit, the specific initiator tRNA, the mRNA and the three initiation factors (72). It is interesting to note that β-galactosidase activity, which is a reflection of the levels of the EbpA-LacZ fusion protein inside the cell, was increased approximately 3.5 -folds when the reporter fusion start codon was ATG versus ATT (Figure 2.8), but a more discreet increase (approximately 1.5 fold) was observed in EbpA surface display on TX5731 carrying ATG as the *ebpA* start codon versus the strains carrying ATT (OG1RF and TX5732) (Figure 2.5). One possibility that could explain this difference would be the existence of additional

regulatory mechanisms participating in the regulation of EbpA levels on the surface of the cells. In light of the current model of Ebp pilus assembly in *E. faecalis* (32, 33), one could infer that modulating the ratios of the major backbone subunit, EbpC, to the minor subunits, EbpA and EbpB, could be important for pilus biogenesis, since an individual pilus fiber is composed of multiple EbpC subunits while in theory only one EbpA and one EbpB subunits are required for the tip and base of one pilus fiber, respectively (32, 33). Therefore, it seems plausible that the ATT start codon of *ebpA* is a way to regulate the ratio of EbpA to EbpC in *E. faecalis*.

Ebp pili are considered one of the major virulence factors of *E. faecalis,* playing a role in biofilm formation, adherence to fibrinogen and in the ability of *E. faecalis* to cause endocarditis and infection in mouse models of ascending UTI and CAUTI (29, 32-34, 36, 37, 69). EbpA has been demonstrated to be the most important pilin in biofilm formation (32, 69), while deletion of *ebpC*, encoding the major pilin, had a minor effect (32) despite abrogating pilus formation; this suggests that EbpA, in monomeric or dimeric form, on the surface of *E. faecalis* cells is capable of sustaining biofilm formation even when it is not part of a pilus polymer (32, 33). In addition, it has been shown that the MIDAS motif present in EbpA's VWA domain is crucial for EbpA-mediated biofilm formation and fibrinogen binding (70). Proteins containing VWA domains, which are widely distributed among the three domains of life, Eukaryota, Archaea and Eubacteria, often participate in cell adhesion and protein-protein interactions (86). Furthermore, other VWA-containing tip pilin proteins, including PilA of *Streptococcus agalatiae* and RrgA of *Streptococcus pneumoniae,* have also been implicated in binding to ECM proteins (87, 88). Considering the demonstrated role of EbpA in biofilm formation (32, 69) and fibrinogen adherence (69), we believed that identity of the EbpA start codon would impact these processes, which have been associated with the ability of *E. faecalis* to cause infection. Indeed we

found that the presence of ATT, compared to ATG, as the start codon of EbpA protein synthesis resulted in less biofilm formation (Figure 2.10) and decreased adherence to fibrinogen (Figure 2.11). Although the reasons behind the advantages or disadvantages of negatively regulating the levels of pilation are unknown, it has been suggested that high expression of pilin surface proteins could involve a fitness cost to the bacteria due to the selective pressure exerted by the immune system (89). Indeed, Danne et al., demonstrated in *Streptococcus gallolyticus* that a mutant overexpressing pili showed reduced survival in human blood compared to a non-piliated mutant (89). In addition, they demonstrated that THP-1 human macrophages showed better opsonophagocytosis of highly-piliated bacterial cells than their non-piliated counterparts (89). Although we cannot discard the possibility that ATT as the start codon of EbpA protein synthesis has a role in *E. faecalis* human infections, the conservation of this rare codon in all sequenced *E. faecalis* strains implies that it appeared long before enterococci became common human colonizers and pathogens, and we speculate that its presence could have aided *E. faecalis* in some way in the environment or an early host, perhaps due the decrease adherence observed in weakly piliated cells, thus favoring dispersal. Regardless of why this change occurred, our results taken together, provide the first example of pilus regulation through the use of a very rare initiation codon and support our hypothesis that **"ATTenuation starts with ATT"**.

CHAPTER 3. Role of the Emp Pilus Subunits of *Enterococcus faecium* in Biofilm Formation, Adherence to Host Extracellular Matrix Components and Experimental Infection

---

*This chapter is based upon work in press in the journal Infection and Immunity with the same title as the one of this chapter (Infect Immun. 2016 Feb 29. pii: IAI.01396-15). I am co-first author of this publication (**Montealegre MC**, Singh KV, Somarajan S, Yadav P, Chang C, Spencer R, Sillanpää J, Ton-That, Murray BE) and I was responsible for preparing the original manuscript and conducted the majority of in-vitro experiments described; Dr. Singh, co-first author of this publication performed the in vivo experiments.* *ASM authors retain the right to reuse the full article in his/her dissertation or thesis. For further information visit http://journals.asm.org/site/misc/reprints.xhtml.*

3.1. INTRODUCTION

The genome of *E. faecium* TX16, also known as DO, encodes four PGCs predicted to form four distinct pilus-like structures (41-44). Indeed, the conditional expression of two distinct types of pili was demonstrated in an *E. faecium* hospital-acquired bloodstream isolate (43). In addition, differential assembly of the pilin proteins encoded by one of these pilin clusters, the PGC-1, has been observed between a bloodstream isolate and a community-derived stool isolate, with the latter strain only displaying the pilin proteins anchored to the cell wall, but not associated with pilus fibers (45).

Another of these pilus clusters, the *empABC* operon (47), is enriched in isolates of clinical origin (90) and we had previously shown that, in the endocarditis-derived *E. faecium* strain TX82, allelic replacement of *empABC* (Δ*empABC::cat*) affected primary attachment and biofilm formation (47). In addition, we found that the Δ*empABC::cat* mutant was significantly attenuated, versus the parental strain TX82, in an experimental model of UTI (47). Furthermore, an epidemiological study found a significant association between the degree of biofilm formation and the presence of the *empABC* operon (91).

The *empABC* operon is composed of three genes, encoding the structural subunit proteins EmpA, EmpB and EmpC; *bps*, encoding the class C sortase, is downstream of the *empABC* operon, separated by a predicted strong transcriptional terminator and shown to be transcribed independently (42, 47) (Figure 3.1). EmpC has been demonstrated to be the major pilin (42, 43, 47), while EmpA and EmpB are predicted to be incorporated into the fiber as minor components (47). However, the role of individual Emp pilus subunits in pilus-associated functions has not been explored previously. In this chapter, we investigated the contribution of each of the subunits of Emp to pilus architecture, biofilm formation, adherence to components of the ECM and infection.

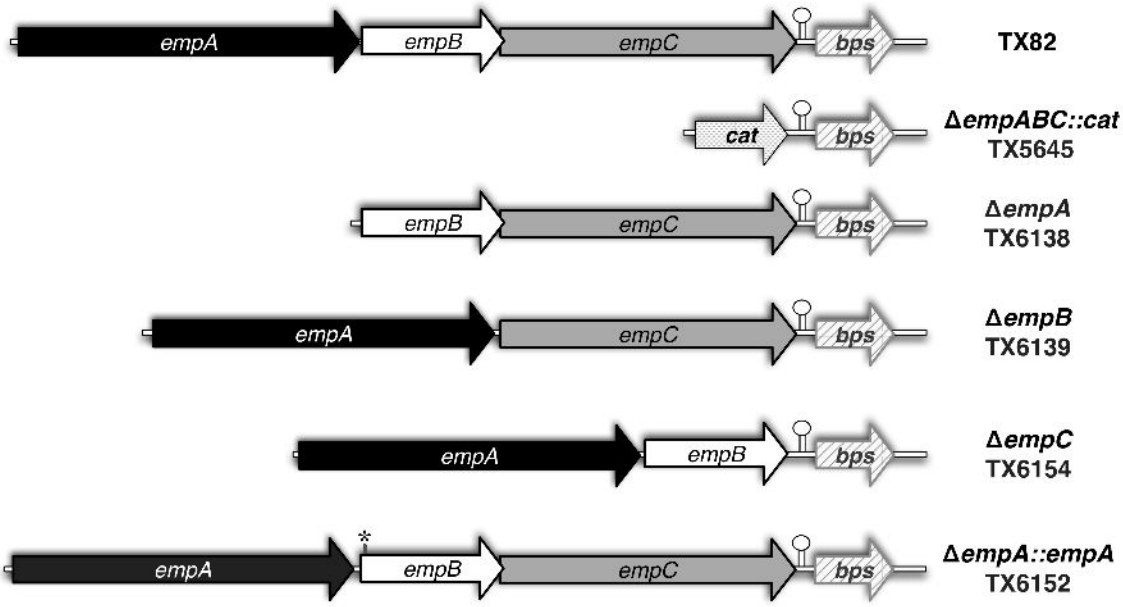

Figure 3.1. Schematic representation of the *emp* operon of *E. faecium* TX82, its deletions derivatives and the *empA* reconstituted strain.

The *emp* operon consist of three genes, *empA*, *empB* and *empC*, encoding the pilin subunits; *bps*, located after a predicted transcriptional terminator (indicated with a lollipop) downstream of *empC*, encodes a class C sortase. The genes deleted from each mutant are indicated and the silent mutation introduced in the *empA* reconstituted strain is indicated with an asterisk. *Sudha Somarajan, Ph.D and Puja Sharma, Ph.D contributed to the generation of the deletion mutants.*

3.2. MATERIAL AND METHODS

Bacterial strains and growth conditions

Relevant characteristics of the bacterial strains and plasmids used in this chapter are described in Table 3-1. *E. coli* strains, used for cloning experiments, were cultured at 37°C in LB (BD) broth or agar. *Enterococcus* strains were routinely grown at 37°C using BHI (BD) broth or agar or TSB-G broth (BD). Ampicillin 100 µg/ml and gentamicin 25 µg/ml were used for selection in *E. coli,* while gentamicin 200 µg/ml was used for enterococci. Enterococcosel agar (BD) supplemented with vancomycin (6 µg/ml) was used to grow the bacteria recovered from the animal experiments. Growth characteristics of TX82, its *emp* deletion derivatives and the *empA* reconstituted strain were assessed in BHI broth, by measuring the OD_{600} and by determining the number of CFUs on BHI agar, as previously described in chapter 2 and in (47).

Construction of markerless deletions of *empA*, *empB* and *empC* genes and generation of an *empA* reconstituted strain (restoration of the *empA* gene in its native location)

Non-polar deletions of the individual genes encoding the pilus subunits EmpA, EmpB and EmpC of *E. faecium* TX82 (Figure 3.1 & Table 3-1) were constructed using a previously described system (75), based on the pHOU1 vector (75, 76). Briefly, a fragment upstream and a fragment downstream of the genes to be deleted were amplified using the primers listed in Table 3-2. The two fragments flanking each gene were fused together by cross-over PCR, cloned into pGEM or TOPO vectors and sub-cloned into pHOU1 (Table 3-1).

Table 3-1. Bacterial strains and plasmids used in chapter 3

Strain or Plasmid	Relevant Characteristic(s)	Reference
Strains		
E. faecium		
TX82	Endocarditis isolate. AMP^R, VAN^R.	(92)
TX5645	TX82 Δ*empABC*::*cat;* allelic replacement of *empABC* with *cat* (chloramphenicol acetyltransferase) gene. CHL^R	(47)
TX6138	TX82 Δ*empA*; *empA* markerless deletion mutant.	This study
TX6139	TX82 Δ*empB*; *empB* markerless deletion mutant.	This study
TX6154	TX82 Δ*empC*; *empC* markerless deletion mutant.	This study
TX6152	TX6138::*empA*; TX82 Δ*empA* with *empA* reconstituted in situ in the chromosome.	This study
E. faecalis		
CK111	OG1Sp *upp4*::P23 *repA4*: conjugative donor that allows pHOU1 replication.	(75)
E. coli		
TG1	*E coli* host strain used for routine cloning	
DH5α	*E coli* host strain used for routine cloning	
EC1000	*E coli* host strain for cloning of RepA-dependent plasmids	(78)
Plasmids		
pGEM-T Easy	Plasmid used for initial cloning of PCR fragments. AMP^R	Promega
Blunt II-TOPO	Plasmid used for initial cloning of PCR fragments. KAN^R	Invitrogen
pHOU1	Conjugative donor plasmid that carries GEN^R and the counterselectable *pheS** gene.	(76)
pQE30	Expression vector	Qiagen
pTEX5636	3192 pb fragment from TX16 *empA* (encoding mature EmpA without signal peptide or cell wall anchor domain) cloned into pQE30 expression vector.	This study

AMP, ampicillin; CHL, chloramphenicol; GEN, gentamicin; KAN, kanamycin VAN, vancomycin. Superscript "R" designates resistance.

Table 3-2. Oligonucleotides used in chapter 3.

Primer Name	Sequence 5′- 3′	Relevant Characteristics
empA-UP-F-NotI	AATATGCGGCCGCGGAGTTCCTTGGGATTCTCTC	Forward for *empA* deletion (upstream fragment), NotI site underlined.
empA-UP-R	CAATCATCCCTACCGTCATTTTTCCCCTCCTTTTTC	Reverse for *empA* deletion (upstream fragment).
empA-DW-F	GGAAAAATGACGGTAGGGATGATTGGTTGTGCG	Forward for *empA* deletion (downstream fragment).
empA-DW-R-PstI	ATATCTGCAGGCCTTCTGTCAGCTTTTCTCCATTCGATG	Reverse for *empA* deletion (downstream fragment), PstI site underlined.
empA-Rev-F-NotI	ATTGCGGCCGCAGAAGACCGGCTGATGGAAA	Forward for *empA* reconstituted strain, NotI site underlined.
empA-Rev-R-BamHI	CGGGATCCAGG**a***GGATCAGGGTAGTCGT	Reverse for *empA* reconstituted strain, BamHI site underlined.
*empA*r-F	GCGGGATCCGACACTACAGATGATCCAAC	Forward for His_6 tag expression of EmpA, BamHI site underlined
*empA*r-R	GCGGTCGAC**TTA**TGGTACTTTTGCCTGATTCG	Reverse for His_6 tag expression of EmpA, SalI site underlined, translational stop codon in bold.
empB-UP-F-BamHI	CGCTGGATCCCAGTCACTACTTCCGATGATACG	Forward for *empB* deletion (upstream fragment), BamHI site underlined.
empB-UP-R	TATACTGTCCGCCTCCATATTTAGCTGCCCCCTCTTTC	Reverse for *empB* deletion (upstream fragment).
empB-DW-F	CAGCTAAATATGGAGGCGGACAGTATATTGAAAGTAGTC	Forward for *empB* deletion (downstream fragment).
empB-DW-R-SmaI	AATATCCCGGGTGATTAACGATCAACTG	Reverse for *empB* deletion (downstream fragment), SmaI site underlined.
empC-UP-F-BamHI	CGCGGATCCCCAAAGTACCAGAAGTCGTC	Forward for *empC* deletion (upstream fragment), BamHI site underlined.
empC-UP-R	TGCACCGATATACACCATTTTTTCACTCCTGTTCT	Reverse for *empC* deletion (upstream fragment).
empC-DW-F	GAGTGAAAAAATGGTGTATATCGGTGCAGGAGTAGT	Forward for *empC* deletion (downstream fragment).

empC-DW-R-EcoRI	CCGGAATTCGAGTGTCCGTCCATTGATTTC	Reverse for *empC* downstream fragment, EcoRI site underlined.
empC-F-(RT)	AGATAAAGGAGCGTCCGTGG	Forward for *empC*, used for RT-PCR.
empC-R-(RT)	AGCTGACACTCCGTCTTTTGG	Reverse for *empC*, used for RT-PCR.
fm-gyrA-F-(RT)	TATTACCTGGACCAGATTTTCCAA	Forward for *gyr*, used for RT-PCR.
fm-gyrA -R-(RT)	TTCTAAGATGTGTGCTCTTGCTTC	Reverse for *gyr*, used for RT-PCR.

*****Silent mutation introduced to differentiate the *empA* reconstituted strain from TX82.

The recombinant pHOU1 plasmids were propagated in *E. coli* EC1000 and transferred to *E. faecalis* CK111 by electroporation (Table 3-1). Double-crossover homologous recombination was achieved by first transferring the plasmids into *E. faecium* TX82 through filter mating with *E. faecalis* CK111 carrying the recombinant plasmids, followed by culturing the gentamicin-resistant *E. faecium* colonies that integrated the plasmid on MM9YEG media supplemented with 10 mM *p*-Cl-Phe. Deletion of the genes was detected by PCR and confirmed by sequencing, with verification of the correct background by PFGE. For generation of the *empA* reconstituted strain (Figure 3.1 & Table 3-1), a 4309 kb fragment that encompasses 439 bp upstream to 480 bp downstream of the *empA* gene was amplified from TX82 (a single silent mutation (Figure 3.1 & Table 3-2) was introduced into the fragment, within the *empB* coding region, to differentiate this reconstituted strain from TX82) and cloned into the pHOU1 vector. Once the fragment was cloned into pHOU1, the approach described above for the generation of the deletions was followed to introduce in situ the *empA* gene into the chromosome of the Δ*empA* strain (Figure 3.1, TX6138).

Reverse transcriptase PCR (RT-PCR)

Total RNA from TX82 and the panel of deletion mutants was isolated from cells grown in TSB-G to mid-logarithmic phase (OD_{600}~0.6). A 5 ml volume of the cultures was mixed with 10 ml of RNA protect reagent (Qiagen, Hilden, Germany), harvested and resuspended in 0.9 ml of TRIzol reagent (Ambion-Thermo Scientific, Waltham, MA). Cells were disrupted by bead beating for 1 min, twice, with cooling on ice in between (BioSpec Products, Bartlesville, OK). RNA extraction and purification was performed using PureLink RNA extraction kit (Ambion) following the manufacturer's instructions. cDNA was synthesized using SuperScriptIII First-Strand Synthesis System (Invitrogen, Carlsbad, CA). Primers, targeting an intragenic region of *empC* (Table 3-2), were used

to evaluate *empC* expression. Expression of the gene encoding gyrase A (*gyrA*) of *E. faecium* was used as an internal control (Table 3-2), as previously described (47). A PCR reaction, in the absence of reverse transcriptase, was used to assure the absence of genomic DNA in the RNA samples.

Antibodies against EmpA

Previously generated goat polyclonal antibodies were used to detect EmpC (42) while rabbit polyclonal antibodies against EmpA were generated in this study. The DNA sequence corresponding to amino acids 30 to 1093 of EmpA from the *E. faecium* strain TX16 (Table 3-2) was cloned into pQE30 (N-terminal His6-tag fusion) expression vector (42), generating the plasmid pTEX5636 (Table 3-1). Expression of rEmpA was induced with 1 mM IPTG and protein purification was performed by nickel affinity chromatography using His-GraviTrap columns (GE Healthcare, Uppsala, Sweden). Protein concentration was determined by absorption spectroscopy at 280 nm using calculated molar absorption coefficient values (93). Rabbit immunization with rEmpA was done following a pre-approved protocol and guidelines by the Animal Welfare Committee of the University of Texas Health Science Center at Houston. In brief, 1 mg of rEmpA in Freund's complete adjuvant (FCA) was subcutaneously injected at multiple sites into a New Zealand white male adult (~3 kg) on day 1. Booster doses prepared in emulsified Freund's incomplete adjuvant (FIA) were given subcutaneously at multiple sites on days 21 and 42. The animal was anesthetized prior to blood collection via cardiac puncture followed by euthanasia. Anti-EmpA antibody titers in rabbit sera were determined by enzyme-linked immunosorbent assay (ELISA) as previously described by (94) with some modifications. Briefly, 96-well plates (Immulon 4HBX, Thermo Fisher Scientific) coated overnight with 1 μg of rEmpA in 50 mM carbonate-bicarbonate buffer, pH 9.6 were used to test the rabbit sera (serial dilutions from 1:200 to 1:25,600).

Detection was perform with peroxidase-conjugated anti-rabbit secondary antibody (Jackson ImmunoResearch Laboratories) and 1-Step™ PNPP substrate (Thermo Fisher Scientific). The highest serum dilution with an absorbance at 405 nm ≥ 0.10 at 3 min after addition of the substrate was the establish as the antibody titer (94).

Immunoelectron microscopy

Immunoelectron microscopy to study Emp pilus architecture in TX82 and its *emp* deletion mutants was performed as previously described (95), with minor modifications. Cells were grown in TSB-G to exponential phase, harvested by centrifugation and then washed with 0.1 M NaCl. Immunogold labeling was performed using the anti-EmpA and anti-EmpC antibodies described above, followed by 18 nm gold-conjugated goat anti-rabbit IgG (1:20 dilution; Jackson ImmunoResearch Laboratories) for EmpA staining or 12 nm donkey anti-goat IgG (1:20 dilution of 1 mg/ml; Jackson ImmunoResearch Laboratories) for EmpC staining. Samples were viewed using a Jeol 1400 transmission electron microscope.

WC ELISA

Surface display of EmpA and EmpC, using TX82, the panel of *emp* deletion mutants and the *empA* reconstituted strain, was measured at mid-logarithmic phase (OD_{600}~0.6) by WC ELISA as described in chapter 2 and following a previously described methodology (32, 96). Rabbit and goat polyclonal antibodies (1:5,000 dilution of 1mg/ml) against EmpA (described above) and EmpC (previously generated in(42)), respectively were used as primary antibodies; while alkaline phosphatase conjugated F(ab')2 fragment goat anti-rabbit IgG and donkey anti-goat IgG (1:5,000 dilution; Jackson Immuno Research Laboratories) were added to the respective wells as secondary antibodies. Detection was performed by measuring the absorbance at 405 nm with a

microplate reader (Thermo Fisher Scientific) after the addition of 1-Step™ PNPP substrate (Thermo Fisher Scientific).

Dot Blot

Dot blot analysis was performed as described Konto-Ghiorhi et al. (87) with slight modifications. In brief, bacteria were grown in TSB-G to an OD_{600} of 0.6, harvested and washed twice with tris-buffered saline (TBS). The nitrocellulose membrane was spotted with approximately 2.3 $x10^6$ CFUs or 2.3 $x10^5$ CFUs, and then blocked with 5% skim milk in TBS. EmpC was detected with the goat anti-EmpC polyclonal antibodies (1:2,500 dilution of 1mg/ml), followed by incubation with peroxidase mouse anti-goat IgG (H+L) (1:20,000 dilution; Jackson Immuno Research Laboratories). Detection was performed using the Super Signal West Pico Chemiluminescent Substrate (Thermo Fisher Scientific).

Biofilm formation assay

In vitro biofilm formation assay was performed as described in chapter 2 (96). In brief, *E. faecium* strains were grown overnight at 37°C in TSB-G broth and then diluted in the same media to an OD_{600} of 0.1, before inoculation into polystyrene plates (BD). Bacteria were allowed to grow for 24 h under static incubation at 37°C. The plates were gently washed three times with PBS, followed by treatment with Bouin's fixative (Sigma-Aldrich). After removing the fixative, the bacterial cells were washed with PBS and stained with 1% crystal violet solution (Sigma-Aldrich). Ethanol:acetone (80:20) was used to solubilize the dye and a microplate reader (Thermo Fisher Scientific) was used to measure the absorbance at 570 nm.

ECM binding assay

Adherence to immobilized fibrinogen and collagen type I was assayed using a crystal violet based staining method as described previously (97) with the some modifications. In brief, Immulon HBX 4 plate wells (Thermo Fisher Scientific) were coated overnight with 10 µg/ml of the ECM proteins, followed by blocking unbound sites with 2% BSA in PBS for 1 h at RT. The *E. faecium* strains grown for 16 h at 37°C in BHI were collected by centrifugation, washed twice with PBS and resuspended in 1% BSA in PBS to an OD_{600} of 1.0. Bacteria were allowed to bind at 37°C for 2 h to the ECM coated wells, followed by two washes with PBS to remove unbound cells. Detection of the adherent cells was performed as described above for the biofilm formation assay.

Mouse UTI model

E. faecium TX82, its *emp* deletion derivatives and the *empA* reconstituted strain, were grown for 24 h in BHI broth, harvested and resuspended to equal OD_{600} in 0.9% saline solution. The bacterial suspensions, estimated to contain 10^8 CFUs, were diluted 1:10 and mixed together in an approx. 1:1 ratio (TX82 with each deletion mutant and Δ*empA*::*empA* with Δ*empA*). In addition, serial dilution of the inoculum were made in 0.9% saline and plated to determine the actual CFUs. Six week-old female ICR mice were inoculated via intraurethral catheterization with the mixed bacterial suspension (approx. 10^6 CFU of each strain) and 48 h after infection, animals were euthanized and CFU counts were determined from kidneys and bladders by plating tissue homogenates onto Enterococcosel agar (BD) with vancomycin (6 µg/ml), as previously described (36). All colonies that grew (up to 47 CFU/organ) were picked into the wells of microtiter plates containing BHI broth + 15% glycerol, grown overnight and then replica plated onto Hybond™ -N+ membranes placed on BHI agar. After overnight growth on the membranes, colonies were lysated to perform high stringency hybridization (98), using

intragenic DNA probes of *ddl* and the corresponding *emp* gene. Hybridization results were used to generate the percentage of each strain recovered from the organs.

Rat infective endocarditis model

Aortic valve endocarditis was induced in male Sprague-Dawley rats by placement of a catheter across the valve, according to our previously published method (94). Twenty-four hours after catheter placement, TX82 or the Δ*empA* deletion mutant (TX6138) grown 24 h at 37°C in BHI broth and resuspended in saline, were inoculated (*i.v.* via tail vein) into 16 rats. In addition, the inoculum was plated onto BHI agar to determine the actual CFU inoculated into the rats. Animals were euthanized 48 h after bacterial inoculation and hearts were ascetically removed. Establishment of bacterial endocarditis was confirmed at autopsy by evidence of vegetations formed around aortic valves and correct placement of the catheter across the valve. Vegetations together with the aortic valve were excised, weighed and homogenized in 1 ml saline. The homogenized tissue was plated on Enterococcosel agar (BD) with 6 μg/ml of vancomycin and colonies were counted after 48 h incubation at 37°C to determine the CFU per gram of vegetation. All the animal experiments described in this study were performed according to protocols used previously in our laboratory (36, 47, 94, 99), and following pre-approved protocol and guidelines by the Animal Welfare Committee of the University of Texas Health Science Center at Houston.

Statistical analyses

GraphPad Prism version 4.00 (GraphPad Sofware) was used for statistical analyses. Unpaired t-test was used to evaluate differences between the strains in the WC ELISA and biofilm formation assays. Analysis of variance (ANOVA) with Bonferroni's multiple comparison post-test was used to compare the results from the

adherence assays. Differences in the length of pilus fibers produced by TX82 and the Δ*empA* were analyzed using unpaired t-test. Paired t-test was used to compare the percentage of bacteria recovered in kidneys and bladders versus the percentage of bacteria inoculated into the mice, while the Mann-Whitney test was used to analyze differences in the $\log_{10}$ CFU of TX82 versus the Δ*empA* deletion mutant recovered from vegetations.

3.3. RESULTS AND DISCUSSION

E. faecium has rapidly emerged as a very important cause of hospital-associated infections (7). Different surface proteins, including pili, have been implicated in enterococcal pathogenesis (5, 100). The *empABC* operon is a three-gene locus (Figure 3.1) that encodes a prototypical pilus structure that consists of a backbone pilin subunit, EmpC, and two minor accessory pilins, EmpA and EmpB (43, 47). In a previous study, we found that allelic replacement of the empABC operon from the endocarditis-derived isolate, TX82, led to significant attenuation in biofilm formation and in a mouse model of UTI (47); however, the role of the individual Emp pilus subunits to pilus-related functions has not yet been explored. Here, we sought to investigate the contribution of EmpA, EmpB and EmpC to pilus architecture, biofilm formation and adherence to components of the ECM and to the ability of E. faecium to cause infection. To address the function of each Emp pilus subunit, we individually deleted each gene of the emp operon from the endocarditis-derived E. faecium isolate TX82 (Δ*empA*, TX6138; Δ*empB*, TX6139; Δ*empC*, TX6154) (Figure 3.1 & Table 3-1). Deletions were designed to be unmarked and non-polar to avoid affecting the remaining pilin genes or the downstream gene, *bps*, that codes for a class C sortase. We also reconstituted in situ the *empA* gene into the chromosome of the Δ*empA* deletion strain (TX6138) to generate strain TX6152 (Figure 3.1 & Table 3-1). Equivalent growth kinetics measured by OD600 (Figure 3.2) and comparable CFUs (data not shown) at all the time points tested were observed between the panel of deletion mutants, the *empA* reconstituted strain and the parental strain.

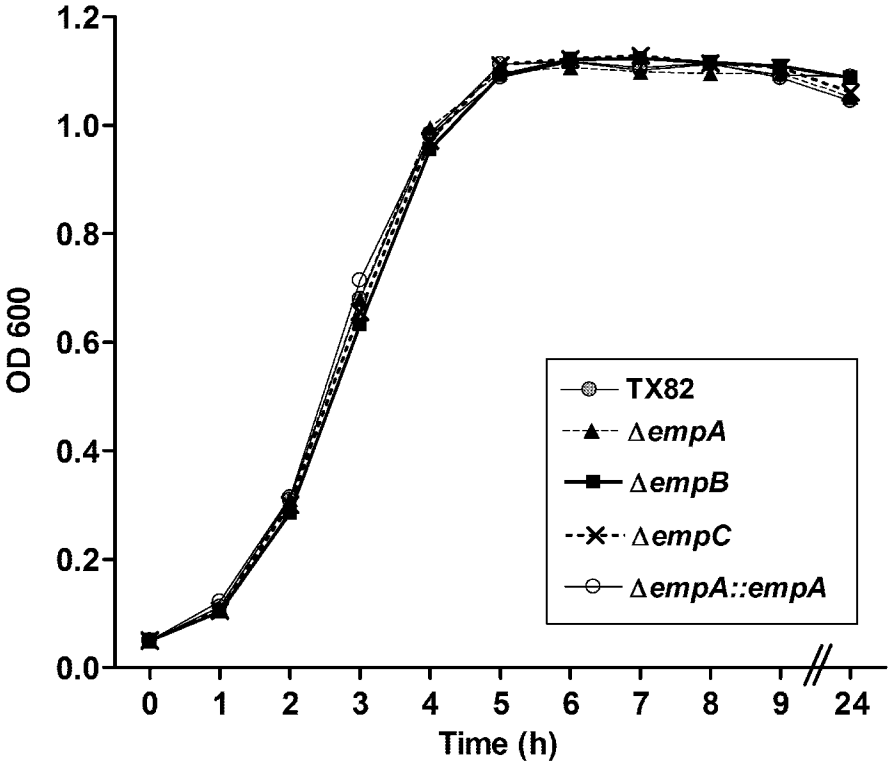

Figure 3.2. Growth curve of *E. faecium*, its isogenic *emp* deletion derivatives and the *empA* reconstituted strain.

Strains were grown in BHI from an initial OD_{600} of 0.05 and samples were taken at indicated time points for OD_{600} measurements.

EmpA localizes at the tip of the fiber while EmpC is distributed along the length of the pilus shaft

We analyzed pilus architecture in TX82 and its deletion derivatives by immunoelectron microscopy using antibodies generated against rEmpA and rEmpC proteins (EmpB localization was not studied since our previous study showed that the homolog of this subunit in *E. faecalis,* EbpB*,* was barely detectable by microscopy or WC ELISA (32)). EmpA is a VWA domain-containing protein predicted to be the tip pilin. As observed in Figure 3.3-A & Figure 3.3-C, EmpA localized at the tip of pilus-like structures; however, it was also abundantly seen on the surface, apparently not forming part of pilus polymers, on TX82 cells (Figure 3.3-A). In agreement with previous studies (42, 43, 47), our microscopy results confirmed EmpC as the major pilin, forming the backbone of the Emp pili (Figure 3.3-B, -C, -E & -G). As expected, the anti-EmpA antibody did not stain the Δ*empA* deletion strain (Figure 3.3-D). In contrast, in the Δ*empB* deletion strain, EmpA was observed on the bacterial surface and as the tip of pilus polymers (Figure 3.3-F), while in the Δ*empC* deletion strain, EmpA was only seen on the bacterial surface (not forming part of pilus polymers) (Figure 3.3-H). Importantly, deletion of *empA* or *empB* did not abrogate pilus polymerization, as pilus-like structures were seen with the anti-EmpC antibody on the Δ*empA* and Δ*empB* strains (Figure 3.3-E & -G); as expected, the anti-EmpC antibody did not stain the Δ*empC* deletion strain (Figure 3.3-I).

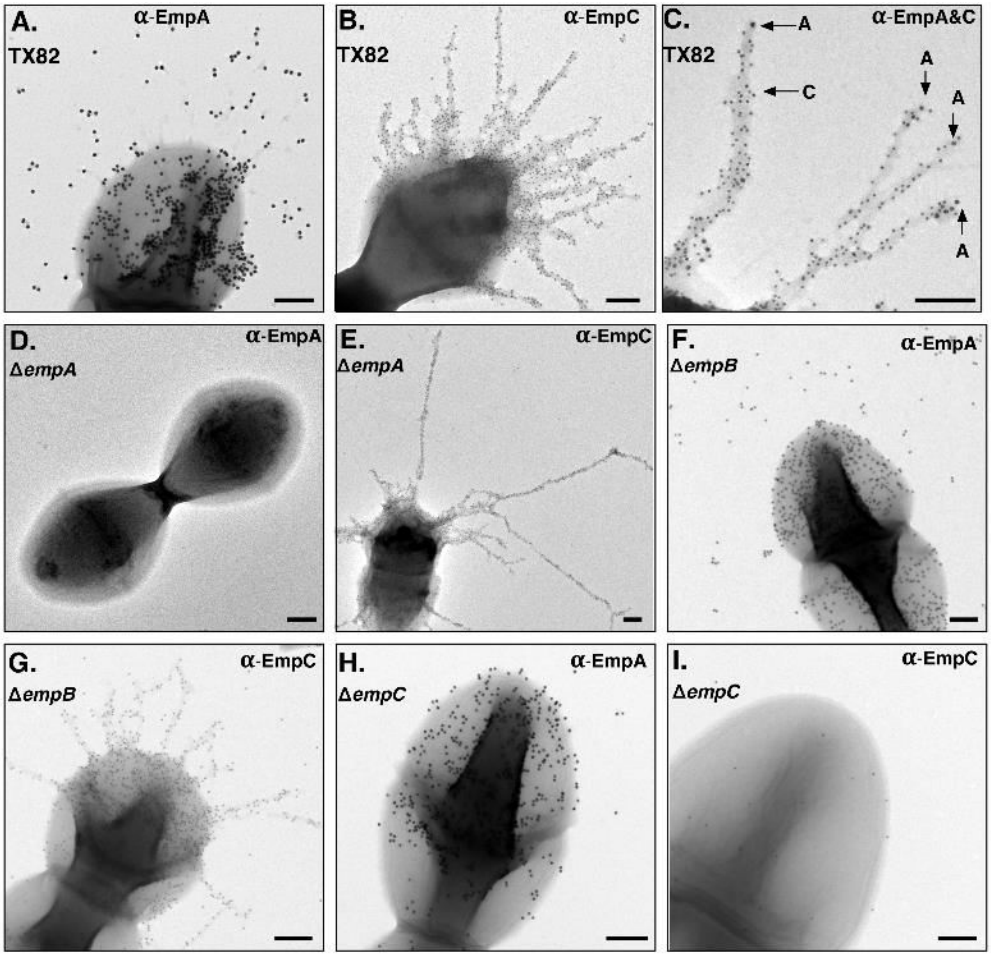

Figure 3.3. Immunoelectron microscopy analysis of pilus architecture in *E. faecium* TX82 and its deletion derivatives.

Cells were grown to mid-log phase in TSB-G and stained with anti-EmpA and/or anti-EmpC antibodies. **(A)** TX82 stained with anti-EmpA (18 nm); **(B)** TX82 stained with anti-EmpC (12 nm); **(C)** TX82 stained with anti-EmpA (18 nm) and anti-EmpC (12 nm); **(D)** Δ*empA* stained with anti-EmpA (18 nm); **(E)** Δ*empA* stained with anti-EmpC (12 nm); **(F)** Δ*empB* stained with anti-EmpA (18 nm); **(G)** Δ*empB* stained with anti-EmpC (12 nm); **(H)** Δ*empC* stained with anti-EmpA (18 nm); **(I)** Δ*empC* stained with anti-EmpC (12 nm). Scale bars indicate a length of 0.2 μm. *Dr. Chungyu Chang performed the majority of IEM.*

EmpA is important for wild-type length of the pilus fiber

Our electron microscopy experiments also provided evidence that the tip subunit, EmpA, is important for determining wild-type length of the pilus fiber. We measured the pilus lengths from 97 and 85 pilus fibers from TX82 and the Δ*empA* deletion strain, respectively, and found that deletion of the *empA* gene caused a significant increase in the length of the pilus fibers (Figure 3.3-E) compared to TX82 cells (Figure 3.3-B). The average length of pili produced by the Δ*empA* deletion strain was 1.22 ± 0.76 μm (mean ± standard deviation) versus 0.69 ± 0.38 μm by TX82 (median for Δ*empA*, 1.03 μm and for TX82, 0.69 μm, $p < 0.0001$; Figure 3.4). This is opposite to the shorter pilus fibers observed in *Actinomyces oris* when the tip subunit, *fimQ*, was deleted (101). In addition, we observed that deletion of *empA* caused a reduction in the number of pili per bacterial cell, which is in accordance with previous findings (101). In *S. agalactiae*, deletion of pilA, the first gene of the operon encoding the pilin adhesin, was associated with longer pilus fibers due to increase transcription of the downstream gene, *pilB*, encoding the shaft (87, 102). We observed only a slight increase in *empC* mRNA levels in the *empA* and *empB* deletion strains, compared to TX82, which suggests that increased expression of *empC* in the Δ*empA* deletion strain is probably not the sole cause of increased length of the pilus fibers in *E. faecium* (Figure 3.5). In contrast, in other Gram-positive organisms, the levels of the shaft subunit have been implicated in the regulation of pilus length (103). While the underlying mechanism for the tip subunit's control of pilus length remains to be determined, this result suggests important differences in the regulation of pilus assembly between enterococci and other Gram-positive bacteria.

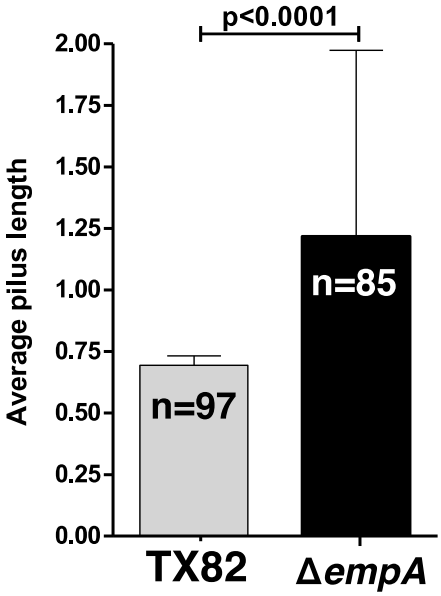

Figure 3.4. Effect of *empA* deletion on pilus fiber length.

Average pilus length (mean ± standard deviation) from 97 and 85 pilus fibers from TX82 and the Δ*empA* deletion strain, respectively. Statistical analysis was performed using the unpaired t-test.

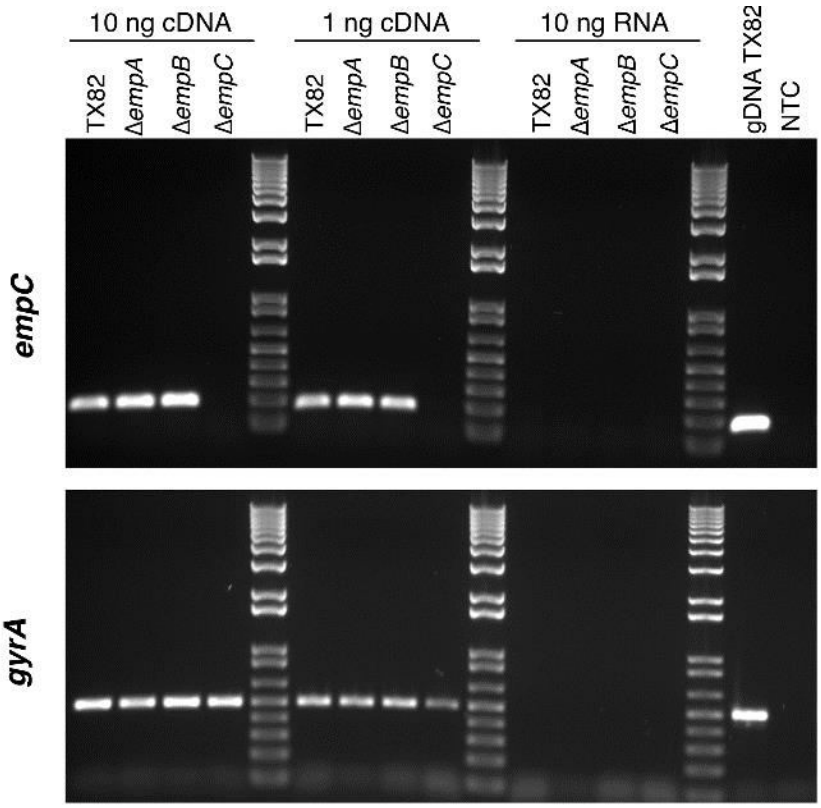

Figure 3.5. Expression of *empC* measured by reverse transcriptase (RT)-PCR.

PCR amplification of *empC* (gel on top) and *gyrA* (gel on bottom; internal control) using 10 ng of cDNA, 1 ng of cDNA or 10 ng of RNA of TX82 and the panel of *emp* deletion strains. Genomic DNA (gDNA) of TX82 and no template control (NTC) were used as controls of the PCR reaction.

Surface display of EmpA and EmpC by TX82, its isogeneic *emp* deletion mutant derivatives and the *empA* reconstituted strain

We next investigated surface display of EmpA and EmpC by the single *emp* deletion mutants and the *empA* reconstituted strain in comparison to the parental strain, TX82, and the previously generated *empABC* operon deletion with *cat* gene allelic replacement (Δ*empABC::cat)* (47). WC ELISA, using our anti-EmpA antisera, revealed that this subunit is abundantly present on the surface of TX82 at mid-exponential phase (Figure 3.6-A). EmpC pilin was also displayed profusely on the surface of TX82 (Figure 3.6-B), as previously demonstrated (47). Consistent with our earlier report (47), we did not detect EmpA or EmpC on the surface of the strain in which the *emp* operon was replaced with *cat* (Δ*empABC::cat*) (Figure 3.6-A & -B). In addition, and as anticipated, the Δ*empA* and Δ*empC* deletion strains did not express EmpA or EmpC on the surface, respectively (Figure 3.6). By WC ELISA we observed that deletion of *empC* and, to a minor extent, deletion of *empB* caused a significant reduction in EmpA surface display versus TX82 cells ($p < 0.0001$ and $p = 0.0070$, respectively; Figure 3.6-A). In addition, EmpC levels on the surface of the Δ*empA* deletion strain were significantly diminished ($p < 0.0001$), while deletion of the *empB* gene did not affect surface display of the shaft pilin subunit ($p = 0.8404$; Figure 3.6-B). No significant differences in EmpA and EmpC levels between TX82 and the *empA* reconstituted strain were observed, indicating restoration of pilin protein levels on the surface of the reconstituted strain ($p = 0.7275$ and $p = 0.4409$, respectively; Figure 3.6).

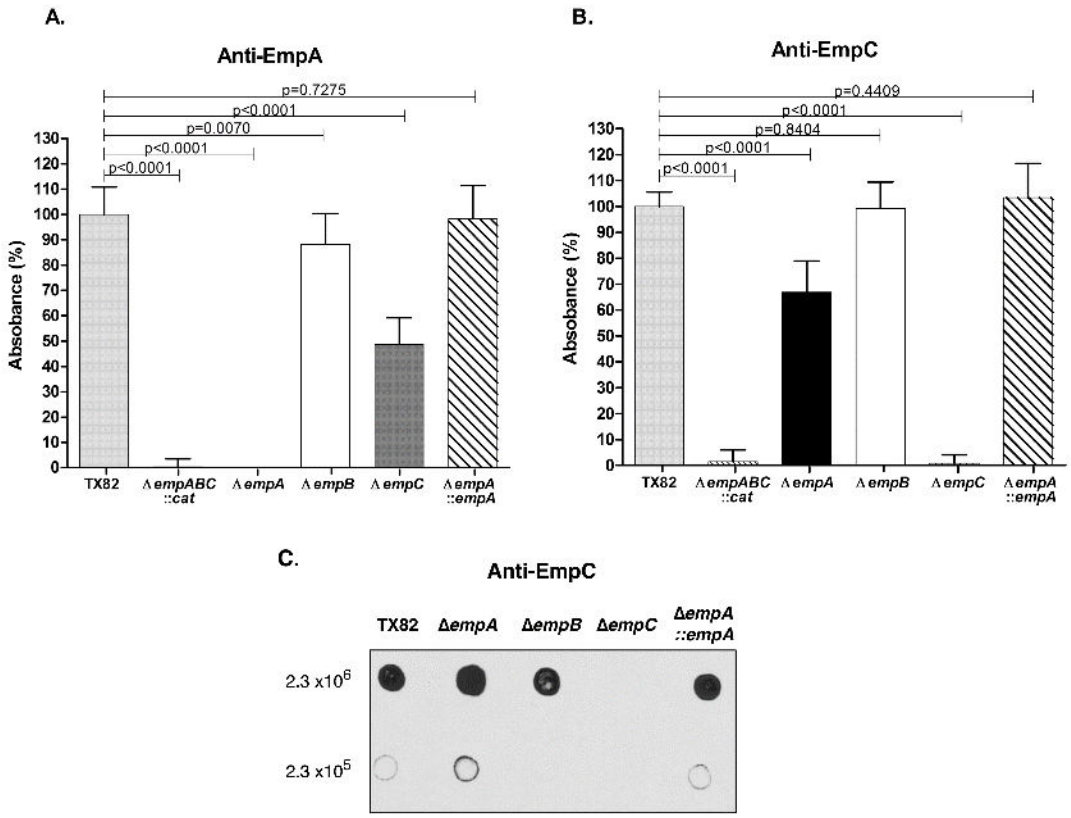

Figure 3.6. Surface display of EmpA and EmpC by *E. faecium* TX82, its deletion derivatives and the *empA* reconstituted strain.

Surface display of **(A)** EmpA and **(B)** EmpC detected by WC ELISA using polyclonal antibodies against EmpA and EmpC, respectively. Bars represent the mean ± standard deviation of the percentage of absorbance measured at 405 nm of each strain compared to TX82, from at least two independent experiments representing 10 wells per strain. Differences between TX82 and its derivatives were analyzed using t-test; p values are indicated in the figure. **(C)** Dot blot on whole bacteria (approximately 2.3 x10^6 CFUs or 2.3 x10^5 CFUs of TX82 and its derivatives) using polyclonal antibodies against EmpC.

Since pili were shown to be longer in the Δ*empA* deletion strain, as compared to TX82, which is inconsistent with the reduced levels of EmpC seen on this strain by WC ELISA (Figure 3.6-B), we further evaluate the levels of EmpC on whole bacteria by an immunodot assay. As observed in Figure 3.6-C, a slight increase in EmpC (not a decrease as seen on WC ELISA), consistent with a slight increase at the mRNA level (Figure 3.5), was observed in the Δ*empA* deletion mutant compared to TX82 and the *empA* reconstituted strain. It is possible that the longer pili on the Δ*empA* deletion strain are more fragile and detach from the bacterial surface during the processing by WC-ELISA. Furthermore, we observed a modest decrease in EmpC levels in the Δ*empB* deletion strain, probably due to release of pilus fibers, consistent with its role as pilus anchor (Figure 3.6; 32). These results, together with our electron microscopy studies, suggest that all the subunits of the pili are important for correct integrity of pilin fibers on the surface of *E. faecium* cells.

EmpA is the main component of Emp pili that mediates biofilm formation

In our previous study, we showed that allelic replacement of the *empABC* operon significantly affected biofilm, with a 75% reduction in biofilm formation in the Δ*empABC::cat* strain versus TX82 (47). Here, we investigated the contribution of each Emp pilus subunit to biofilm formation. As seen in Figure 3.7, deletion of *empA* reduced biofilm formation to the same extent as observed with the deletion of the operon, indicating that the tip subunit, EmpA, is the main component of the Emp pili mediating biofilm formation ($p < 0.0001$). In addition, when *empA* was reconstituted in situ, biofilm formation was restored ($p > 0.05$).

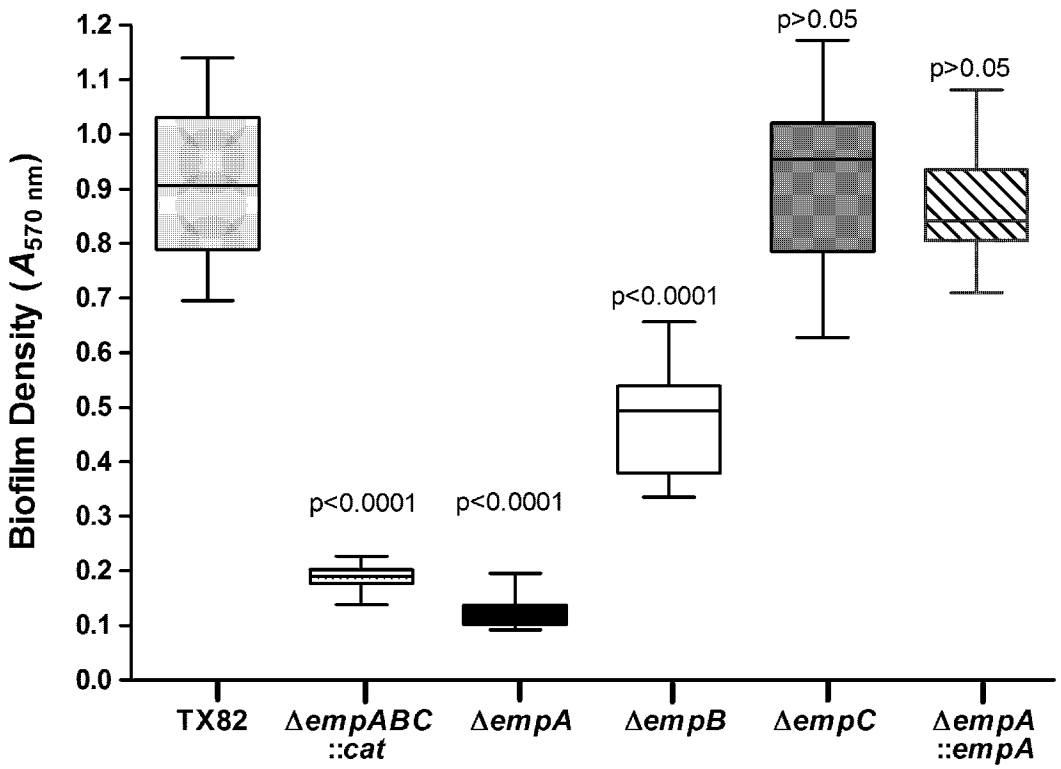

Figure 3.7. Contribution of each Emp pilin subunit to biofilm formation.

Cells grown 24 h in TSB-G were analyzed for biofilm formation using a crystal violet based assay. Median values measured at 570 nm, interquartile ranges and minimum and maximum values (whiskers) from three independent experiments representing 30 wells per strain are indicated. t-test was used to compare biofilm density values between TX82 and its derivatives; p values are indicated in the figure.

Surprisingly, we found the major backbone pilin, EmpC, to be dispensable for this process ($p > 0.05$), which is consistent with abundant EmpA seen in the surface of the Δ*empC* deletion strain (Figure 3.3-H); while deletion of *empB* led to a significant decrease in biofilm formation ($p < 0.0001$; Figure 3.7). These results indicate that EmpA and, to a lesser extent EmpB, play important roles in biofilm formation, even when the EmpC pili backbone is absent.

EmpA and EmpB are important for adherence to ECM proteins

Adherence to ECM proteins is proposed to be the first step in the infection process of *E. faecium* (104). Our group previously demonstrated, using a sensitive radioactive assay, that strain TX82 shows high levels of adherence to fibrinogen and collagen type I (104). Since pili in other Gram-positive organisms have been implicated in binding to ECM proteins (87, 88), including recent reports that demonstrated that EbpA of *E. faecalis* mediates adherence to host fibrinogen (69, 96), known to be exposed/released after trauma (69), our hypothesis was that Emp pili contributed to the adherence capacity of TX82. We investigated, by using a crystal violet based ECM binding assay, the involvement of each Emp pilus subunit to the adherence of *E. faecium* TX82 to fibrinogen and collagen type I. As observed in Figure 3.8, deletion of *empA* and *empB* significantly reduced fibrinogen ($p < 0.001$) and collagen I ($p < 0.05$ and $p < 0.01$, respectively) adherence compared to TX82, suggesting that these two subunits contribute to the adherence capacity of TX82. The *empA* reconstituted derivative showed almost wild-type levels of adherence ($p > 0.05$) and the Δ*empC* deletion strain showed no attenuation in binding; in fact, its fibrinogen binding ability was increased compared to TX82 ($p < 0.01$; Figure 3.8).

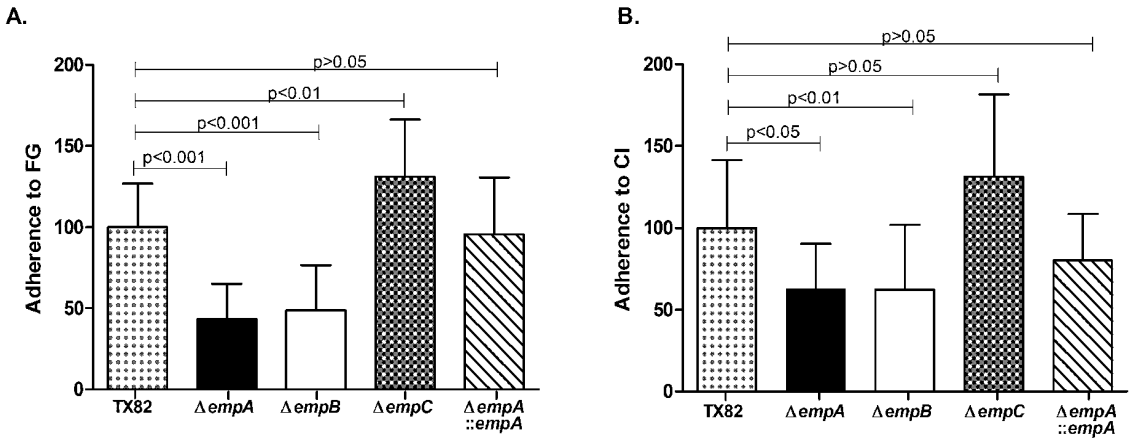

Figure 3.8. Contribution of each Emp pilin subunit to ECM adherence.

Adherence of *E. faecium* TX82, its *emp* deletion derivatives and the *empA* reconstituted strain to immobilized **(A)** fibrinogen and **(B)** collagen type I. Bars represent the mean ± standard deviation of the percentage of adherence of each strain compared to TX82 (defined as 100%) from four independent experiments representing 29 wells per strain. Statistical analysis was performed using ANOVA with Bonferroni's post-test; p values are indicated in the figure.

In other Gram-positive organisms, including *Corynebacterium diphtheriae,* deletion of the gene encoding shaft subunit, also did not affect the adherence phenotype, although pilus assembly was abolished (105). The fact that deletion of *empC* showed an increase in binding is intriguing; one possibility is that, in the absence of EmpC, other cell wall-associated proteins, including EmpA, could have a closer or tighter interaction with components of the ECM.

The three pilin subunits encoded by the *emp* operon are important in a mouse model of UTI

In order to elucidate the role of the individual Emp pilin subunits in infection, we evaluated each of the deletion strains in a mouse model of UTI. We found that, after 48 hours of infection, each of the deletion mutants were significantly attenuated in kidneys ($p = 0.028 – p = 0.048$) and in bladders ($p < 0.0001 – p = 0.0124$) versus TX82 (Figure 3.9-A, -B & -C). These results indicate that EmpA, EmpB and EmpC are all require for full virulence of *E. faecium* TX82 in the UTI model. It is worth mentioning that, even though the *empC* deletion strain showed no attenuation in our in vitro assays (biofilm (Figure 3.7) and ECM adherence (Figure 3.8)), our in vivo model results demonstrated the importance of this subunit in the virulence of *E. faecium* (Figure 3.9-C). We also evaluated the *empA* reconstituted strain (Δ*empA::empA*) versus the Δ*empA* deletion mutant and found significantly higher percentage of the reconstituted strain, in kidneys ($p = 0.0153$) and bladders ($p < 0.0008$), compared to the *empA* deletion strain (Figure 3.9-D), confirming the involvement of EmpA to *E. faecium* pathogenesis in UTI.

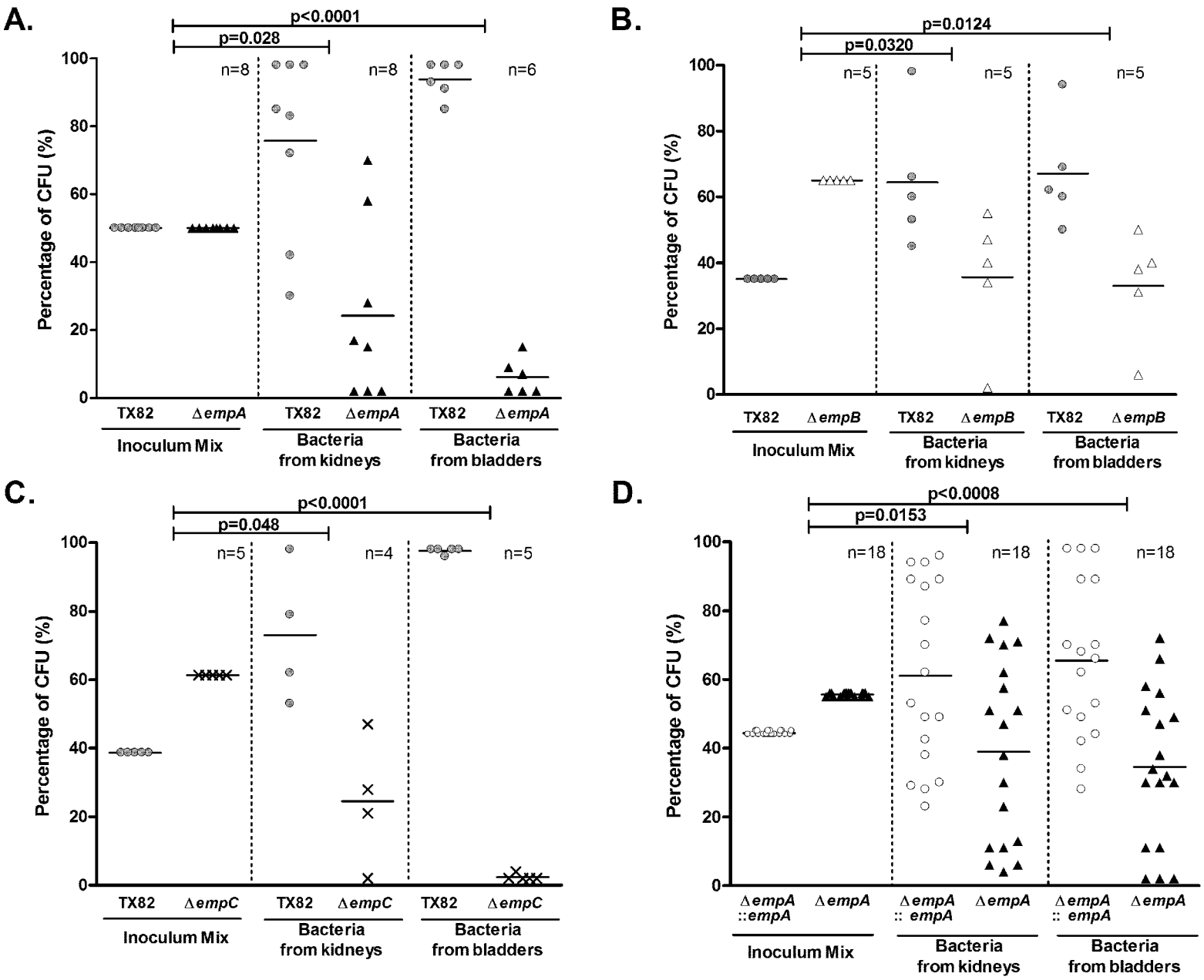
A.
p<0.0001
p=0.028
n=8
n=8
n=6
Percentage of CFU (%)
100
80
60
40
20
0
TX82
ΔempA
TX82
ΔempA
TX82
ΔempA
Inoculum Mix
Bacteria from kidneys
Bacteria from bladders
B.
p=0.0124
p=0.0320
n=5
n=5
n=5
Percentage of CFU (%)
TX82
ΔempB
TX82
ΔempB
TX82
ΔempB
Inoculum Mix
Bacteria from kidneys
Bacteria from bladders
C.
p<0.0001
p=0.048
n=5
n=4
n=5
Percentage of CFU (%)
TX82
ΔempC
TX82
ΔempC
TX82
ΔempC
Inoculum Mix
Bacteria from kidneys
Bacteria from bladders
D.
p<0.0008
p=0.0153
n=18
n=18
n=18
Percentage of CFU (%)
ΔempA ::empA
ΔempA
ΔempA :: empA
ΔempA
ΔempA :: empA
ΔempA
Inoculum Mix
Bacteria from kidneys
Bacteria from bladders

Figure 3.9. Attenuation of *empA*, *empB* and *empC* deletion mutants in a mouse UTI model, using a mixed inoculum.

Mice were infected with a mixed bacterial suspension of TX82 and the **(A)** Δ*empA* deletion strain, **(B)** Δ*empB* deletion strain and **(C)** Δ*empC* deletion strain or **(D)** the *empA* reconstituted strain (Δ*empA::empA)* and Δ*empA* deletion strain. Horizontal lines represent the mean of percentage of total bacteria inoculated into each mouse and recovered 48 h after infection in kidneys and bladders. In some instances no bacteria were recovered (two in panel A (bladder) and one in panel C (kidney)). Results were analyzed using a paired t-test; p values are indicated in the figure.

Importance of EmpA in an endocarditis model

EmpA has a VWA with a MIDAS motif. Given the demonstrated role of tip pilin proteins containing VWA domains in cell adhesion and pathogenesis (37, 86-88) and our result that implicated EmpA in biofilm formation, ECM adherence and UTI, our hypothesis was that this subunit plays an important role in endovascular infection. As shown in Figure 3.10, we found that after monoinoculation of TX82 and the Δ*empA* deletion mutant in a rat endocarditis model, the $\log_{10}$ CFUs of bacteria recovered from the vegetations were significantly lower in the rats inoculated with the *empA* deletion strain compared to TX82 ($p = 0.0088$; Figure 3.10), suggesting that EmpA is also important in the pathogenesis of endocarditis.

Considering that the *empABC* operon is found in the majority of isolates of clinical origin (96 to 100%, depending on the clinical source), but is also frequently found in nonclinical isolates (73 and 77 % of fecal and animal isolates harbor the *emp* operon, respectively) (90), Emp pili represent an excellent target for vaccine development. In addition, success in preventing endocarditis infection by a monoclonal antibody that targets the Ebp pili of *E. faecalis* has been demonstrated (70). Furthermore, it was recently shown that immunization with EbpA, the counterpart of EmpA in *E. faecalis*, provides protection against catheter-associated bladder infection in mice (69). Our finding that EmpA is important for *E. faecium* biofilm formation, ECM adherence and infection suggests that this pilin subunit could be a potential target for the development of alternative therapeutic approaches to counteract this multidrug resistant pathogen.

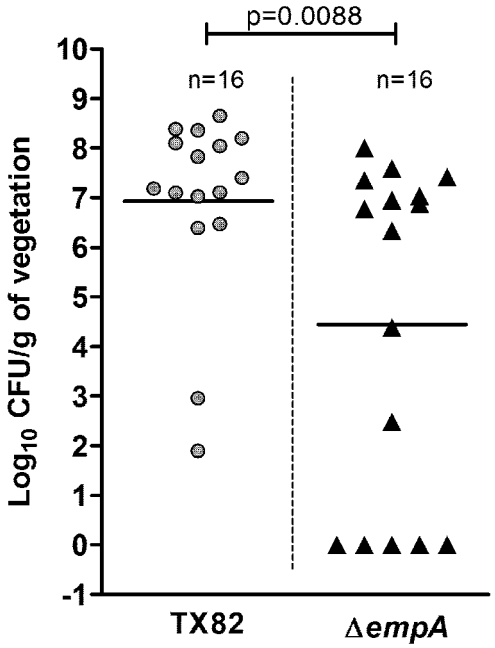

Figure 3.10. Effect of *empA* deletion in a rat model of infective endocarditis.

Monoinfection experiment using 10^9 CFU inocula of TX82 or the Δ*empA* deletion strain. Data are expressed as $\log_{10}$ CFUs/g of bacteria recovered 48 h after infection from vegetations (horizontal lines represent the geometric mean CFU/g). Results were analyzed using the Mann-Whitney test; p value is indicated in the figure.

CHAPTER 4. Gastrointestinal Tract Colonization Dynamics by Different *Enterococcus faecium* Clades

*This chapter is based upon work published in The Journal of Infectious Diseases with the same title as the one of this chapter (J Infect Dis. 2015). I am co-first author of this publication (**Montealegre MC**, Singh KV, Murray BE) and I was responsible for preparing the original manuscript, conducted the in vitro competition experiments and participated in the in vivo experiments described; the in-vivo experiments were conducted by Dr. Singh, co-first author of this publication. A special acknowledgement to Karen Jacques-Palaz for her technical assistance. The right to include the article in full or in part in a thesis or dissertation, provided that this is not published commercially remains with the authors. For additional information visit http://www.oxfordjournals.org/en/help/faq/authors/online-licensing.html.*

4.1. INTRODUCTION

Different studies have demonstrated the existence of large differences in the accessory (51, 56, 59) and core genome (57, 59) between the *E. faecium* clades; however, very little is known about the factors that promote the predominance of subclade A1 strains in the hospital setting. Some have suggested that the transition of *E. faecium* from commensal to pathogen is a consequence of the enriched accessory genome of subclade A1 strains, including acquired antibiotic resistance determinants (106), genomic islands (56), and insertion sequences (55, 107). Putative virulence factors are also found to be enriched in subclade A1 strains (108); however, only a few of these have been experimentally proven to contribute to pathogenesis (109, 110).

GIT colonization with antibiotic-resistant enterococci generally precedes infection (15). In addition, it has been demonstrated that during hospitalization, ampicillin-resistant *E. faecium* strains rapidly replace ampicillin-susceptible, commensal *E. faecium* strains (22, 111). Interestingly, after a patient is discharged from the hospital, ampicillin-resistant *E. faecium* tend to wane (111). Although the replacement of commensal clade B strains by subclade A1 *E. faecium* in the hospital environment could be related to greater fitness, colonization capacity or virulence potential of subclade A1 strains, our hypothesis is that commensal clade B strains have a better ability to colonize the GIT than clade A isolates, which would explain the vast predominance of clade B in humans in the community and why antibiotic-resistant *E. faecium* strains are often replaced once patients leave the hospital.

In an attempt to better understand the dynamics of *E. faecium* colonization, we evaluated the ability of 12 *E. faecium* strains from clades A1, A2 and B to colonize the GIT of mice, individually as well as in competition with a strain of a different clade.

4.2. MATERIALS AND METHODS

Bacterial strains, routine growth conditions and general techniques

E. faecium used from subclades A1 and A2 and clade B and their relevant characteristics are listed in Table 4-1, including five strains that grouped genetically into subclade A1, three strains from subclade A2 and four strains from clade B. The strains were chosen to cover a spectrum of ampicillin MICs and to represent different sequence types (STs; Table 4-1). PFGE was performed as previously described (112), with some modifications, to confirm that the strains selected were not closely related (data not shown). Isolates were routinely grown at 37°C using BHI broth or agar (BD). Mueller Hinton II broth (cation adjusted; BD) was used for susceptibility testing while enterococcosel agar (EA; BD) was used to grow bacteria recovered from animals.

Susceptibility testing

MICs of ampicillin (Sigma-Aldrich), erythromycin (Sigma-Aldrich), gentamicin (Sigma-Aldrich), and vancomycin (Sigma-Aldrich) were determined by broth microdilution according to Clinical and Laboratory Standards Institute (CLSI) guidelines.

Murine GIT model

GIT colonization studies used six-week-old female ICR mice (Harlan Laboratories). Mice were prescreened for enterococci before and after decolonization (Figure 4.1) by plating dilutions of fecal pellets on EA, a selective medium for enterococci, with 8 µg/ml of nitrofurantoin (EA-NIT8). We used a decolonization regimen, with some modifications, that has been previously used to successfully establish enterococci in the GIT of mice (18, 113, 114).

Table 4-1. *E. faecium* strains used in chapter 4 and MICs of selected antimicrobial agents.

Clade	Strain Name	Source (isolation site)	Country of Isolation/ Year	ST[b]	MICs[a] (µg/ml)				Reference
					AMP	ERY	GEN	VAN	
A1	C68	Hospitalized patient (feces)	USA/1996	16	128	>256	>1024	128	(115)
	1.230.933	Hospitalized patient (blood)	USA/2005	18	128	>256	16	>256	(51)
	TX82	Endocarditis Patient (blood)	USA/1999	17	64	256	4	>256	(92)
	TX0133A	Endocarditis Patient (blood)	USA/2006	17	64	>256	16	>256	(116)
	TX16 (DO)	Endocarditis Patient (blood)	USA/1992	18	16	>256	16	0.5	(117)
A2	EnGen12	Hospitalized patient (ascites)	NLD/1995	27	0.5	>256	16	>256	(59)
	EnGen35	Hospitalized patient (gut)	NLD/1979	66	1	4	8	0.5	(59)
	EnGen21	Hospitalized patient (feces)	NLD/2002	5	8	>256	8	>256	(59)
B	Com15	Healthy volunteer (feces)	USA/2007	583	≤ 0.25	16	8	1	(51)
	TX1330	Healthy volunteer (feces)	USA/1994	107	1	0.25	8	1	(118)
	E980	Healthy volunteer (feces)	NLD/1998	94	≤ 2	32	8	0.5	(56)
	1.141.733	Hospitalized patient (wound)	USA/2005	327	2	16	16	1	(51)

[a.] AMP, ampicillin; ERY, erythromycin; GEN, gentamicin; VAN, vancomycin. [b.] Multi-locus sequence type.

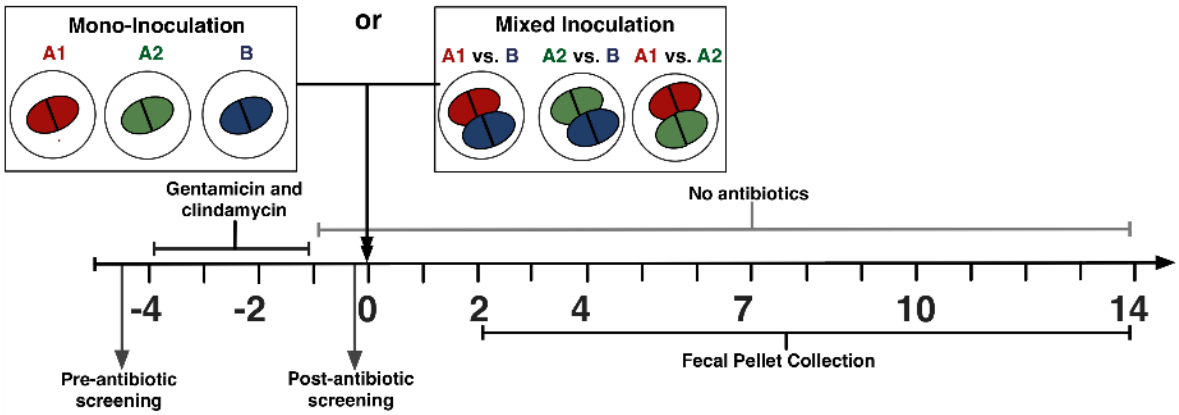

Figure 4.1. Schematic representation of the GIT colonization mouse model used in this study.

In brief, five to seven mice per strain in mono-inoculation and four mice per combination in the competitions assays were first decolonized for four days with 1 mg/ml of gentamicin (113) in drinking water plus subcutaneous injections of clindamycin (2.4 mg/day/mouse) (114). Antibiotics were stopped 24 h prior to gavage of bacteria, to allow elimination of drug (18) (Figure 4.1). Each strain was administered individually (for the mono-inoculation assays; Table 4-2) or in combination (for the competition assays) with a strain of a different clade (Table 4-3), in a suspension estimated by OD_{600} to contain approximately 10^7 to 10^9 CFUs; the actual number of CFUs was determined by plating serial dilutions of each inoculum made in 0.9% saline onto EA-NIT8 (all the *E. faecium* strains studied grew well on EA-NIT8; Table 4-2 & Table 4-3).

Fresh stool pellets, one per mouse obtained by gentle abdominal massage, were collected directly in sterile pre-weighted Eppendorf tubes on days 2, 4, 7 and 10 or 14 post-inoculation (Figure 4.1), weighted, serially diluted in 0.9% saline and plated EA-NIT8. After incubation for 48 h at 37°C, *E. faecium* colonies were initially counted based on colony appearance; to further confirm their identity, 12 random colonies in the mono-inoculation and 47 random colonies in the competition assays per animal and time point were picked and grown overnight in microtiter plates containing BHI broth plus 15% glycerol. The colonies were then replica plated onto Hybond™ -N+ membranes placed on BHI agar and, after overnight growth, bacteria were lysated for DNA hybridization under high-stringency conditions.

Table 4-2. Colony forming units (CFUs) in the inocula used in the in vivo mono-inoculation experiments and presence (+) and absence (-) of markers used to distinguish the isolated colonies.

Clade	Strain Name	Inoculum CFUs	NIT[a]	ERY[b]	VAN[c]	*ddl*$_{Efm}$	IS*16*	*acm*
A1	C68	2.3×10^9	+	+	+	+	+	+
	1,230,933	4×10^9	+	+	+	+	+	+
	TX82	1.4×10^8	+	+	+	+	+	+
	TX0133A	2×10^9	+	+	+	+	+	+
	TX16 (DO)	1.6×10^9	+	+	+	+	+	+
A2	EnGen12	5×10^7	+	+	+	+	-	-
	EnGen35	3.3×10^9	+	-	-	+	-	-
	EnGen21	5×10^8	+	+	+	+	-	+
B	Com15	2.5×10^9	+	-	-	+	-	+
	TX1330	2.2×10^9	+	-	-	+	-	+
	E980	2.05×10^9	+	-	-	+	-	+
	1,141,733	3.6×10^9	+	-	-	+	-	+

[a.] EA with 8 µg/ml of nitrofurantoin, [b.] EA with 256 µg/ml of erythromycin, [c.] EA with 128 µg/ml of vancomycin

Table 4-3. Strain pairs and CFUs in the inocula used in the mixed inoculation experiments and antibiotics and probes used to differentiate the strains.

	Strain Pairs (Inoculum CFUs/ml)		Used to differentiate the strains in the pairs (µg/ml)
A1 vs. B	**A1**	**B**	
1	C68 (4.3 x10^{9})	Com15 (2.95 x10^{9})	ERY (256), VAN (128), IS*16*
2	TX82 (5 x10^{7})	Com15 (5 x10^{7})	ERY (256), VAN (128), IS*16*
3	C68 (1.45 x10^{9})	TX1330 (2.3 x10^{9})	ERY (256), VAN (128), IS*16*
4	TX16 (2.95 x10^{9})	E980 (2.75 x10^{9})	ERY (256), VAN (128), IS*16*
A2 vs. B	**A2**	**B**	
5	EnGen12 (1.1 x10^{9})	TX1330 (2.3 x10^{9})	ERY (256), VAN (128), *acm*
6	EnGen35 (1.5 x10^{8})	Com15 (5 x10^{7})	*acm*
7	EnGen21 (2.95 x10^{9})	E980 (2.75 x10^{9})	ERY (256), VAN (128)
A1 vs. A2	**A1**	**A2**	
8	C68 (1.45 x10^{9})	EnGen12 (1.1 x10^{9})	IS*16*, *acm*
9	TX82 (1.5 x10^{8})	EnGen35 (5x10^{7})	ERY (256), VAN (128)
10	TX16 (2.95 x10^{9})	EnGen21 (2.95 x10^{9})	ERY (256), VAN (128)

Hybridization DNA probes for *ddl*$_{Efm}$, for species confirmation (119). IS*16* (107), present only in the subclade A1 strains and *acm* (120), absent from two A2 subclade isolates, were used for distinguishing the strains (Table 4-2 & Table 4-3). In addition, when antibiotic selection could be used (Table 4-1, Table 4-2 & Table 4-3), colonies were replica plated onto EA with 256 µg/ml of erythromycin and/or EA with 128 µg/ml of vancomycin. Results were used to calculate the number of CFUs/g (for the mono-inoculation assays) and percentages of bacteria recovered (for the competition assays) from fecal pellets. PFGE was performed using random colonies from each experiment to confirm the strain identity (data not shown).

Growth curves and in vitro competition assays

To assess growth characteristics**,** bacteria from overnight cultures were inoculated at an initial OD_{600} of 0.05 and grown for 24 h at 37°C with gentle shaking. OD_{600} readings were taken every hour from 0 to 8 hours, with a final reading at 24 hours. In addition, aliquots were removed at 0, 2, 4, 8 and 24 hours for CFU determination on BHI agar (47). For the in vitro competition studies, we performed three independent replicates with three different strain pairs (two pairs A1 versus B and 1 pair involving A2 versus B). In brief, the strains grown individually overnight were inoculated at an approximately 1:1 ratio into 10 ml of BHI broth and grown for 24 hours at 37°C with gentle shaking. At time 0, 4 and 24 hours, samples were collected and serial dilutions as described above were plated onto BHI agar. To distinguish and obtain the percentage of each strain, at least 47 colonies per time point were randomly selected and plated onto BHI and antibiotic selective plates (vancomycin 128 µg/ml and erythromycin 256 µg/ml) or hybridized with the *acm* probe, as described above for the in vivo competition (Table 4-3).

Statistical Analysis

Statistical analyses were performed using GraphPad Prism version 4.00 (GraphPad Sofware). Differences in the geometric mean $\log_{10}$ CFUs/g from the mono-inoculation assays were evaluated using an unpaired t-test. Paired t-test was used to analyze the data from the in vitro and in vivo competition experiments, comparing the percentages of each strain recovered at different time points versus the percentages in the inoculum.

4.3. RESULTS

Representatives of *E. faecium* clades colonize the GIT of mice at similar levels after mono-inoculation

We studied 12 *E. faecium* strains, of which five grouped genetically into subclade A1, three were from subclade A2 (59), and four from clade B (Table 4-1); for clarity, the clade or subclade designation is at times written as a subscript. Compared with the clade B strains, the clade A strains generally showed higher MICs; of note, MICs ≥ 128 µg/ml of erythromycin and vancomycin were only observed within clade A (Table 4-1). We first evaluated the effectiveness of antibiotic pre-treatment, previously used to facilitate colonization of enterococci by reducing the endogenous flora (18, 113, 114); as shown in Figure 4.2, this treatment was effective in reducing the load of bacteria. To assess clade-related differences in colonization capacity of the *E. faecium* strains, we next evaluated the ability of the 12 strains to colonize the GITs of mice after mono-inoculation. The geometric mean $\log_{10}$ CFUs/g for each strain recovered from the fecal pellets are shown in Figure 4.3 (see also Figure 4.4 for detailed results). The greatest number of CFUs/g were observed at day 2, with most strains recovered in the range of 10^8 to 10^9 CFUs/g, except TX82$_{A1}$ (4.91×10^7 CFUs/g) and TX0133A$_{A1}$ (1.51×10^7 CFUs/g). As time progressed, the number of enterococcal CFUs found in the fecal pellets decreased, although the majority of strains were still present in high levels at day 4 (between 10^7 to 10^9 CFUs/g), and counts of only TX0133A$_{A1}$, TX1330$_B$ and E980$_B$ were below this range. At day 7, some strains were still present at high levels, including C68$_{A1}$, 1.230.933$_{A1}$ and TX16$_{A1}$, EnGen12$_{A2}$ and Com15$_B$ (range, 10^7 to 10^8 CFUs/g), while the others were recovered at lower levels (range, 10^3-10^6 CFUs/g).

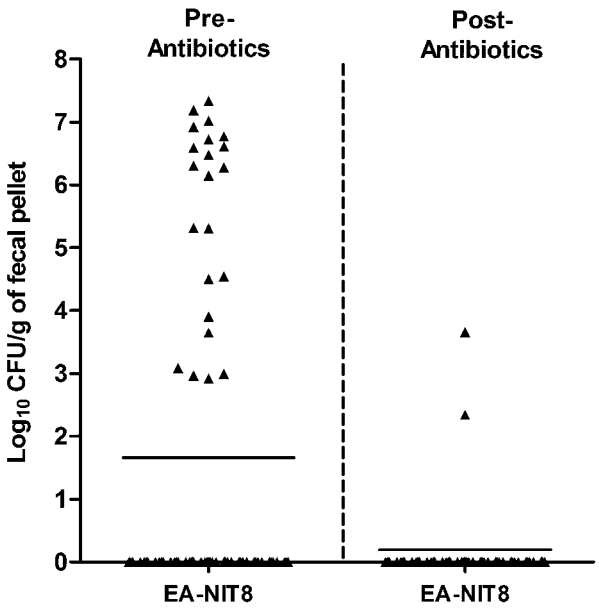

Figure 4.2. Recovery of bacteria pre- and post-decolonization antibiotics.

Log_{10} CFUs/g recovered from fecal pellets pre- and post-antibiotic decolonization treatment on EA-NIT8. Each symbol represents the log_{10} CFUs/g recovered from each of the 72 mice used in the mono-inoculation assays. The horizontal lines indicate the geometric mean log_{10} CFUs/g.

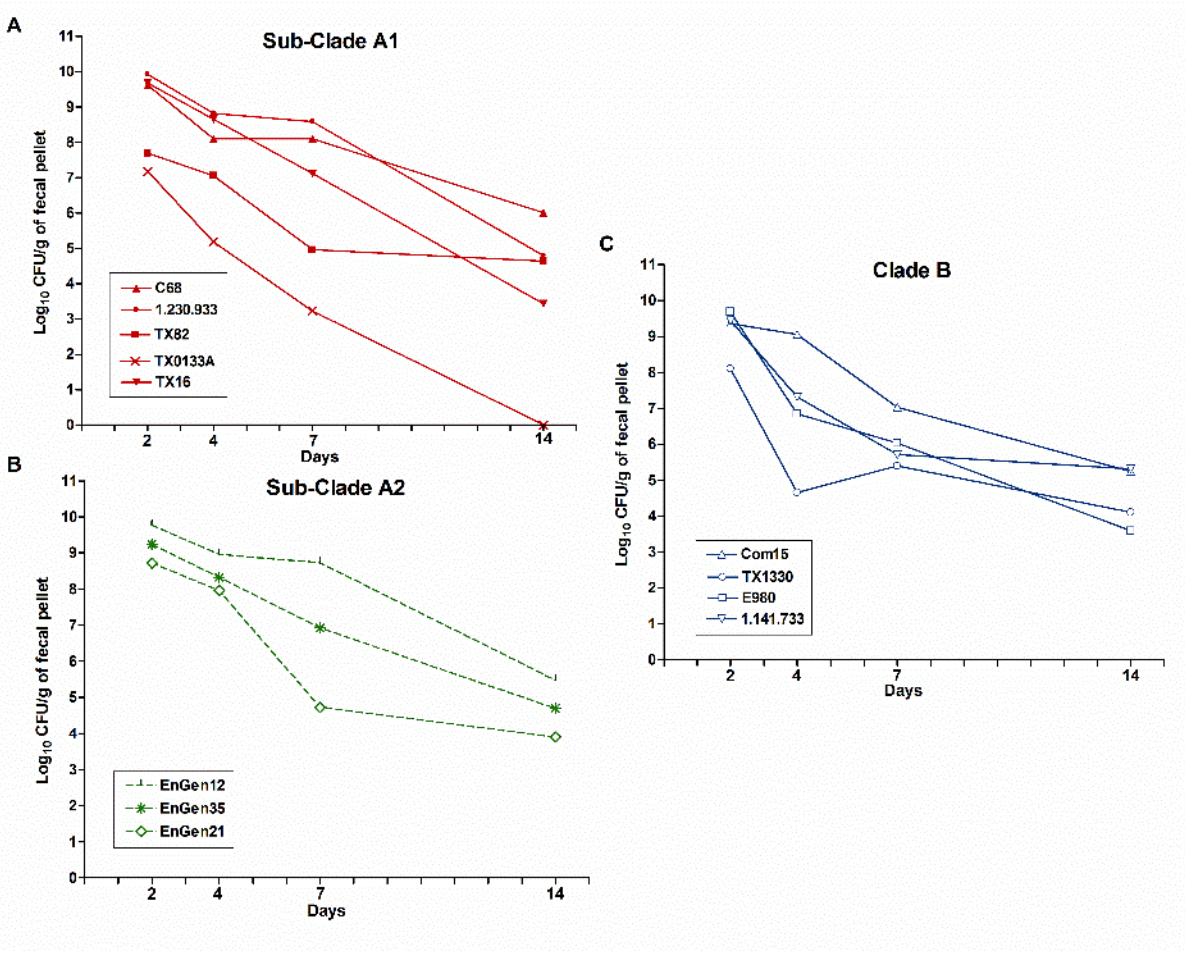

Figure 4.3. GIT colonization by the 12 *E. faecium* strains after mono-inoculation.

Geometric mean $\log_{10}$ CFUs/g of each strain recovered from fecal pellets on days 2 to 14 on EA with 8 µg/ml nitrofurantoin (EA-NIT8) after orogastric administration of **(A)** subclade A1 strains (1.4 x 10^8 – 4 x 10^9 CFU), **(B)** subclade A2 strains (5 x 10^7 – 3.3 x 10^9 CFU) and **(C)** clade B strains (2.05 x 10^9 – 3.6 x 10^9 CFU) (see Table 4-2 for the inoculum counts of each strain). Each symbol represents the geometric mean CFUs/g recovered from fecal pellets of five to seven mice per strain (see Figure 4.4 for detailed results).

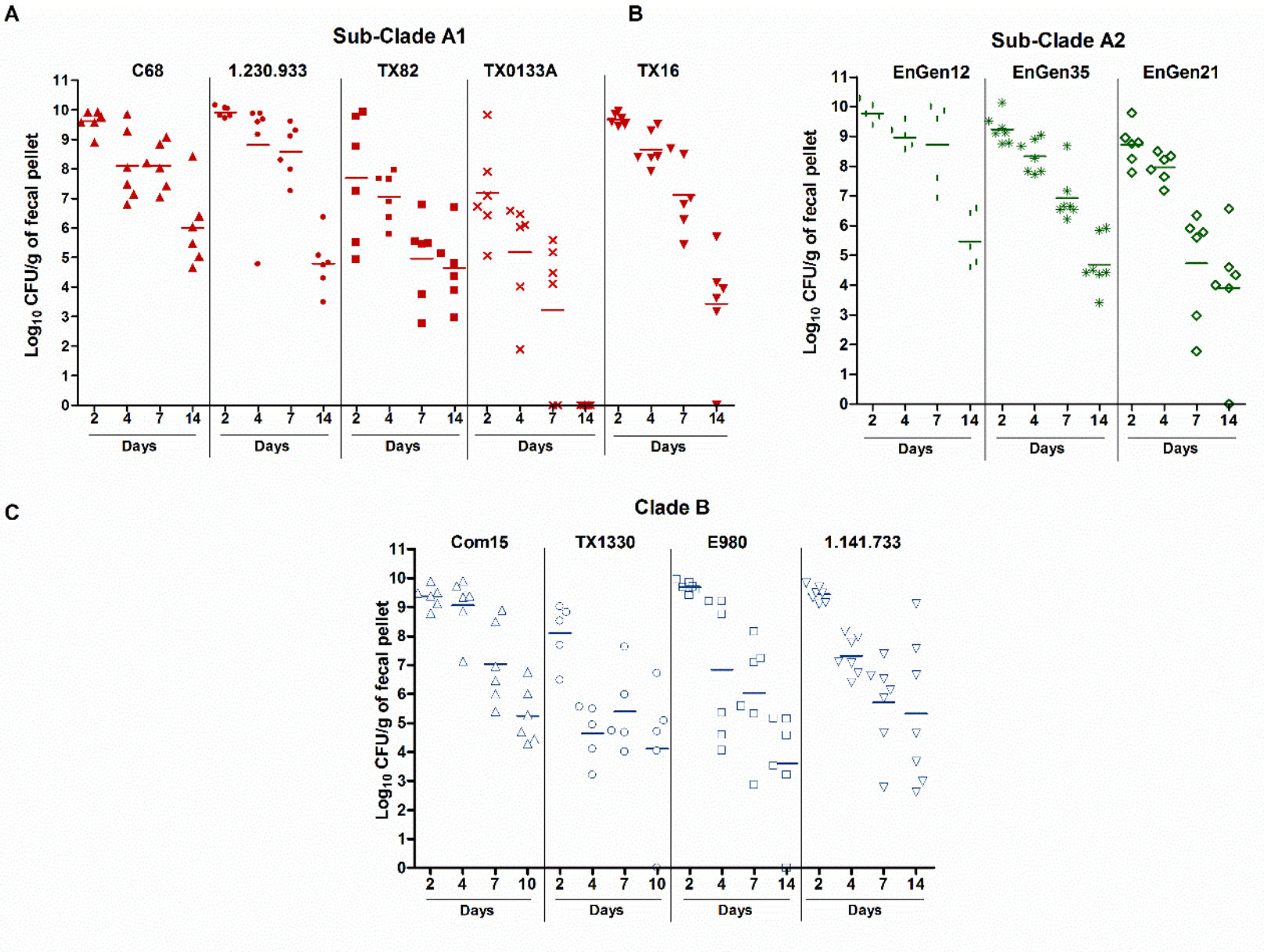
A
Sub-Clade A1
C68
1.230.933
TX82
TX0133A
TX16
Log10 CFU/g of fecal pellet
Days
B
Sub-Clade A2
EnGen12
EnGen35
EnGen21
C
Clade B
Com15
TX1330
E980
1.141.733

Figure 4.4. Detailed GIT colonization by the 12 *E. faecium* strains after mono-inoculation.

Log_{10} CFUs/g of each strain recovered from fecal pellets on days 2 to 14 on EA-NIT8 after orogastric administration of **(A)** subclade A1 strains ($1.4 \times 10^8 - 4 \times 10^9$ CFU), **(B)** subclade A2 strains ($5 \times 10^7 - 3.3 \times 10^9$ CFU) and **(C)** clade B strains ($2.05 \times 10^9 - 3.6 \times 10^9$ CFU) (see Table 4-2 for the inoculum counts of each strain). Each symbol represents the log_{10} CFUs/g recovered from fecal pellets of individual mice; the horizontal lines indicate the geometric mean log_{10} CFUs/g recovered of each strain.

All the strains, except TX0133A_{A1}, were detected at day 14 after inoculation (Figure 4.3 & Figure 4.4). To determine whether there were overall differences in the levels of colonization between the clades, we compared the composite geometric mean $\log_{10}$ CFUs/g by clades and found no statistically significant difference in the colonization levels at any of the time points evaluated ($p > 0.05$; Figure 4.5).

E. faecium clade B strains outcompete clade A strains as persistent colonizers of the GITs of mice when present together (competition assay)

To access the effect on colonization of inoculating strains together, we again first pretreated mice as described above. Then, a bacterial suspension containing an approximately 1:1 ratio, based on OD_{600}, of a strain from one clade and a strain from a different clade, were administered to the mice (Figure 4.1); the actual ratio was later determined by plating to assess the number of CFUs of each strain in the inoculum (Table 4-3). The results of in vivo competition assays are shown in Figure 4.6, Figure 4.7 and Figure 4.8. When subclade A1 strains were evaluated with clade B strains (four different strain pairs tested; see Table 4-3), although the dynamics of colonization varied between pairs, in three of the four strain pairs tested, the commensal clade B strain significantly outcompeted the HA subclade A1 strain at day 14 ($p < 0.0008$ to 0.0118; Figure 4.6). Specifically, Com15$_B$ predominated over the subclade A1 strains C68$_{A1}$ (Figure 4.6-A) and TX82$_{A1}$ (Figure 4.6-B); this difference was statistically significant at day 7 and 14 for both pairs and, for Com15$_B$ versus TX82$_{A1}$, as early as day 2 (Figure 4.6-B). Interestingly, TX1330$_B$, although significantly outcompeted at early time points (days 2 and 4), eventually outcompeted C68$_{A1}$ at days 7 and 14 (Figure 4.6-C). Only with TX16$_{A1}$ versus E980$_B$ did the A1 strain predominate at all time points (Figure 4.6-D).

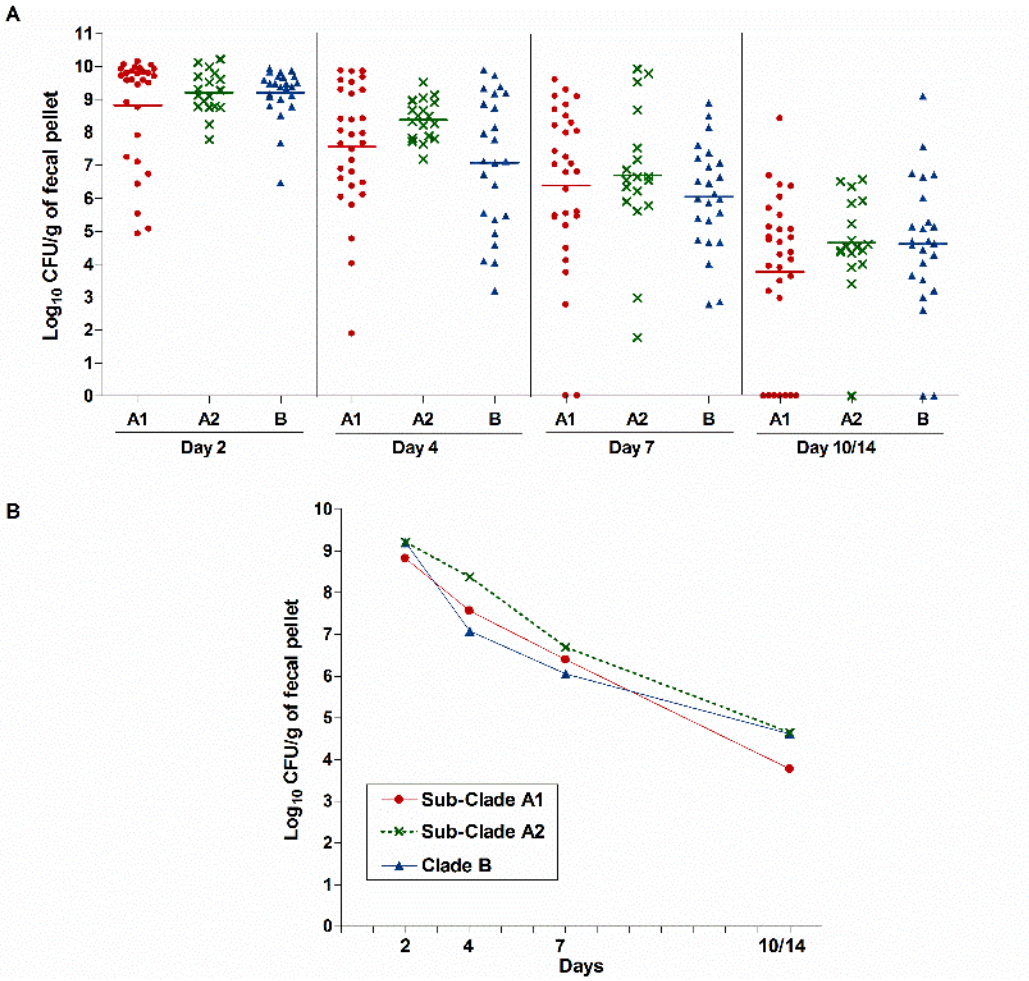

Figure 4.5. Aggregate GIT colonization by the different *E. faecium* clades after mono-inoculation of 12 strains.

(A) Distribution of the numbers of bacteria recovered from fecal pellets on days 2 to 14 on EA-NIT8 after orogastric administration of the 12 *E. faecium* strains. Each symbol represents the $\log_{10}$ CFUs/g recovered from fecal pellets of individual mice; the horizontal lines indicate the geometric mean $\log_{10}$ CFUs/g of all strains of each clade or subclade. **(B)** Composite comparison of numbers of bacteria by clades. Each symbol represents the geometric mean $\log_{10}$ CFUs/g recovered from fecal pellets of 30, 18 and 24 mice, after orogastric administration of the subclade A1, subclade A2 and clade B strains, respectively.

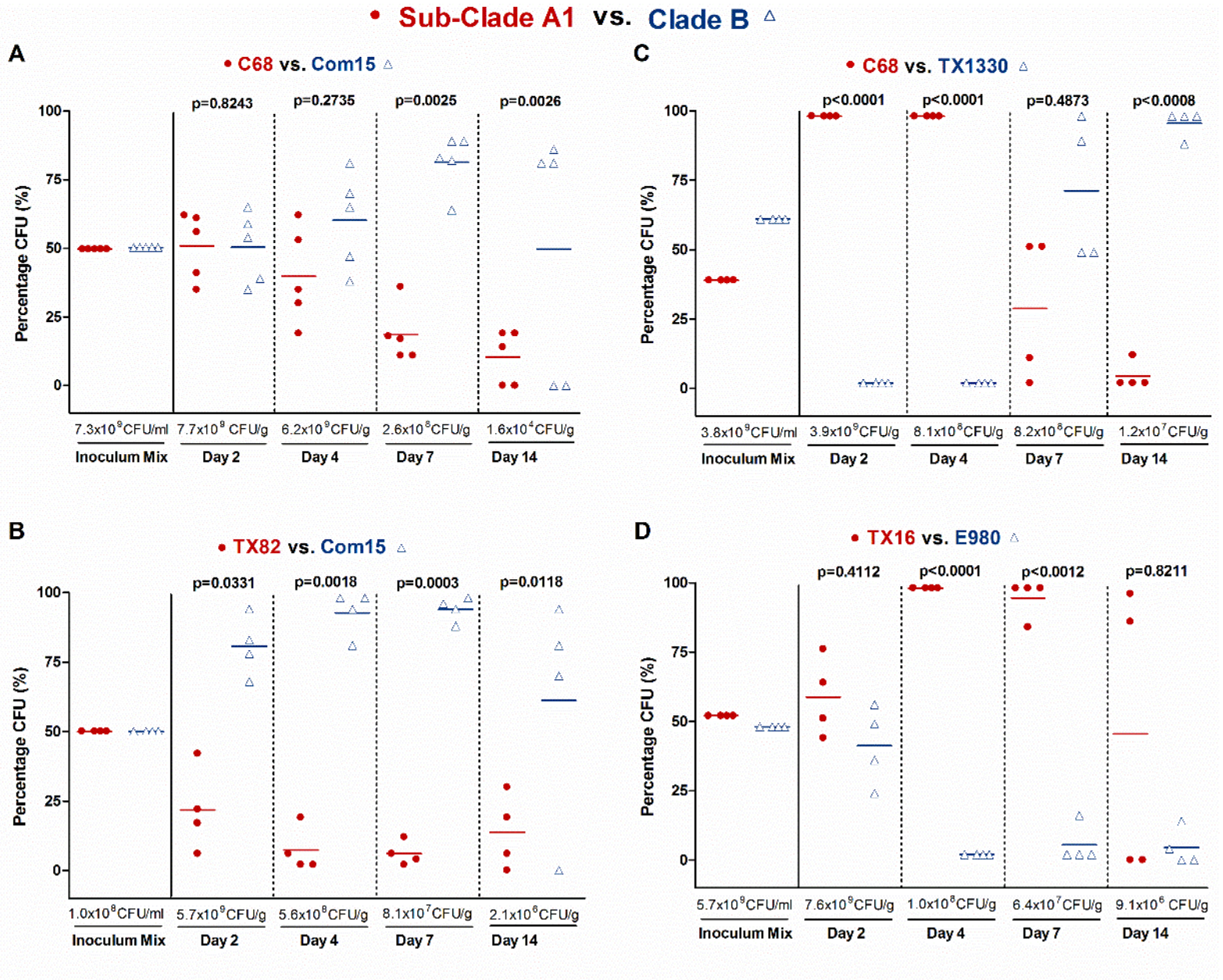
• Sub-Clade A1 vs. Clade B △
A
• C68 vs. Com15 △
Percentage CFU (%)
100
75
50
25
0
p=0.8243
p=0.2735
p=0.0025
p=0.0026
7.3x10^9CFU/ml
7.7x10^9 CFU/g
6.2x10^9CFU/g
2.6x10^8CFU/g
1.6x10^4CFU/g
Inoculum Mix
Day 2
Day 4
Day 7
Day 14
C
• C68 vs. TX1330 △
p<0.0001
p<0.0001
p=0.4873
p<0.0008
3.8x10^9CFU/ml
3.9x10^9CFU/g
8.1x10^8CFU/g
8.2x10^6CFU/g
1.2x10^7CFU/g
B
• TX82 vs. Com15 △
p=0.0331
p=0.0018
p=0.0003
p=0.0118
1.0x10^8CFU/ml
5.7x10^9CFU/g
5.6x10^8CFU/g
8.1x10^7CFU/g
2.1x10^6CFU/g
D
• TX16 vs. E980 △
p=0.4112
p<0.0001
p<0.0012
p=0.8211
5.7x10^9CFU/ml
7.6x10^9CFU/g
1.0x10^8CFU/g
6.4x10^7CFU/g
9.1x10^6 CFU/g

Figure 4.6. GIT colonization by *E. faecium* subclade A1 versus clade B strains after mixed inoculation.

Percentage of CFUs of subclade A1 versus clade B from the inoculum mix and from fecal pellets recovered at days 2, 4, 7 and 14 after mixed inoculation of the A1 versus B strain-pairs **(A)** C68 versus Com15, **(B)** TX82 versus Com15, **(C)** C68 versus TX1330 and **(D)** TX16 versus E980. The horizontal lines indicate the means; the geometric mean $\log_{10}$ CFUs/g of total *E. faecium* recovered from fecal pellets on EA-NIT8 are indicated at the bottom of each graph below the "X" axes. The p values were calculated using paired t-test for the percentage of bacteria recovered in the fecal pellets versus that of the inoculum mix.

Competition between clade A2 and clade B was also evaluated using three different strains from each clade (three strain pairs were tested; see Table 4-3). With these pairs, we observed the predominance of the clade B strain over the clade A2 strains as early as day 2 (Figure 4.7); for the strain pairs $EnGen35_{A2}$ versus $Com15_{B}$ (Figure 4.7-B) and $EnGen21_{A2}$ versus $E980_{B}$ (Figure 4.7-C), this difference was significant from day 2 onward, while $TX1330_{B}$ significantly predominated over $EnGen12_{A2}$ from day 4 onward ($p = 0.0092$; Figure 4.7-A). These results support our hypothesis that, in the absence of concurrent antibiotics, when commensal clade B strains are present with clade A strains, the former are better able to persist as colonizers of GIT.

We also asked whether differences in colonization exist when a strain of subclade A1 is co-inoculated with a strain of subclade A2 (Table 4-3). As depicted in Figure 4.8, in two of the three pairs evaluated, the subclade A1 strain outcompeted the subclade A2 strain, whereas with one pair, $EnGen35_{A2}$ predominated over $TX82_{A1}$ at all time points (Figure 4.8).

E. faecium clade B strains also predominated over the clade A strains in vitro

The clear predominance of clade B strains versus clade A in the in vivo competition assays led us to study the in vitro growth of selected strains. When grown individually, the clade B strains studied, TX1330 and Com15, showed equivalent growth kinetics based on OD_{600} (data not shown) and CFU counts (Figure 4.9-A). In contrast, the subclade A1 strains, C68 and TX82, showed a slight and prominent growth delay, respectively, evidenced by decreased OD_{600} (data not shown) and CFU counts (Figure 4.9-A).

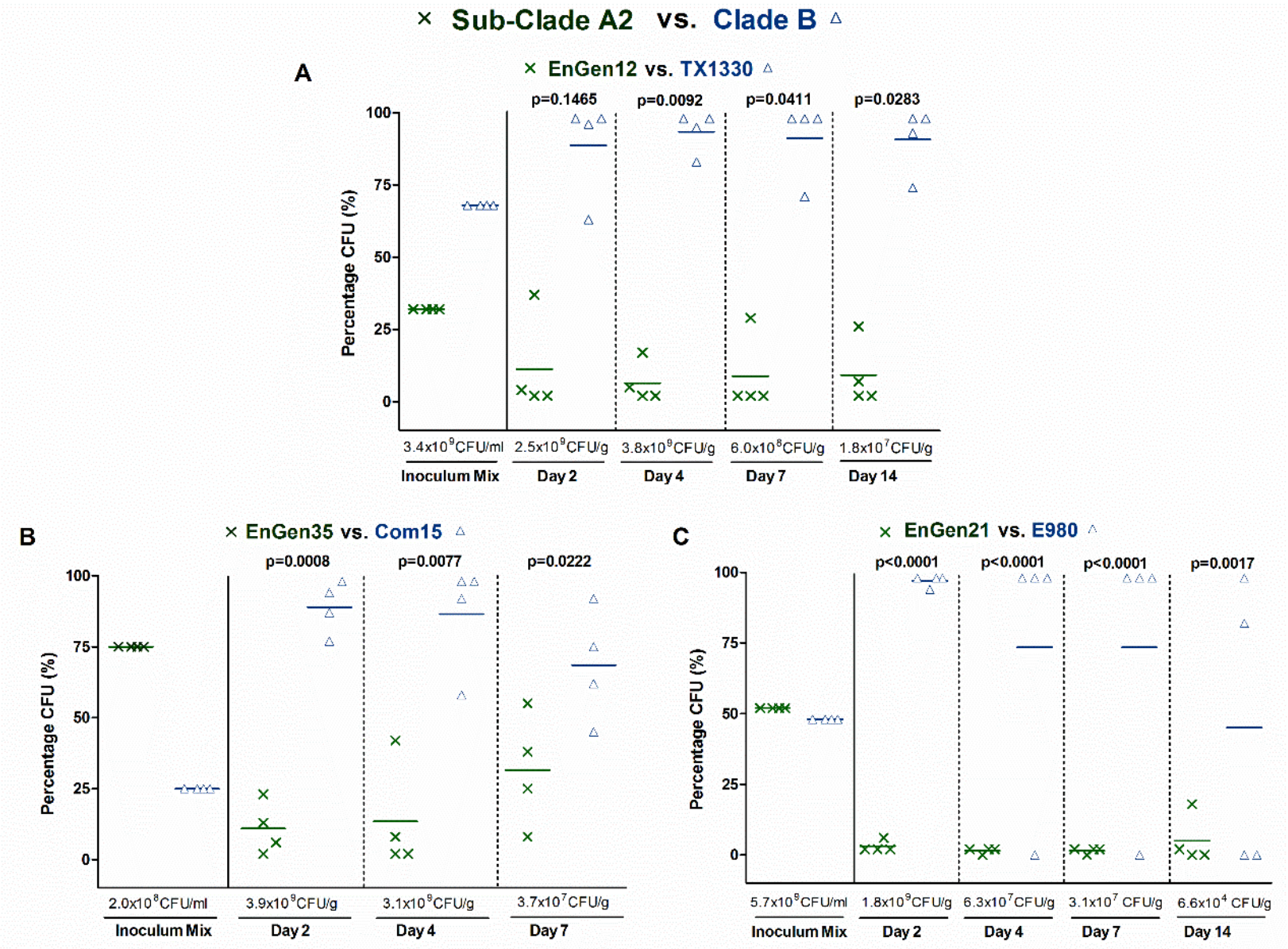
× Sub-Clade A2 vs. Clade B △
A
× EnGen12 vs. TX1330 △
p=0.1465
p=0.0092
p=0.0411
p=0.0283
Percentage CFU (%)
100
75
50
25
0
3.4x10^9CFU/ml
2.5x10^9CFU/g
3.8x10^9CFU/g
6.0x10^8CFU/g
1.8x10^7CFU/g
Inoculum Mix
Day 2
Day 4
Day 7
Day 14
B
× EnGen35 vs. Com15 △
p=0.0008
p=0.0077
p=0.0222
Percentage CFU (%)
2.0x10^8CFU/ml
3.9x10^9CFU/g
3.1x10^9CFU/g
3.7x10^7CFU/g
Inoculum Mix
Day 2
Day 4
Day 7
C
× EnGen21 vs. E980 △
p<0.0001
p<0.0001
p<0.0001
p=0.0017
Percentage CFU (%)
5.7x10^9CFU/ml
1.8x10^9CFU/g
6.3x10^7CFU/g
3.1x10^7 CFU/g
6.6x10^4 CFU/g
Inoculum Mix
Day 2
Day 4
Day 7
Day 14

Figure 4.7. GIT colonization by *E. faecium* subclade A2 versus clade B strains after mixed inoculation.

Percentage of CFUs of subclade A2 versus clade B from the inoculum mix and from fecal pellets recovered at days 2, 4, 7 and 14 after mixed inoculation of the A2 versus B strain pairs **(A)** EnGen12 versus TX1330, **(B)** EnGen35 versus Com15, **(C)** EnGen21 versus E980. The horizontal lines indicate the means; the geometric mean $\log_{10}$ CFUs/g of total *E. faecium* recovered from fecal pellets on EA-NIT8 are indicated at the bottom of each graph below the "X" axes. The p values were calculated using paired t-test for the percentage of bacteria recovered in the fecal pellets versus that of the inoculum mix.

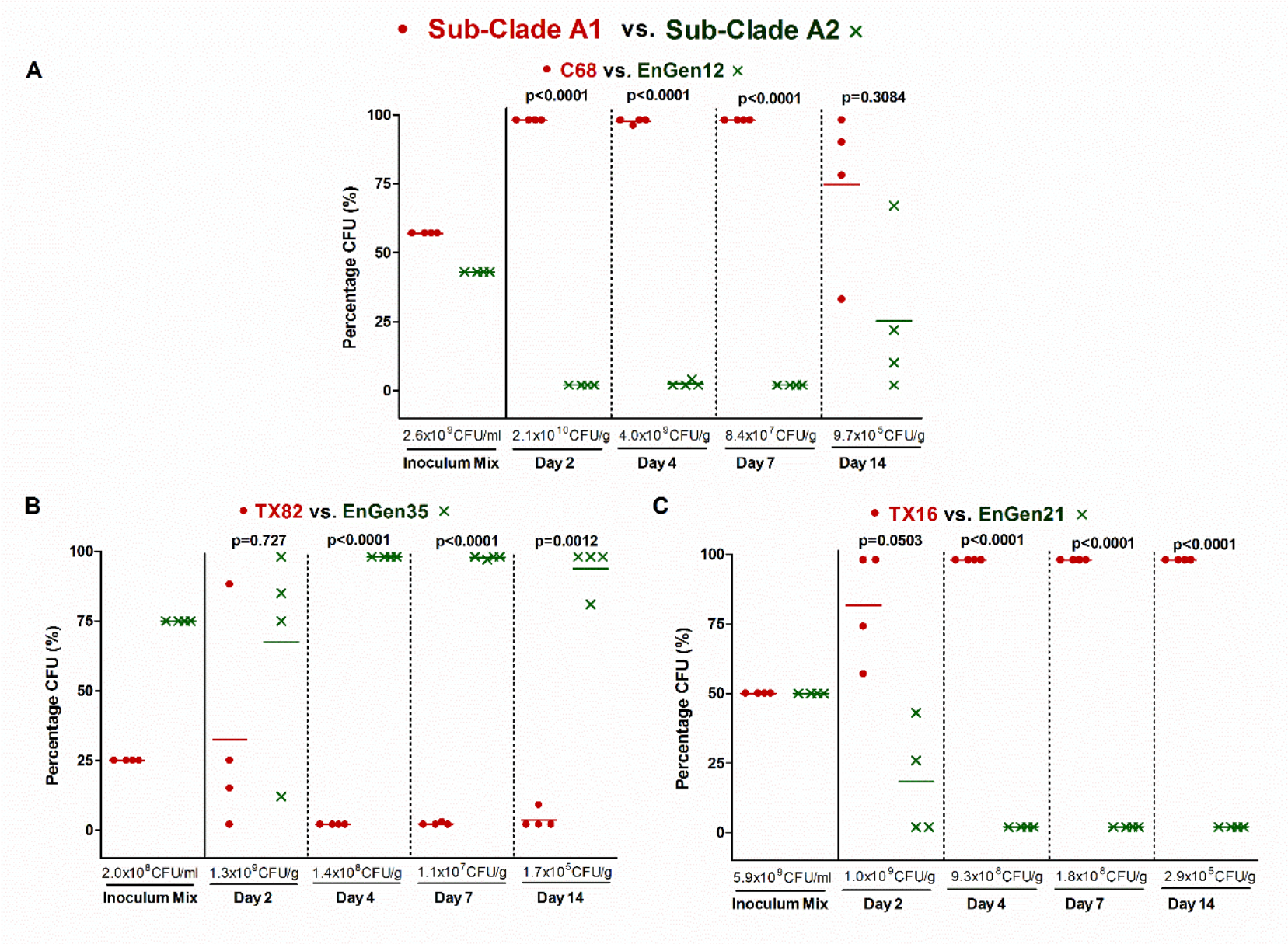
• Sub-Clade A1 vs. Sub-Clade A2 ×
A
• C68 vs. EnGen12 ×
p<0.0001
p<0.0001
p<0.0001
p=0.3084
Percentage CFU (%)
100
75
50
25
0
2.6x10^9CFU/ml
2.1x10^10CFU/g
4.0x10^9CFU/g
8.4x10^7CFU/g
9.7x10^5CFU/g
Inoculum Mix
Day 2
Day 4
Day 7
Day 14
B
• TX82 vs. EnGen35 ×
p=0.727
p<0.0001
p<0.0001
p=0.0012
Percentage CFU (%)
2.0x10^8CFU/ml
1.3x10^9CFU/g
1.4x10^8CFU/g
1.1x10^7CFU/g
1.7x10^5CFU/g
Inoculum Mix
Day 2
Day 4
Day 7
Day 14
C
• TX16 vs. EnGen21 ×
p=0.0503
p<0.0001
p<0.0001
p<0.0001
Percentage CFU (%)
5.9x10^9CFU/ml
1.0x10^9CFU/g
9.3x10^8CFU/g
1.8x10^8CFU/g
2.9x10^5CFU/g
Inoculum Mix
Day 2
Day 4
Day 7
Day 14

Figure 4.8. GIT colonization by *E. faecium* subclade A1 versus subclade A2 strains after mixed inoculation.

Percentage (%) CFU of subclade A1 versus subclade A2 from the inoculum mix and from fecal pellets recovered at days 2, 4, 7 and 14 after mixed inoculation of the A2 versus B strain-pairs **(A)** C68 versus EnGen12, **(B)** TX82 versus EnGen35 **(C)** TX16 versus EnGen21. The horizontal lines indicate the means; the geometric mean $\log_{10}$ CFUs/g of total *E. faecium* recovered from fecal pellets on EA-NIT8 are indicated at the bottom of each graph below the "X" axes. The p values were calculated using paired t-test for the percentage of bacteria recovered in the fecal pellets versus that of the inoculum mix.

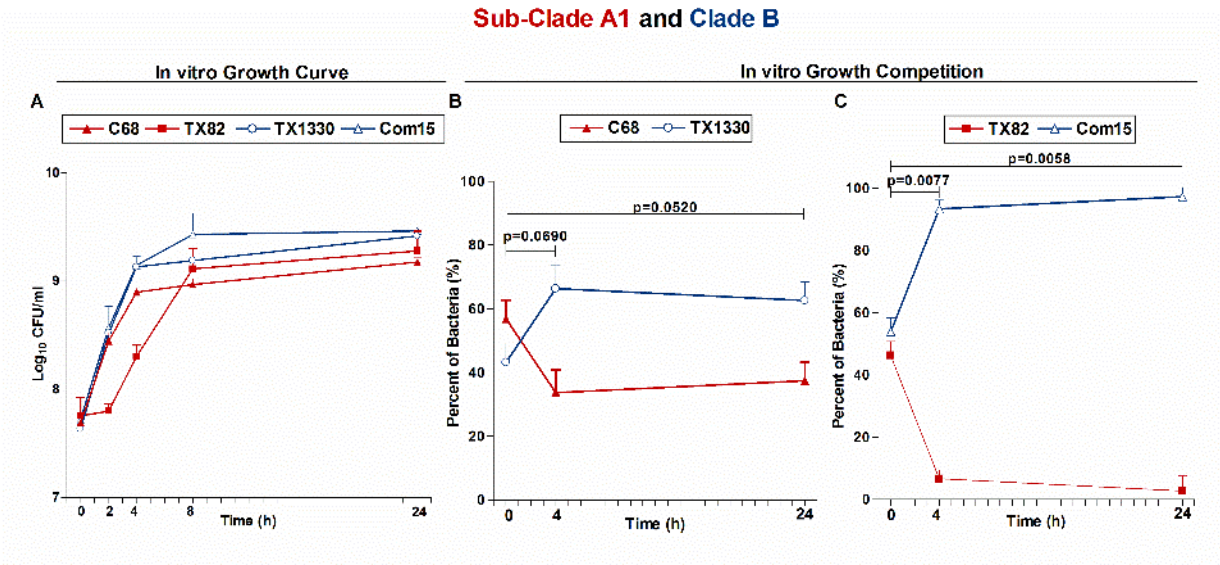

Figure 4.9. In vitro growth of subclade A1 and clade B *E. faecium* strains alone and in competition.

(A) In vitro growth curves of strains $C68_{A1}$, $TX1330_{B}$, $TX82_{A1}$ and $Com15_{B}$. Bacteria were grown alone in BHI broth for 24 h at 37°C, and aliquots were removed at 0, 2, 4, 8 and 24 h for CFU determination. In vitro growth competition of strains **(B)** C68 versus TX1330 and **(C)** TX82 versus Com15. Strains were inoculated at an approximately 1:1 ratio into 10 ml of BHI broth and grown for 24 h at 37°C, aliquots were removed at 0, 4 and 24 h and serial dilutions were plated on BHI agar. Each symbol represents the means percentage ± standard deviation from 3 independent experiments; p values were calculated using paired t-test.

In contrast, the subclade A1 strains, C68 and TX82, showed a slight and prominent growth delay, respectively, evidenced by decreased OD_{600} (data not shown) and CFU counts (Figure 4.9-A). Consistent with the growth kinetics of the individual strains, in in vitro growth competition, the clade B strains also predominated over the subclade A1 strains (Figure 4.9-B & -C) and this difference was significant with the pair $TX82_{A1}$ versus $Com15_{B}$ (6.6% versus 93.4% and 2.8% versus 97.2% at 4 h and 24 h, respectively) (Figure 4.9-C). When the subclade A2 strain (EnGen35) and the clade B strain (Com15) were grown individually, similar growth kinetics at the earlier time points (2 and 4 h) were observed; however, $EnGen35_{A2}$ had fewer CFU/ml than $Com15_{B}$ at the later time points (8 and 24 h; Figure 4.10-A). In the in vitro competition assay, a slight predominance of $Com15_{B}$ over $EnGen35_{A2}$ was observed at 4 h, although almost equal percentages of each strain were present at 24 h (Figure 4.10-B). In summary, the differences seen in the in vitro competition growth generally mirrored the differences seen in growth curves when grown alone. That is, the clade B strain grew better than clade A strains when grown alone and they also grew better (outcompeted) the clade A strains when grown together.

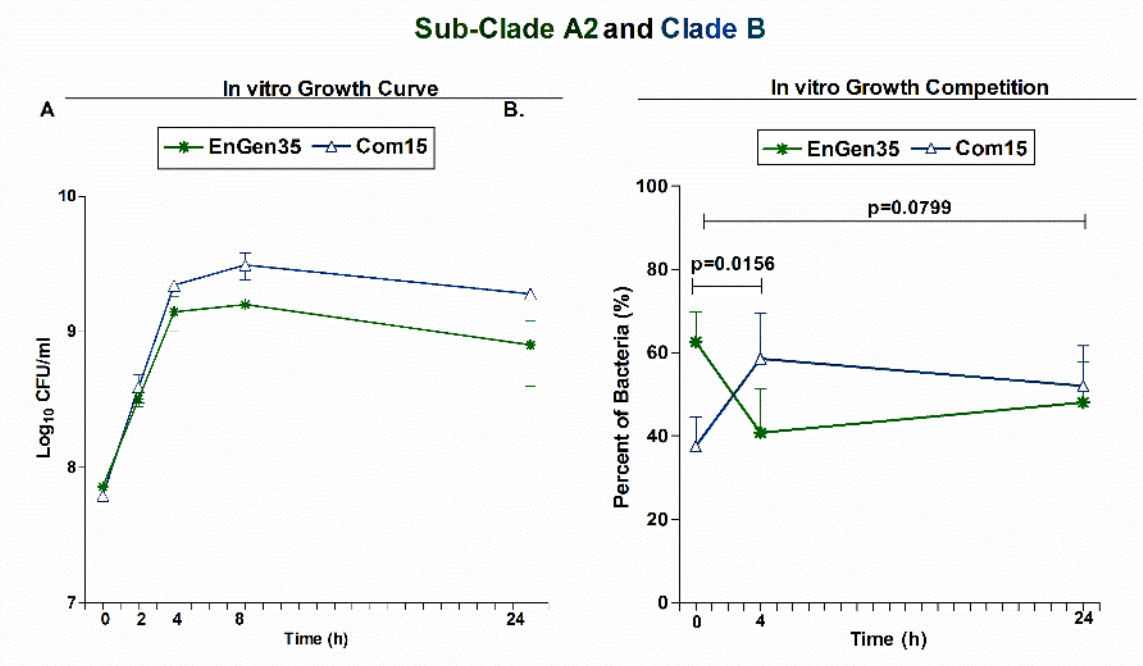

Figure 4.10. In vitro growth of subclade A2 and clade B *E. faecium* strains alone and in competition.

(A) In vitro growth curves of EnGen35$_{A2}$ and Com15$_{B}$. Bacteria were grown in BHI broth for 24 h at 37°C, and aliquots were removed at 0, 2, 4, 8 and 24 h for CFU determination. In vitro growth competition of strains **(B)** EnGen35$_{A2}$ versus Com15$_{B}$. Strains were inoculated at an approximately 1:1 ratio into 10 ml of BHI broth and grown for 24 h at 37°C, aliquots were removed at 0, 4 and 24 h and serial dilutions were plated on BHI agar. Each symbol represents the means percentage ± standard deviation from 3 independent experiments; p values were calculated using paired t-test.

4.4. DISCUSSION

GIT colonization and in particular intestinal overgrowth by antibiotic-resistant enterococci are recognized risk factors for infection (15). Clade B (CA) *E. faecium* are commonly found in healthy individuals but rarely cause infections; conversely, subclade A1 (HA) strains are responsible for the majority of infections and hospital outbreaks worldwide but are rarely reported colonizing healthy individuals in the community (57, 59). The complex dynamics of GIT colonization by *E. faecium* and the different health/disease associations of the *E. faecium* clades prompted us to investigate the ability of representative *E. faecium* strains from each clade to colonize the GIT of mice. After administering each strain individually, we were able to establish all the strains, regardless of the clade, in the GITs of mice (Figure 4.3 & Figure 4.4); while the colonization dynamics varied between the strains, we did not find significant differences (Figure 4.5) in the ability of the clades to colonize the mouse GIT, as assessed by pooled CFU comparison. Interestingly, our in vitro growth curves, albeit with a limited number of strains, suggested a reduction in fitness for the clade A strains (Figure 4.9-A & Figure 4.10-A); however, this reduced growth in vitro of the clade A strains did not seem to parallel the density of the strain achieved in vivo after mono-inoculation (Figure 4.3 & Figure 4.4), an outcome that is not unexpected since laboratory media do not replicate the complex conditions that bacteria may encounter in the GIT (e.g., availability of nutrients, host immune response and the presence of competitors). In addition, the fact that the pan-genome of *E. faecium* is predicted to be unlimited (56) suggests that a clade could acquire genes that have the potential to increase its fitness under certain environmental conditions; indeed, one gene cluster encoding a carbohydrate phosphotransferase system specifically enriched in isolates of clinical origin (clade A) was found important for GIT colonization during antibiotic treatment (121) (differential

use of carbohydrates has been suggested as one of the main drivers of the divergent evolution of the different *E. faecium* clades (59)).

Since competition assays have been suggested to be more sensitive for measuring fitness (122), we also asked whether differences in the colonization capacity of the clades could be observed when a strain from one clade was co-inoculated into mice with a strain from a different clade. Interestingly, we observed predominance of the clade B strains over the clade A strains in six of the seven pairs tested (Figure 4.6 & Figure 4.7). In addition, the vitro competition assays also suggested a competition advantage of clade B strains over clade A strains (Figure 4.9-B-C & Figure 4.10-B), just as their growth also appeared better when grown alone, as mentioned above. What is surprising is that the in vivo mono-inoculation experiments did not show an in vivo difference when the strains were inoculated alone. Whether clade B strains, in competition, are better able to acquire nutrients, tolerate stress of the GIT, withstand host innate immune responses or directly suppress A1 strains is not known. In any case, these results support our hypothesis that clade B strains have a colonization advantage over clade A, at least in the absence of concurrent antibiotic treatment. This outcome is similar to findings from a recent study of *E. faecalis*, in which it was shown that a commensal isolate was more persistent than the nosocomial isolate in a murine GIT colonization model (123). A previous search for clade-specific orthologs (i.e. present in all isolates of one clade but absent in the other) revealed that the *E. faecium* clade B, but not clade A, harbors a set of genes that encode factors that could potentially mediate an interaction with eukaryotic cells, suggesting the possibility that clade B strains may be more closely associated with cells of the GIT than clade A strains (51). In addition, it is possible that the increased occurrence of resistance genes in clade A strains (Table 4-1), compared with clade B strains, could pose a fitness cost for the bacteria in the absence of

antibiotics, resulting in growth rate reduction and/or a decrease in their competitive ability in vivo and in vitro, as previously suggested (122, 124). Although we did not evaluate isogenic strains to determine the fitness cost of a particular resistance determinant, it is interesting to note that the only instance in which a subclade A1 strain outcompeted a clade B strain was when a vancomycin-susceptible subclade A1 strain, TX16 (DO), was in competition with the clade B strain, E980 (Figure 4.6-D). Indeed, the acquisition of VanA-type vancomycin resistance by enterococci (125) as well as in other species (126), has been associated with a substantial fitness cost. In addition, among the subclade A1 strains evaluated, TX16 showed the lowest MIC of ampicillin (Table 4-1). The absence in TX16 of certain resistances associated with clade A1 strains (44, 68) and its relatively early isolation suggest that this strain may have arisen early in the evolution of clade A1.

In summary, we showed that clade B strains displayed an in vitro growth advantage over subclade A1 strains both when grown alone as well as when grown in mixed cultures. Interestingly, in vivo after mono-inoculation, subclade A1 strains showed no significant defect in their ability to colonize the GIT of mice, as they were recovered in approximately equal numbers to clade B and subclade A2 strains. However, we demonstrated the predominance of clade B strains over clade A strains in an in vivo competition model of GIT colonization, perhaps as a consequence of a direct antagonistic interaction between the strains or a better ability to compete for the same niche. These results appear to explain the vast predominance of clade B versus clade A in humans in the community and the observation that ampicillin- and vancomycin-resistant *E. faecium* acquired during hospitalization diminish in number and seem to disappear with time after patients leave the hospital (22, 111, 127, 128), while commensal isolates seem to reemerge in these individuals.

CHAPTER 5. Differential Penicillin-Binding Protein 5 (PBP5) levels in the *Enterococcus faecium* Clades

5.1. INTRODUCTION

Ampicillin-resistant *E. faecium* has emerged as one of the leading pathogens in the hospital setting (5, 7). In the USA, the incidence of infections caused by ampicillin-resistant *E. faecium* started to increase during the 1980s, accompanied by a progressive increase in the ampicillin MICs over time (129, 130); currently, the majority of *E. faecium* isolated in hospitals around the USA are resistant to this β-lactam antibiotic (5, 7), which has been mainly attributed to the presence of PBP5 (65, 129, 130). The proposed mechanism of PBP5-mediated action is its intrinsic low affinity for β-lactam antibiotics, allowing peptidoglycan synthesis (transpeptidation) and bacterial growth when the other PBPs are inhibited by the drug (66, 67).

High-level ampicillin resistance in clinical isolates of *E. faecium* has been primarily associated with variants of PBP5 with even lower affinity for β-lactams (58, 68, 131-133). In particular, specific amino acid changes in the C-terminal transpeptidase domain of PBP5 have been implicated with increased β-lactam MICs (58, 131, 132). A methionine-to-threonine or alanine substitution at position 485 (Met-485-Thr/Ala) and the addition of aspartic acid or serine after amino acid 466 (Asp-466' or Ser-466'), both positions located close to the active site of the enzyme, have been associated with the highest levels of resistance to β-lactam antibiotics (58, 68, 132-134). In addition, other amino acid substitutions, including an alanine for isoleucine or threonine at position 499 (Ala-499-Ile/Thr), a glutamine for valine at position 629 (Glu-629-Val) and a proline for serine at position 667 (Pro-667-Ser) have been implicated in resistance to β-lactams (58, 68, 132). Rice et al. demonstrated that single substitutions in positions 485, 499, 629 and 466' had low impact in the ampicillin MICs, but when these mutations were present in combination the levels of resistance were amplified (131). However, in clinical isolates, there is not an absolute correlation between these substitutions and high-levels of

ampicillin resistance (58). In addition, factors other than the PBP5 mutations, including increased PBP5 production, have been suggested to play a role in elevating the MICs of ampicillin and other β-lactams (65, 135-137).

Interestingly, the two main *E. faecium* lineages found in humans: the hospital-associated clade (subclade A1) and the community-associated clade (clade B) (57, 59) differ in their ampicillin phenotype, which is attributed to the presence of two distinct allelic forms of the *pbp5* gene that differ by approximately 5% (58). Most of the subclade A1 strains are resistant to ampicillin (MIC ≥ 16 μg/ml) and harbor the consensus *pbp5-R* allele, while the majority of clade B strains are susceptible to ampicillin (MIC ≤ 2 μg/ml) and harbor the consensus *pbp5-S* allele (58). In contrast, subclade A2 strains, associated primarily with animals and estimated to have split from subclade A1 75 years ago (59), were shown to display ampicillin MICs that range between 0.5 to 128 μg/ml, with the majority of isolates analyzed harboring a "hybrid-like" *pbp5* (*pbp5-S/R*), considered an intermediate allele between *pbp5-S* and *pbp5-R* (68). It is interesting to note that, in addition to the amino acid changes in the transpeptidase domain of PBP5 described above, the different *pbp5* alleles have a number of other amino acid variations and silent polymorphisms throughout the PBP5 protein and *pbp5* gene, respectively (58, 68).

On the basis of the observation that, in some clinical *E. faecium* isolates (presumably from subclade A1), increased amounts of PBP5 have been associated with elevated β-lactams MICs, we postulated that differences in PBP5 levels exist between the *E. faecium* clades; in particular, we inferred that PBP5 protein levels are higher in clade A ampicillin-resistant strains compared to clade B and subclade A2 ampicillin-susceptible strains. In this chapter, we examined PBP5 protein abundance by western

blot, as well as the genetic environment upstream of *pbp5,* from 16 *E. faecium* strains from clades A1, A2 and B that carry different variants of the *pbp5* allele and cover the spectrum of ampicillin MICs.

5.2. MATERIALS AND METHODS

Bacterial strains, plasmids, routine growth conditions and susceptibility testing

Relevant characteristics of the *E. faecium* and *E. coli* strains used in this chapter are described in Table 5-1 and Table 5-2, respectively. *E. faecium* were routinely grown at 37°C in BHI broth or agar (BD). In some instances, the clade or subclade designation of the strains is written as a subscript. *E. coli* strains were cultured at 37°C using LB (BD) broth or agar. Ampicillin susceptibility testing was performed by broth microdilution in Mueller Hinton II broth (cation adjusted; BD) following the Clinical and Laboratory Standards Institute (CLSI) guidelines or by E-test (bioMérieux, Marcy-l'Étoile, France). Kanamycin (Sigma-Aldrich) 50 µg/ml was used for selection of *E. coli* with the pET28a(+) vector and derivatives.

Expression and purification of soluble recombinant PBP5-S from $Com15_B$ and PBP5-R from $C68_{A1}$

Fragments of *pbp5-S* and *pbp5-R* were amplified from genomic DNA of the *E. faecium* strains $Com15_B$ and $C68_{A1}$, respectively, using the primers F-rPBP5 and R-rPBP5, containing the NdeI and BamHI restriction sites, respectively (Table 5-3). These fragments, lacking the first 108 bp of the *pbp5* coding sequence that corresponds to the 36 amino acids encoding the transmembrane domain, were cloned into the pET28a(+) vector using the NdeI and BamHI sites. The resulting recombinant plasmids, pTEX4302.1 (*pbp5-S* from Com15) and pTEX2193.1 (*pbp5-R* from C68), were propagated in *E. coli* TG1 cells and then transformed into *E. coli* BL21(DE3) cells for expression (Table 5-2).

Table 5-1. Relevant characteristics of the *E. faecium* strains used in chapter 5.

Clade	Strain Name	Source (Isolation site)	Country /Year	ST[a]	AMP[b] MIC (µg/ml)	PBP5-S/R type[c]	Reference
B	Com15	Healthy volunteer (feces)	USA/2007	583	0.19[d]	S_{21}/R_0	(51)
	TX1330	Healthy volunteer (feces)	USA/1994	107	1	S_{20}/R_1	(118)
	1.141.733	Hospitalized patient (wound)	USA/2005	327	1	S_{20}/R_1	(51)
	TX2050	Unknown	USA/1971	296	1	S_{20}/R_1	(138)
	E980	Healthy volunteer (feces)	NLD/1998	94	1	S_{17}/R_4	(56)
A2	EnGen12	Hospitalized patient (ascites)	NLD/1995	27	0.5	S_{13}/R_8	(59)
	EnGen35	Hospitalized patient (gut)	NLD/1979	66	1	S_8/R_{13}	(59)
	EnGen21	Hospitalized patient (feces)	NLD/2002	5	8	S_8/R_{13}	(59)
	EnGen52	Hospitalized patient (blood)	NLD/2002	332	128	S_8/R_{13}	(59)
	EnGen24	Hospitalized patient (urine)	NLD/2001	210	32	S_2/R_{19}	(59)
	EnGen25	Hospitalized patient (stomach)	NLD/1965	92	128	S_0/R_{21}	(59)
A1	TX16 (DO)	Endocarditis Patient (blood)	USA/1992	18	16	S_4/R_{17}	(117)
	TX82	Endocarditis Patient (blood)	USA/1999	17	64	S_1/R_{20}	(92)
	C68	Hospitalized patient (feces)	USA/1996	16	128	S_1/R_{20}	(115)
	1.230.933	Hospitalized patient (blood)	USA/2005	18	128	S_1/R_{20}	(51)
	1.231.502	Hospitalized patient (blood)	USA/2005	203	128	S_1/R_{20}	(51)

[a.] Multi-locus sequence type; [b.] Ampicillin; [c.] PBP5-S/R type as described by Pietta et al., indicating that X positions match the PBP5-S consensus and Y positions match the R consensus. [d.] MIC determined by E-test.

Table 5-2. Relevant characteristics of the *E. coli* strains and plasmids used in chapter 5.

Strain or Plasmid	Relevant Characteristic(s)	Reference
***E. coli* Strains**		
TG1	Host strain used for routine cloning	
BL21 (DE3)	Strain used for overexpression of recombinant PBP5.	Life Technologies
Plasmids		
pGEM-T Easy	Plasmid used for initial cloning of PCR fragments; AMP^R.	Promega
pET28a(+)	Expression vector carrying T7lac promoter, adds an N-terminal His tag; KAN^R.	Novagen
pTEX4302.1	pET28a(+) derivative carrying a 1929 bp fragment of the *pbp5-S* gene from *E. faecium* $Com15_{B.}$ The fragment lacks the first 108 bp of the PBP5 coding sequence, which corresponds to the transmembrane domain region.	This study
pTEX2193.1	pET28a(+) derivative carrying a 1929 bp fragment of the *pbp5-R* gene from *E. faecium* $C68_{A1.}$ The fragment lacks the first 108 bp of the PBP5 coding sequence, which corresponds to the transmembrane domain region.	This study

AMP, Ampicillin; KAN, Kanamycin; Superscript "R" designates resistance.

Table 5-3. Oligonucleotides used in chapter 5.

Primer Name	Sequence 5'- 3'	Relevant Characteristics
rPBP5		
F-rPBP5	GGAATTCCATATGCAAGAAA CCCAAGCAGTA	Forward for expression of Δ1-36 rPBP5; NdeI site underlined.
R-rPBP5	CGGGATCCTTATTGATAATTT TGGTTGAG	Reverse for expression of Δ1-36 rPBP5; BamHI site underlined.
***pbp5* upstream region** (These primers were designed to confirm the presence or absence of a 201 bp deletion upstream of *pbp5*)		
psr-F-del	AGTATCCAAACGAACCTTCC	Forward for *psr*; used to amplify the 3' end of *psr* and the intergenic region between *psr* and *pbp5.*
pbp5-R-del	GCCTGTTCGATTTTTGCCG	Reverse for *pbp5*; used to amplify the 3' end of *psr* and intergenic region between *psr* and *pbp5.*
***pbp5* upstream region of TX82$_{A1}$ and 1.230.933 $_{A1}$** (These primers were designed based on the upstream region of *pbp5* in the complete genome sequence of the *E. faecium* strain Aus0004)		
hisJ-F	CCGTCACACCTTTTGCTTTT	Forward for a gene encoding a putative histidinol phosphate phosphatase (HisJ); used with the *pbp5*-R$^{115-134}$ primer.
gnat-F	TCAACGGCTCTATCTGCTCA	Forward for a gene, *gnat,* encoding a putative acetyltransferase; used with the *pbp5*-R$^{115-134}$ primer
pbp5-R$^{115-134}$	CCAGCTTCTACTGCTTGGGT	Reverse for *pbp5*; used to amplify the region immediately upstream of *pbp5*.

E.coli BL21(DE3) harboring pTEX4302.1 and pTEX2193.1 plasmids were grown at 37°C in LB medium containing 50 µg/ml kanamycin to mid-log phase. Expression was induced at 16°C by the addition of ß-d-1-thiogalactopyranoside to 0.4 mM and an additional incubation for 17 h. Purification was performed by a series of chromatographies[1], as previously described with minor modifications (139).

Generation of anti-rPBP5-S and anti-rPBP5-R antibodies[2]

Polyclonal antibodies against rPBP5-S and rPBP5-R were separately generated using a previously described scheme (94, 140) and following a pre-approved protocol and guidelines by the Animal Welfare Committee of the University of Texas Health Science Center at Houston. In brief, male Sprague-Dawley rats were subcutaneously injected at multiple sites with 1 mg of rPBP5-S or rPBP5-R suspended in Freund's complete adjuvant (FCA) at day 1, followed by two booster doses of 1 mg of rPBP5-S or rPBP5-R prepared in Freund's incomplete adjuvant (FIA) at days 14 and 28. Blood was collected at day 42, followed by euthanasia of the animal. Antibody titers were determined by ELISA as previously described in chapter 3 and in (94). Prior to their use, anti-rPBP5-S and anti-rPBP5-R antibodies were absorbed with *E. coli* BL21(DE3) lysates to remove any anti-*E. coli* antibodies, if present.

PBP5 detection by western blot

Cells grown overnight in BHI broth were inoculated into fresh BHI broth at a starting optical density 600nm (OD_{600}) of 0.05 and grown at 37°C with gentle shaking until reaching an OD_{600} of 1.1 ± 0.1. Cultures were centrifuged at 3900 rpm for 10 min and the

---

[1] Dr. Milya G. Davlieva performed the PBP5 protein purification.
[2] Dr. Kavindra V. Singh generated the polyclonal antibodies.

pellets were rapidly chilled on dry ice and stored at -80°C until used. Cells were resuspended in 1 ml of 1X PBS, disrupted twice by 1 min bead beating pulses at maximum speed, followed by centrifugation to recover the supernatant. Protein concentrations were measured using the Pierce Bicinchoninic Acid (BCA) Protein Assay Kit (Thermo Fisher Scientific) according to the manufacturer's instructions. Samples, normalized to equal protein concentrations (19 µg), were boiled in SDS-containing sample buffer and separated by SDS-PAGE (10% acrylamide). Coomassie staining was used to ensure that equivalent amounts of protein were loaded into each lane (data not shown). Samples were transferred to a PVDF membrane (EMD Millipore, Darmstadt, Germany) and analyzed with the absorbed rat antisera against PBP5-S or PBP5-R, followed by incubation with peroxidase conjugated goat anti-rat IgG, light chain specific (Jackson Immuno Research Laboratories). As positive controls, 10 ng of purified recombinant PBP5-S and PBP5-R proteins were loaded into a lane. Intensity of the bands was analyzed using Image J software (http://imagej.nih.gov/ij/).

Analyses of the genetic environment upstream of the *pbp5* gene

Whole genome sequences for 15 of the 16 strains included in this study were available in the NCBI website http://www.ncbi.nlm.nih.gov/genome and were used to retrieved the upstream region of *pbp5.* DNA and protein multiple sequence alignments were performed using the alignment tool MUSCLE from the EBI website http://www.ebi.ac.uk/Tools/msa/muscle/. Bioinformatic analyses were confirmed by PCR, using the primers listed in Table 5-3.

5.3. RESULTS AND DISCUSSION

The 16 *E. faecium* strains, their ampicillin MICs and PBP5 types are shown in Table 5-1. We used the PBP5 type designation (S_XR_Y) described by Pietta et al. (68), based on the 21 positions previously reported to consistenly vary between PBP5-S and PBP5-R (58). Consistent with our previous reports, clade B strains showed ampicillin MICs ≤ 2 µg/ml, subclade A1 strains displayed MICs ≥ 16 µg/ml, while the subclade A2 strains MICs ranged from 0.5 to 128 µg/ml (58, 68). It is important to note that, although two of the six subclade A2 strains studied have MICs of 128 µg/ml, they were chosen from 13 A2 strains with a median MIC of 4 µg/ml.

Western blot, with a polyclonal serum raised against r-PBP5-S from $Com15_B$, showed that PBP5 protein levels were higher in the ampicillin-resistant strains from clade A compared to those in the highly ampicillin-susceptible strains from clade B and subclade A2 (Figure 5.1). When PBP5 levels were detected with a polyclonal serum raised against r-PBP5-R from $C68_{A,}$ comparable results were obtained (Figure 5.2), indicating that differences observed between strains are due to differences in protein abundance and not in the affinity of the antibodies for a particular type of PBP5 (Figure 5.1 & Figure 5.2). Furthermore, comparable results were obtained in independent experiments (biological and technical replicates).

When comparing strains of the same clade or subclade, we observed a correlation between the ampicillin MIC (Table 5-1), the PBP5 sequence type (Table 5-1) and the levels of PBP5 protein (Figure 5.1 & Figure 5.2)

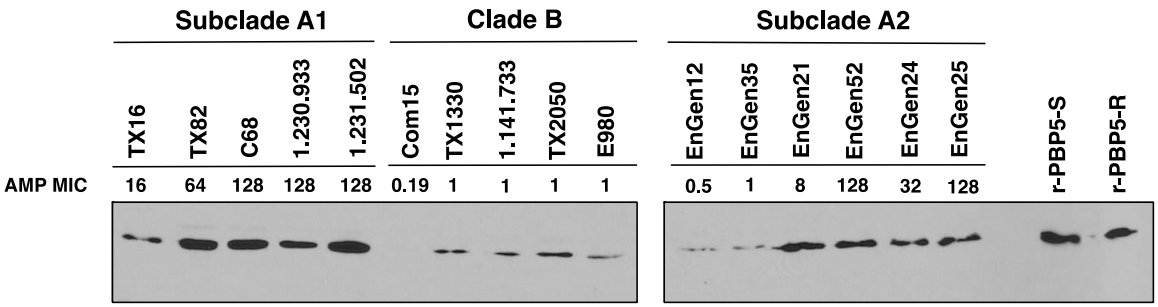

Figure 5.1. Expression of PBP5 by western blot with polyclonal serum raised against rPBP5-S.

Proteins were separated by SDS-PAGE, transferred to a PVDF membrane and PBP5 was detected with a polyclonal serum raised against-r-PBP5-S from Com15 (see Figure 5.2 for re-probed membrane with a polyclonal serum raised against rPBP5-R from strain C68). The *E. faecium* strains and ampicillin MICs are indicated above the image (See Table 5-1 for detailed description of the strains); 10 ng of recombinant PBP5-S and PBP5-R were loaded into the last two lanes as a control.

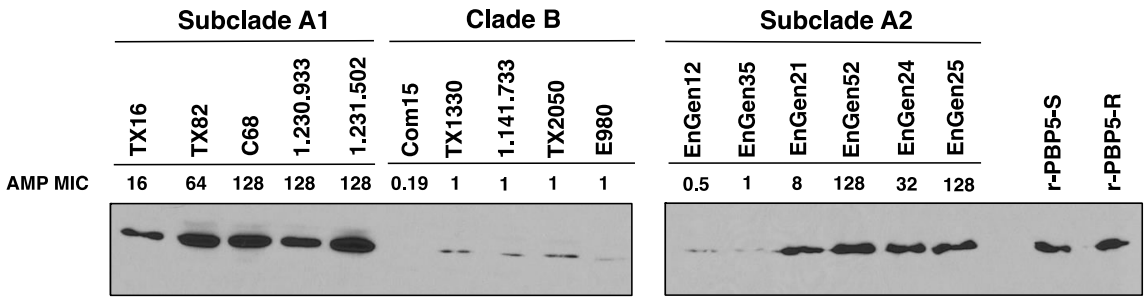

Figure 5.2. Expression of PBP5 by western blot with a polyclonal serum raised against rPBP5-R.

Antibodies used to detect PBP5 in Figure 5.1 were removed and the membrane was re-probed with a polyclonal serum raised against-r-PBP5-R from C68 (See Table 5-1 for detailed description of the strains).

Within subclade A1, TX16 (DO) displays moderate resistance to ampicillin (MIC = 16 µg/ml) (58, 68), which correlates with its reduced PBP5 protein levels (Figure 5.1 & Figure 5.2) compared to the other subclade A1 strains studied with higher ampicillin MICs (MICs ≥ 64 µg/ml). However, in addition to its lower *pbp5* expression compared to other subclade A1 strains, TX16 (PBP5-S_4/R_{17}) also lacks two amino acid changes (Asp/Ser-466' and Met-485-Thr/Ala) that have been linked with the highest levels of ampicillin resistance (58, 68), which also could explain its moderate ampicillin MIC.

When subclade A2 strains were compared to each other, higher PBP5 protein levels (Figure 5.1 & Figure 5.2) were observed in the strains with reduced ampicillin susceptibility (EnGen21, EnGen52, EnGen24 and EnGen25; MICs = 8-128 µg/ml) compared to the highly susceptible ones (EnGen12 and EnGen35; MICs = 0.5-1 µg/ml). Within subclade A2, we also analyzed three strains that displayed considerably different ampicillin MICs (EnGen35 = 1 µg/ml, EnGen21 = 8 µg/ml and EnGen52 = 128 µg/ml) but that have same number of amino acid changes (PBP-S_8/R_{13}) associated with the R form of the protein (EnGen35 and EnGen52 have the same amino acid sequence in these 21 positions, while EnGen21 diverged in one position; Table 5-4). Interestingly, reduced PBP5 protein levels in EnGen35 may account for its very low MIC compared to EnGen21 and EnGen52 (Figure 5.1 & Figure 5.2). Conversely, PBP5 protein levels between EnGen21 and EnGen52 were comparable (Figure 5.1 & Figure 5.2), suggesting that other factors, including the seven amino acid differences (six outside of the 21 consensus positions) between the PBP5 sequences of these two strains (68), could also play a role in the different ampicillin MICs (Table 5-4 & Table 5-5).

Table 5-4. Amino acid sequence in the 21 positions previously reported to vary between PBP5-S and PBP5-R of the *E. faecium* strains EnGen35$_{A2}$, EnGen21 $_{A2}$ and EnGen52 $_{A2}$.

Strain	MIC (µg/ml)	PBP5 -S/R type	24	27	34	66	68	85	100	144	172	177	204	216	324	466'	485	496	499	525	586	629	667
PBP5-S-Consensus	**≤2**		**V**	**S**	**R**	**G**	**A**	**E**	**E**	**K**	**T**	**L**	**D**	**A**	**T**	**-**	**M**	**N**	**A**	**E**	**V**	**E**	**P**
EnGen35	1	S_8/R_{13}	A	G	Q	E	A	E	Q	Q	A	I	D	S	A	-	M	K	T	D	V	E	P
EnGen21	8	S_8/R_{13}	A	G	Q	E	A	E	Q	Q	A	I	D	S	A	-	M	K	I*	D	V	E	P
EnGen52	128	S_8/R_{13}	A	G	Q	E	A	E	Q	Q	A	I	D	S	A	-	M	K	T	D	V	E	P
PBP5-R Consensus	**≥16**		**A**	**G**	**Q**	**E**	**T**	**D**	**Q**	**Q**	**A**	**I**	**G**	**S**	**A**	**S**	**A/ T**	**K**	**T/I***	**D**	**L**	**V**	**S**

*Isoleucine at position 499 is commonly found in strain from clade A2 with “hybrid-like” PBP5 sequences.

Table 5-5. Amino acid changes outside the 21 positions previously reported to vary between PBP5-S and PBP5-R of the *E. faecium* strains EnGen35$_{A2}$, EnGen21$_{A2}$ and EnGen52$_{A2}$.

Strain	MIC (µg/ml)	39	314	401	406	509	606
PBP5-S-Consensus	**≤2**	**T**	**T**	**A**	**P**	**D**	**S**
EnGen35	1	N	T	A	P	D	S
EnGen21	8	T	T	S	P	D	S
EnGen52	128	N	I	A	A	E	F
PBP5-R Consensus	**≥16**	**T**	**T**	**A**	**P**	**D**	**S**

When comparing clade B strains to each other, similar low PBP5 protein levels were observed between TX1330, 1.141.733 and TX2050 and E980 (MICs = 1 µg/ml), albeit the later showed a small decrease relative to the others; on the other hand, Com15 showed a significant reduction in PBP5 quantity (the band was only visible when the film was overexposed) (Figure 5.1 & Figure 5.2), which is in accordance with its hyper-susceptibility (MICs = 0.19 µg/ml; Table 1).

The upstream region of *pbp5* has been suggested to contribute to ampicillin resistance. Initial evidence for a role of this region comes from studies in *E. hirae* where an 87 bp deletion in the 5' region of an open reading frame (ORF) located upstream of *pbp5* was associated with increased PBP5 levels in a resistant mutant. This finding led to the designation of this ORF as *p*enicillin-binding protein *s*ynthesis *r*epressor (*psr*) (141); however, the direct role of Psr in *pbp5* repression has not yet been established (142). Interestingly, Massida et al. showed that Psr is involved in the regulation of different cell surface-related processes in *E. hirae* including lysozyme sensitivity, autolysis, and the levels of rhamnose in the cell wall (143). Furthermore, a role for the *pbp5* upstream region in the *E. faecium* subclade A1 strain, C68, was also shown (142). When the *pbp5* gene of C68 was cloned along with its upstream region containing two ORFs, *ftsW* and *psr,* the ampicillin MICs were higher, compared to when the gene was cloned in the same vector with only its own promoter region (64-128 µg/ml versus 8-16 µg/ml) (142). However, in strain C68, Psr seems not to participate in the regulation of *pbp5* transcription (142). The role of the second ORF, *ftsW,* is unknown, but studies of a homologous gene in *E. coli* showed that the product of this gene is a transmembrane protein that interacts with PBP3 in *E. coli* (144).

When I analyzed the sequence upstream of *pbp5*, in the 15 *E. faecium* strains with available whole genome sequences included in this study, a broad degree of genetic

variations, including large and small DNA fragment insertions and deletions, as well as single nucleotide polymorphisms (SNPs), was observed. Interestingly, we found some alterations in this upstream region that correlated with increased PBP5 abundance and ampicillin resistance. One of the changes associated with the highest ampicillin MICs is a 201 bp deletion that encompasses 137 bp of the 3' end of *psr* and 64 bp of the intergenic region of *psr* and *pbp5* (Figure 5.3). This deletion was confirmed by PCR, using the primers *psr*-F-del and *pbp5*-R-del that anneal on *psr* and *pbp5*, respectively, in five strains (EnGen52$_{A2}$, Engen24$_{A2}$, EnGen25$_{A2}$, C68$_{A1}$ and 1.231.502$_{A1}$). Of note, four of the five strains with the highest ampicillin MIC (128 µg/ml) had this deletion (Figure 5.4).

In the remaining three resistant strains from subclade A1, TX16, TX82 and 1.230.993 (MICs = 16-128 µg/ml) and in strain EnGen21 from subclade A2 (MIC = 8 µg/ml), I found evidence of two major insertional events. In TX16$_{A1}$ and EnGen21$_{A2}$ (MICs = 8-16 µg/ml), a 1346 bp fragment, that includes a 1179 pb transposase with 99% identity between these two strains, is inserted in the same exact position within the intergenic region of *psr* and *pbp5* (Figure 5.5) (an insertion of this size was also visualized in the PCR shown in Figure 5.4).

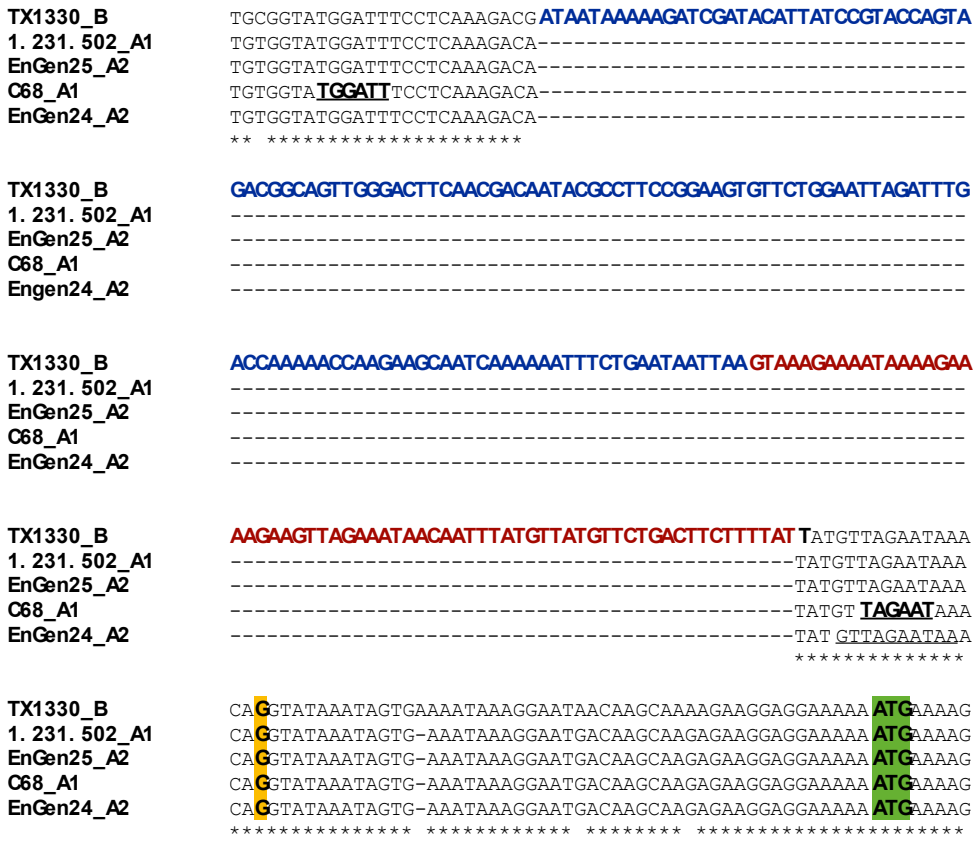

Figure 5.3. Alignment of the upstream region of *pbp5* from the *E. faecium* strains $1.231.502_{A1}$, $EnGen25_{A2}$, $C68_{A1}$ and $EnGen24_{A2}$ against $TX1330_{B}$.

The 201 bp region deleted is shown in blue (corresponding to 137 bp of the 3' end of *psr*) and in red (corresponding to the intergenic region between *psr* and *pbp5*). The transcriptional start site of the *pbp5* gene, demonstrated by Rice et al. (142), and the predictive translational start codon are highlighted in yellow and green, respectively. The putative -10 and -35 boxes predicted in strain C68 are in bold and underlined (142).

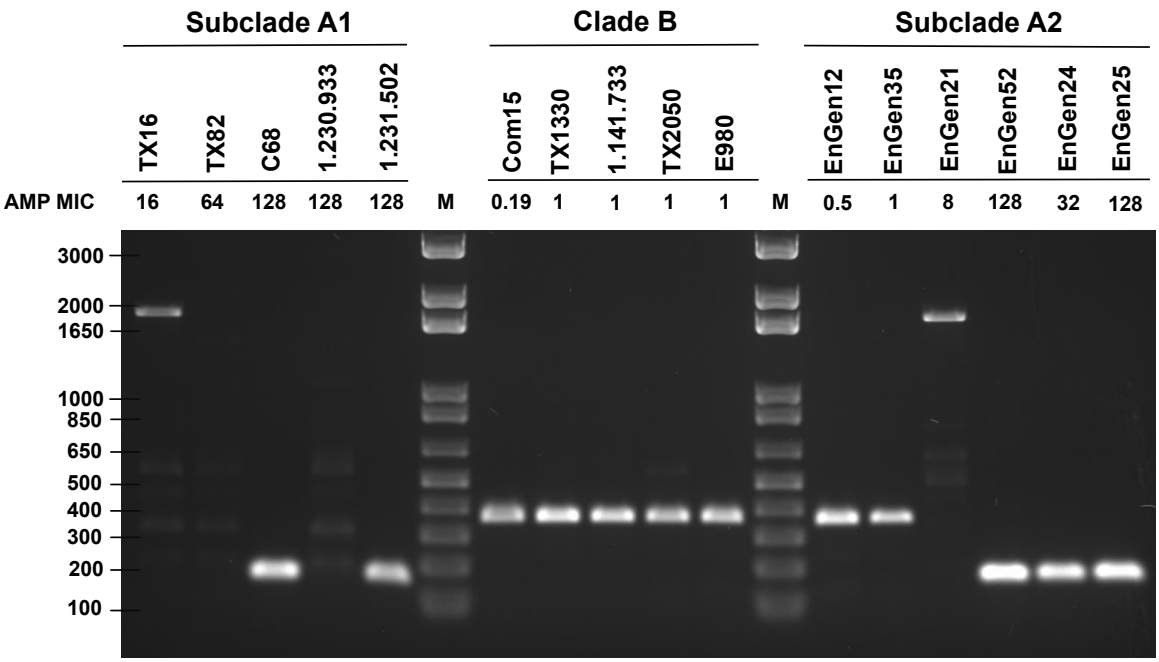

Figure 5.4. PCR upstream of *pbp5* using the primers *psr*-F-del and *pbp5*-R-del that anneal on *psr* and *pbp5*, respectively.

The *E. faecium* strains and ampicillin MICs are indicated above the image (See Table 5-1 for detailed description of the strains). The 201 bp deletion was confirmed in strains $C68_{A1,}$ $1.231.502_{A1,}$ $EnGen52_{A2,}$ $EnGen24_{A2}$ and $EnGen25_{A2,}$ while an insertion was detected in strains $TX16_{A1}$ and $EnGen21_{A2}$. In contrast, no PCR product was obtained for $TX16_{A1,}$ and $1.231.933_{A1.}$

```
TX1330_B        AGAAGTTAGAAATAACAATTTATGTTATGT----------------------------
EnGen21_A2      AGAAGTTAGAAATAACAATCTATGTTATGTTTTGACTTGAGAGTATAAAATATTTTGTGT
DO_A1           AGAAGTTAGAAATAACAATCTATGTTATGTTCTGACTTGAGAGTATAAAATATTTTGTGT
                ****************** **********

TX1330_B        ------------------------------------------------------------
EnGen21_A2      AAATGAAAAAATCCATACAAAAAAGGAAGTCCCTTCTGTAGAATAAAGTTAACGACAACC
DO_A1           AAATGAAAAAATCCATACAAAAAAGGAAGTCCCTTCTGTAGAATAAAGTTAACGACAACC

TX1330_B        ------------------------------------------------------------
EnGen21_A2      AATTCACAGAAAAGAGGACTTCCCTATGAATGATTTTACTACAGAAATTGTGCAAACTCT
DO_A1           AATTCACAGAAAAGAGGACTTCCCTATGAATGATTTTACTACAGAAATTGTGCAAACTCT

TX1330_B        ------------------------------------------------------------
EnGen21_A2      AGTCACTAAAGGCGATTTAAATGAATTATTCCGTTCGCACTTAGAAAAAGCGATAAACAC
DO_A1           AGTCACTAAAGGCGATTTAAATGAATTATTCCGTTCGCACTTAGAAAAAGCGATAAACAC

TX1330_B        ------------------------------------------------------------
EnGen21_A2      ACTCCTACGGACTGAATTAACGGCTTTTTTAGATTACGAAAAATATGATCGCACTGGTTT
DO_A1           ACTCCTACGGACTGAATTAACGGCTTTTTTAGATTACGAAAAATATGATCGCACTGGTTT

TX1330_B        ------------------------------------------------------------
EnGen21_A2      TAATTCAGGTAATTCGAGAAACGGTTCTTACTTTCGATCAATCAAAACCGAATATGGTGA
DO_A1           TAATTCAGGTAATTCGAGAAACGGTTCTTACTTTCGATCAATCAAAACCGAATATGGTGA

TX1330_B        ------------------------------------------------------------
EnGen21_A2      ATTAACATTGGAAATACCTAGAGATCGTAATGGTGAGTTTAAACAACAAACTTTACCAGC
DO_A1           ATTAACATTGGAAATACCTAGAGATCGTAATGGTGAGTTTAAACAACAAACTTTACCAGC

TX1330_B        ------------------------------------------------------------
EnGen21_A2      CTACAAAAGAACAAACGATACATTGGAAACCACTATTATCCATTTATTCGAAAAAGGTGT
DO_A1           CTACAAAAGAACAAACGATACATTGGAAACCACTATTATCCATTTATTCGAAAAAGGTGT

TX1330_B        ------------------------------------------------------------
EnGen21_A2      TACGATGTCTGAAATTGCTGATTTGATCGAAAAAATGTACGGTCATCACTATACTCCACA
DO_A1           TACGATGTCTGAAATTGCTGATTTGATCGAAAAAATGTACGGTCATCACTATACTCCACA

TX1330_B        ------------------------------------------------------------
EnGen21_A2      AACCATGTCCAACATGACTAAAGTTCTGACTGAAGAAGTAAATGCCTTTAAATCCAGAGC
DO_A1           AACCATGTCCAACATGACTAAAGTTCTGACTGAAGAAGTAAATGCCTTTAAATCCAGAGC

TX1330_B        ------------------------------------------------------------
EnGen21_A2      CTTAAATGATAAGTATGTCGCTATTTTTATGGACGCTACTTACATTCCACTAAAACGTCA
DO_A1           CTTAAATGATAAGTATGTCGCTATTTTTATGGACGCTACTTACATTCCACTAAAACGTCA
```

```
TX1330_B        ------------------------------------------------------------
EnGen21_A2      AACTGTATCCAAAGAAGCGATTTATATTGCCATTGGTATACGAGAAGACGGCACTAAAGA
DO_A1           AACCGTATCCAAAGAAGCGATTTATATTGCCATTGGTATACGAGAAGACGGCACTAAAGA

TX1330_B        ------------------------------------------------------------
EnGen21_A2      AGTACTGAGTTATGCGATTGCTCCAACTGAATCAACATACGTTTGGAATGAGCTGCTACA
DO_A1           AGTACTGAGTTATGCGATTGCTCCAACTGAATCAACATACGTTTGGAATGAGCTGCTACA

TX1330_B        ------------------------------------------------------------
EnGen21_A2      GGATATTAACTCCAGAGGAGTTCAAGAAGTCTTGCTTTTTTATTACGGACGGCTTAAAAGG
DO_A1           GGATATTAACTCCAGAGGAGTTCAAGAAGTCTTGCTTTTTTATTACGGACGGCTTAAAAGG

TX1330_B        ------------------------------------------------------------
EnGen21_A2      CATGAAAGATACTATCCATCAAATTTATCCTAAAGCAAAATATCAGCATTGTTGTATCCA
DO_A1           CATGAAAGATACTATCCATCAAATTTATCCTAAAGCAAAATATCAGCATTGTTGTATCCA

TX1330_B        ------------------------------------------------------------
EnGen21_A2      TGTATCTCGTAATATCGCTCATAAAGTACGTGTCAAAGACCGAAAAGAAATCTGTGATGA
DO_A1           TGTATCTCGTAACATCGCTCATAAAGTACGTGTCAAAGACCGAAAAGAAATCTGTGATGA

TX1330_B        ------------------------------------------------------------
EnGen21_A2      CTTTAAGGCTGTTTATCAAGCTAACTCAAAAGAAGAAGCGAATACCTTCTTATCCGGCAT
DO_A1           CTTTAAGGCTGTTTATCAAGCTAACTCAAAAGAAGAAGCGAATACCTTCTTATCCGGCAT

TX1330_B        ------------------------------------------------------------
EnGen21_A2      GATTGAGAAATGGAAGAAAAACTATCCTAAAGTGACGCAGTCACTCATAGAAAACCAAGA
DO_A1           GATTGAGAAATGGAAGAAAAACTATCCTAAAGTGACGCAGTCACTCATAGAAAACCAAGA

TX1330_B        ------------------------------------------------------------
EnGen21_A2      CTTATTAACTTTTTATGATTTTCCACCTAGCATTCGTAGAACCATTTACTCAACCAATCT
DO_A1           CTTATTAACTTTTTATGATTTTCCACCTAGCATTCGTAGAACCATTTACTCAACCAATCT

TX1330_B        ------------------------------------------------------------
EnGen21_A2      AATCGAGTCTTTCAATAAGCAAATTAAAAGATACAGCCGTAGAAAAGAGCAGTTTCAAAA
DO_A1           AATCGAGTCTTTCAATAAGCAAATTAAAAGATACAGCCGTAGAAAAGAGCAGTTTCAAAA

TX1330_B        ------------------------------------------------------------
EnGen21_A2      TGAAGAATCACTAGAACGCTTTCTAGTCAGCATTTTTGATACATACAATCAAAAATTTCT
DO_A1           TGAAGAATCACTAGAACGCTTTCTAGTCAGCATTTTTGATACATACAATCAAAAATTTCT

TX1330_B        ------------------------------------------------------------
EnGen21_A2      AAACAGAAGCCATAAAGGTTTTCAACAGGTAACCGATACATTAGTTTCAATGTTTACTGA
DO_A1           AAACAGAAGCCATAAAGGTTTTCAACAGGTAACCGATACATTAGTTTCAATGTTTACTGA
```

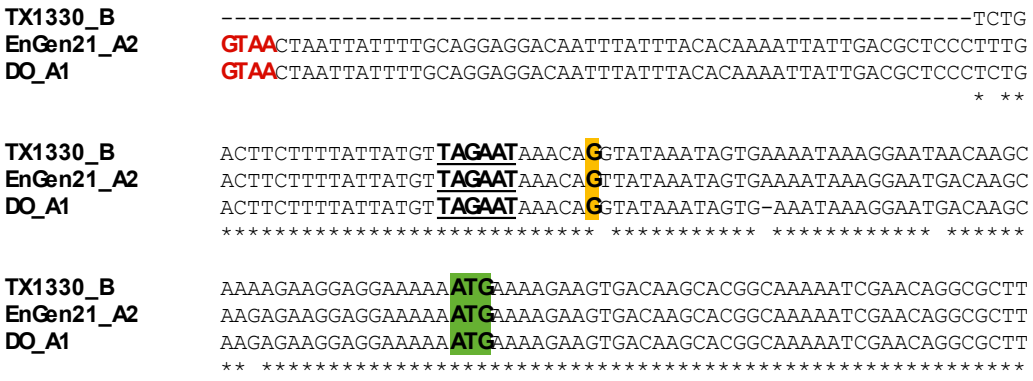

Figure 5.5. Alignment of the upstream region of *pbp5* from the *E. faecium* strains EnGen21$_{A2}$ and TX16 (DO)$_{A1}$ against TX1330$_{B}$.

The transposase sequence is shown in red. The transcriptional start site of the *pbp5* gene, demonstrated by Rice et al. (142), and the translational start codon are highlighted in yellow and green, respectively. The putative -10 box predicted in strain C68 is in bold and underlined (142).

On the other hand, no PCR product using the primer pair *psr*-F-del-*pbp5*-R-del was obtained for strains $TX82_{A1}$ and $1.230.933_{A1}$ (MICs = 64-128 µg/ml) (Figure 5.4), which suggested a different genetic arrangement in the upstream region of these strains. When I analyzed the region upstream of *pbp5* in the draft genome of $TX82_{A1}$ and $1.230.933_{A1}$ a series of gaps in the sequence were detected; however, sequence alignments and PCR results, designed to close these gaps (Table 5-3), strongly suggest that the *pbp5* upstream sequence of these two strains is similar to the *pbp5* upstream sequence of the subclade A1 strain, Aus0004 (data not shown). The region between the *psr* and the *pbp5* gene in Aus0004 includes three different ORFs, IS*Efm1*, *gnat* and *hisJ,* predicted to encode a transposase, an acetyltransferase and a histidinol phosphate phosphatase, respectively (Figure 5.6). Of note, although these large deletion and insertional events likely affect the promoter region of *pbp5*, specifically the region upstream of the putative -10 sequence predicted by Rice et al. (142), we can not discard a role of Psr, since all the strains with ampicillin MICs ≥ 8 µg/ml had alterations in the sequence of the *psr* gene (data not shown) that could render this protein non-functional.

In addition, I found several other small insertions, deletions and SNPs, between clades that could be associated with the differential expression of PBP5. A single nucleotide deletion between the demonstrated *pbp5* transcriptional start (142) and the predicted ATG translational start was observed in clade A ampicillin-resistant strains versus clade B and subclade A2 ampicillin susceptible strains. In addition, a 5 bp deletion in the intergenic region of *psr* and *pbp5* was observed in the clade A background compared to the clade B background (data not shown). In contrast, all the strains from clade B have a full-length *psr* gene located immediately upstream of *pbp5* and no deletions or insertions in the *pbp5-psr* intergenic region were observed.

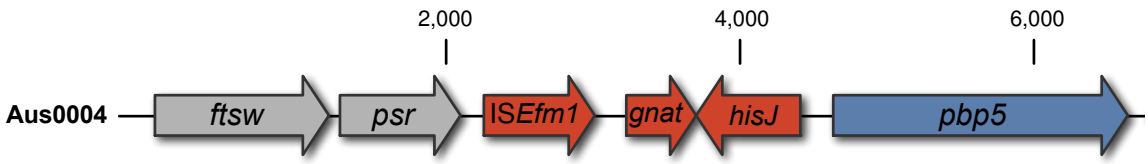

Figure 5.6. Genetic environment of *pbp5* in the *E. faecium* strain Aus0004.

Three ORFs, IS*Efm1, gnat* and *hisJ* (shown in red), are located in between *psr* and *pbp5* and are predicted to code for a transposase, an acetyltransferase and a histidinol phosphate phosphatase of the HisJ family, respectively.

High-level ampicillin resistance in *E. faecium* has been primarily associated with sequence mutations in the transpeptidase domain of the low-affinity PBP5 (58, 68, 131-133); however, earlier reports also pointed to increased production of PBP5 as a contributor to resistance, in particular in isolates with intermediate MICs (16 to 64 µg/ml) (65, 134, 135). Here, we found that ampicillin-resistant strains, including highly resistant strains with MICs > 64 µg/ml from subclades A1 and A2, showed higher PBP5 protein levels compared to ampicillin-susceptible clade B and subclade A2 strains (Figure 5.1 & Figure 5.2). This is in contrast to what was reported by Rybkine et al., who found an apparent decrease in PBP5 protein abundance in isolates with MICs greater than 16 µg/ml (132). Conversely, our results are in accordance with previous findings by Fontana et al. that reported that the PBP5 protein levels in highly ampicillin-resistant strains are elevated (135). The controversial role of PBP5 overproduction in ampicillin resistance might be explained, at least in part, by the fact that most of the earlier studies used radiolabeled penicillin as a measure of PBP5 quantity, an experimental approach that also measures the ability of PBP5 to bind to the labeled compound (135), which has been shown to be decreased by the presence of specific PBP5 mutations (131).

Overall, the results presented in this chapter provide further insight into PBP5-mediated resistance, highlighting that, in addition to amino acid sequence alterations in PBP5, overproduction of this protein is also observed in highly resistant strains from clade A. In addition, this finding underscores the contribution of the clade background in the regulation of PBP5 abundance and points to differences in the upstream region of *pbp5* as likely contributors to the differential levels of PBP5. Further studies are warranted in order to elucidate the underlying mechanism for the differential regulation of PBP5 levels between the *E. faecium* clades.

CHAPTER 6. CONCLUDING REMARKS AND FUTURE PERSPECTIVES

The rising clinical importance of members of the genus *Enterococcus*, primarily *E. faecalis* and *E. faecium* (5, 7), has prompted a number of investigations on factors that contribute to the pathogenesis and recent emergence of these organisms as important causes of infections. However, many aspects of the mechanisms used by enterococci to cause infections are still not understood. Considerable attention has been given to enterococcal surface proteins, including pili. The first part of this dissertation was focused on the Ebp pili of *E. faecalis* (**Chapter 2**) and its ortholog, the Emp, in *E. faecium* (**Chapter 3**). The work presented here indicates that Ebp and Emp pili display important differences in their regulation and function, despite the high homology between its subunits. Expression of the Ebp pili of *E. faecalis* seems more tightly controlled as compared to that of Emp pili of *E. faecium*. Studies in our lab have indicated that, after *E. faecalis* cells are grown in BHI media, less than 10% of the bacteria express pili on the surface (29). However, it has been demonstrated that the use of a different growth media, namely TSB-G, the addition of serum to BHI broth (BHI-S) or the presence of bicarbonate, enhances Ebp surface display (29, 40). It is important to note that when transcript levels of the *ebpABC* operon were compared, no significant differences were observed under the different growth conditions studied (29). This finding suggested that regulation of Ebp levels on the surface under different growth conditions might occur post-transcriptionally. Different stages of the pilus biogenesis pathway could be subject to this regulation, including translation, secretion across the membrane, polymerization of the pilus fiber and/or anchoring of the pili to the bacterial cell wall (39).

In **Chapter 2** of this dissertation, I demonstrated that a non-canonical initiation codon, ATT, is used as the start of EbpA translation. This codon was found conserved in all *E. faecalis* isolates sequenced to date; in contrast, an ATG codon, at the equivalent

position, was predicted as the translational start of several EbpA orthologs in other enterococcal species, including *E. faecium* (96). The presence of this rare start codon as the start of EbpA protein synthesis downregulates the rates of EbpA translation, which in turns diminishes the levels of EbpA on the surface of the cells, compared to an engineered ATG start codon (96). Regulating the levels of EbpA exposed on the surface of the cells could be important for establishing a precise ratio between EbpA (the tip) and EbpC (the shaft) of the pilus fiber as, in principle, only one subunit of EbpA is required to initiate the polymerization of pilus fibers that contained multiple EbpC subunits (96). It would be interesting to address in future studies if the ratio of the Emp subunits is controlled in *E. faecium* and if so, the molecular mechanism underlying this regulation.

Studies have demonstrated that downregulating the expression of immunogenic surface proteins could have positive effect for the bacterium in the context of human infections by diminishing the pressure exerted by the host immune system (89). By reducing the amount of EbpA on the surface, *E. faecalis* reduces its ability to form biofilms and adhere to fibrinogen (96); while these processes are important in the infection process, their reduction could potentially aid *E. faecalis* cells in dispersion to new sites and/or dissemination into the environment (96). Therefore, another interesting line for future research would be to establish if differences in the levels of pilation directly impact colonization and/or virulence using experimental animal models.

Based on what it is known about the strength of Shine-Dalgarno (SD) sequence, the optimal spacing between the SD sequence and the start codon, and the adenine rich region upstream of the SD region (145, 146), we postulate that EbpA abundance is also fine-tuned by additional features in its mRNA. In this regard, we observed differences in the sequence and location of the SD sequence between *ebpA* and the other subunits of

the *ebp* operon (*ebpB* and *ebpC*), and between *ebpA* and its ortholog gene in *E. faecium*, *empA,* which could suggest that EbpA levels are further downregulated by additional mechanisms.

In **Chapter 3**, fundamental insights into the function of the Emp subunits were presented. EmpA was shown to be located at the tip of the pilus fiber, but the vast majority was seen attached to the surface of *E. faecium* cells, presumably as monomers. In addition, it was found that, of the three subunits of Emp, EmpA is the most relevant subunit in biofilm formation and adherence to ECM proteins. These results are consistent with our previous findings on the tip subunit of the *E. faecalis* Ebp (32). Furthermore, we found that deletion of *empA* caused the production of very long pilus-like structures, a phenomenon that was also observed by deletion of *ebpA* from *E. faecalis* (32). Since, in addition to longer pili, a marked reduction in the number of pilus fibers per bacterial cell was observed in our immunoelectron microscopy studies, one can predict that the availability of the tip subunits, EmpA and EbpA, in *E. faecium* and *E. faecalis*, respectively, may be important for efficient initiation of pilus polymerization. One possibility that could help explain the phenotype observed is that, when initiation of pilus polymerization occurs in the absence of a tip subunit, by a mechanism yet to be determined, pilus polymerization continues beyond typical wild-type lengths due to availability of the shaft subunit and reduction in the number of sites for initiation of pilus polymerization.

The findings presented in **Chapter 3** also show that EmpB, the base or anchor of the pilus fiber, is important for biofilm formation and ECM adherence, while EmpC, the shaft pilin of the Emp, is completely dispensable for these processes. This is different from our lab's findings in *E. faecalis*, where deletion of *ebpC,* and not deletion of *ebpB,*

affected the ability of the cells to form biofilms, although this reduction was small in magnitude (32). Despite the fact that deletion of *empC* did not affect biofilm or ECM adherence in *E. faecium*, it was found that this subunit as well as the other Emp subunits, EmpA and EmpB, are important in a model of UTI. Furthermore, we provided evidence that EmpA is important for *E. faecium* pathogenicity in an endocarditis model. Overall, the results presented in **Part I** of this dissertation contribute to our understanding of pili regulation and function in enterococci. One can envision that targeting the tip subunit of the enterococcal pili, EbpA and EmpA, could be an excellent choice for vaccine or drug development in a pathogen characterized by high levels of resistance to the commonly used antibiotic therapies. Indeed, it has been demonstrated that vaccination with EbpA affects *E. faecalis* ability to form biofilm and to bind to fibrinogen and protects mice in a CAUTI model (69). Success in targeting the Ebp pili, by the use of a monoclonal antibody against EbpC, was also demonstrated by Pinkston et al. (70).

In **Part II,** the focus shifted towards *E. faecium*. First, in **Chapter 4**, colonization by different strains that belong to the three known *E. faecium* clades (59) was explored. By using a mouse model, we found that, after monoinoculation of the strains, colonization was similar between the *E. faecium* clades; however, the in vitro growth of clade A strains was reduced relative to clade B strains (147). Interestingly, the dynamics observed when a strain from clade B was co-inoculated into the GIT with a strain of clade A reflects the colonization pattern seen in humans; that is, vast predominance of clade B in humans in the community and re-colonization of individuals who acquired clade A VRE nosocomially, with clade B strains soon after discharge from the hospital (22, 111, 127, 128). We found that, in six of seven in vivo co-inoculation experiments (A with B), clade B predominated over clade A, starting at day 2 in some pairs and after 14

days in all six pairs (147). In these experiments, in an attempt to resemble conditions in the community setting, no antibiotic treatment was given to the mice after they were fed with bacteria. One possible drawback of this study is that the colonization abilities of the strains in the murine model are not an accurate representation of the colonization abilities of the strains in humans; however, mice have been extensively used as a model organism for studying enterococcal colonization (15, 17, 121, 148-151).

The mechanism underlying the predominance of clade B over clade A isolates when co-inoculated is currently unknown, and represents an interesting topic for future research. In *E. faecalis,* it was demonstrated that the multidrug resistant strain V583 was eradicated by *E. faecalis* commensals of the GIT bacterial consortium, by a mechanism that involves pheromone responsive plasmids (152). On the other hand, Kommineni et al. showed that the production of an enterococcal bacteriocin (bac-21), encoded in a sex-pheromone responsive plasmid (pPD1), confers a competitive advantage to *E. faecalis* compared to enterococci indigenous of the mouse GIT or to an *E. faecalis* strain lacking pPD1 (153). Preliminary evidence suggests that, in the majority of the *E. faecium* strain pairs we studied, killing of the hospital strain by the commensal strain is not the reason why commensal strains predominated. Therefore, it is more likely that clade B strains are better able to compete for resources or for a niche, or that they have enhanced ability to cope with conditions in the gut, including the host immune system and/or the thousands of other organisms present in this environment. It also would be interesting to investigate if clade A and clade B colonize the same niche of the GIT. On this subject, it was recently shown that vancomycin-resistant *E. faecium* co-localize in the same region of the colon with another important nosocomial pathogen, *Klebsiella pneumoniae,* but most likely they reside in separate niches (154).

Another interesting line of investigation would be to address the effect of concurrent antibiotic treatment on the ability of the clades to colonize the GIT of mice, in order to investigate if the dynamics seen in the absence of antibiotics change upon antibiotic therapy. Since clade A strains display higher levels of resistance compared to clade B strains, we believe that antibiotic treatment would give the clade A isolates a fitness advantage over clade B isolates and other bacterial species of the microbiota that will impact the colonization dynamics. Although this prediction may seem obvious, it is complicated by parenteral delivery of antibiotics, which may or may not reach concentrations in the gut sufficient to inhibit other bacteria or select for one clade versus the other. Indeed, evaluating the effect of parenteral cephalosporin therapy, which is commonly used in the clinical setting, on the colonization dynamics of the *E. faecium* clades would be of high clinical relevance, since this therapy is associated with increased risk of developing enterococcal infections at variety of sites (155). In addition, it has been demonstrated that treatment with third-generation cephalosporins, such as ceftriaxone, preceded *E. faecium* overgrowth in 93% of patients (156).

Overall, the results presented in **Chapter 4** advanced our knowledge about the complex dynamics of GIT colonization by the *E. faecium* clades and open new avenues for future research aimed at deciphering the factors that contribute to the emergence of *E. faecium* as a prominent pathogen in the hospital environment. By understanding the reasons that promote *E. faecium* colonization, we could increase our capacity to identify individuals at risk for development of infections. These studies could also potentially lead to the design of therapeutic strategies aimed at diminishing intestinal colonization, which in turn should translate into decreased rates of infections.

In **Chapter 5**, the focus was on one core gene, *pbp5*, which shows sequence variation between the *E. faecium* clades. Previous studies have demonstrated that the distinct allelic types of *pbp5*, *pbp5-S* and *pbp5-R,* are associated with susceptibility and resistance to ampicillin, respectively; however, sequence differences alone could not explain the array of different ampicillin MICs seen in *E. faecium* (58, 68). The results presented in this chapter indicate that, in addition to different *pbp5* allelic types carried by the *E. faecium* clades, there are marked differences in PBP5 abundance that, in the majority of the strains, correlate with their ampicillin phenotype. Furthermore, we presented evidence of the extensive differences in the region upstream of the *pbp5* gene among the strains studied that may account for the differential abundance of PBP5. Considering that β-lactam resistance in *E. faecium* is a worldwide therapeutic problem, it will be of significant clinical interest to investigate the mechanism by which PBP5 levels are up-regulated in clade A resistant strains versus clade B/A2 susceptible strains.

In some instances, however, neither the PBP5 type nor its protein levels could account for the ampicillin MICs, which suggests that additional factors contribute to the differences in the ampicillin phenotypes among clinical isolates of *E. faecium.* In this regard, Zhang et al., using a transposon mutant library, identified a number of genes associated with ampicillin resistance (157). In that study, by the generation of non-polar markerless deletions or by disrupting the coding sequence using an insertional approach, it was found that three genes with roles in cell wall biogenesis, *ddcP*, ldt_{fm} and *pgt*, can contribute to ampicillin resistance in *E. faecium* (157). One could further investigate if differences in the sequence and/or expression levels of these recently identified ampicillin determinants could explain the yet unaccountable differences in the ampicillin MICs between certain *E. faecium* isolates. In addition, it is possible that other

factors could mediate activation or repression of PBP5 function or that PBP5 works in concert with other proteins to mediate resistance.

Taken together, the work presented in this dissertation offers important contributions to the understanding of the enterococcal pili including a mechanism that is part of the complex regulatory network that controls Ebp pilus expression in *E. faecalis* and the role that the Emp pili play in the pathogenesis of *E. faecium* infections. Furthermore, this work begins to shed light on the colonization dynamics of the *E. faecium* clades and also addresses how differences in the PBP5 levels between the clades are linked to the differential resistance to ampicillin. Overall, the results presented here are likely to lead to interesting future studies that could help explain why enterococci, in particular *E. faecium*, has recently become a more frequent cause of infections in hospitals.

REFERENCES

1. **Ludwig W**, **Seewaldt E**, **Renate K-B**, **Schleifer KH**, **Magrum L**, **R WC**, **Fox GE**, **Stackebrandt E**. 1985. The Phylogenetic Position of *Streptococcus* and *Enterococcus*. J Gen Microbiol **131**:543–551.
2. **Parte AC**. 2013. LPSN-list of prokaryotic names with standing in nomenclature. Nucleic Acids Res **42**:D613–D616.
3. **Van Tyne D**, **Gilmore MS**. 2014. Friend Turned Foe: Evolution of Enterococcal Virulence and Antibiotic Resistance. Microbiology **68**:337–356.
4. **Murray BE**. 1990. The life and times of the *Enterococcus*. Clin Microbiol Rev **3**:46–65.
5. **Arias CA**, **Murray BE**. 2012. The rise of the *Enterococcus*: beyond vancomycin resistance. Nat Rev Microbiol **10**:266–278.
6. **Franz CMAP**, **Huch M**, **Abriouel H**, **Holzapfel W**, **Gálvez A**. 2011. Enterococci as probiotics and their implications in food safety. Int J Food Microbiol **151**:125–140.
7. **Sievert DM**, **Ricks P**, **Edwards JR**, **Schneider A**, **Patel J**, **Srinivasan A**, **Kallen A**, **Limbago B**, **Fridkin S**, **for the National Healthcare Safety Network (NHSN) Team and Participating NHSN Facilities**. 2013. Antimicrobial-Resistant Pathogens Associated with Healthcare-Associated Infections: Summary of Data Reported to the National Healthcare Safety Network at the Centers for Disease Control and Prevention, 2009–2010. Infect Control Hosp Epidemiol **34**:1–14.
8. **Tedim AP**, **Ruiz-Garbajosa P**, **Corander J**, **Rodríguez CM**, **Cantón R**, **Willems RJ**, **Baquero F**, **Coque TM**. 2015. Population Biology of Intestinal *Enterococcus* Isolates from Hospitalized and Nonhospitalized Individuals in Different Age Groups. Appl Environ Microbiol **81**:1820–1831.
9. **Hollenbeck BL**, **Rice LB**. 2012. Intrinsic and acquired resistance mechanisms in *enterococcus*. Virulence **3**:421–569.
10. **Werner G**, **Coque TM**, **Franz CMAP**, **Grohmann E**, **Hegstad K**, **Jensen L**, **van Schaik W**, **Weaver K**. 2013. Antibiotic resistant enterococci-tales of a drug resistance gene trafficker. Int J Med Microbiol **303**:360–379.
11. **Uttley AH**, **Collins CH**, **Naidoo J**, **George RC**. 1988. Vancomycin-resistant

enterococci. Lancet **1**:57–58.

12. **Leclercq R**, **Derlot E**, **Duval J**, **Courvalin P**. 1988. Plasmid-Mediated Resistance to Vancomycin and Teicoplanin in *Enterococcus faecium*. N Engl J Med **319**:157–161.

13. **Bonten MJ**, **Willems R**, **Weinstein RA**. 2001. Vancomycin-resistant enterococci: why are they here, and where do they come from? Lancet Infect Dis **1**:314–325.

14. **Cattoir V**, **Leclercq R**. 2013. Twenty-five years of shared life with vancomycin-resistant enterococci: is it time to divorce? J Antimicrob Chemother **68**:731–742.

15. **Ubeda C**, **Taur Y**, **Jenq RR**, **Equinda MJ**, **Son T**, **Samstein M**, **Viale A**, **Socci ND**, **van den Brink MR**, **Kamboj M**, **G PE**. 2010. Vancomycin-resistant *Enterococcus* domination of intestinal microbiota is enabled by antibiotic treatment in mice and precedes bloodstream invasion in humans. J Clin Invest **120**:4332–4341.

16. **Taur Y**, **Xavier JB**, **Lipuma L**, **Ubeda C**, **Goldberg J**, **Gobourne A**, **Lee YJ**, **Dubin KA**, **Socci ND**, **Viale A**, **Perales MA**, **Jenq RR**, **van den Brink MRM**, **Pamer EG**. 2012. Intestinal Domination and the Risk of Bacteremia in Patients Undergoing Allogeneic Hematopoietic Stem Cell Transplantation. Clin Infect Dis **55**:905–914.

17. **Donskey CJ**, **Hanrahan JA**, **Hutton RA**, **Rice LB**. 2000. Effect of Parenteral Antibiotic Administration on the Establishment of Colonization with Vancomycin-Resistant *Enterococcus faecium* in the Mouse Gastrointestinal Tract. J Infect Dis **181**:1830–1833.

18. **Pultz NJ**, **Shankar N**, **Baghdayan AS**, **Donskey CJ**. 2005. Enterococcal surface protein Esp does not facilitate intestinal colonization or translocation of *Enterococcus faecalis* in clindamycin-treated mice. FEMS Microbiol Lett **242**:217–219.

19. **Brandl K**, **Plitas G**, **Mihu CN**, **Ubeda C**, **Jia T**, **Fleisher M**, **Schnabl B**, **DeMatteo RP**, **G PE**. 2008. Vancomycin-resistant enterococci exploit antibiotic-induced innate immune deficits. Nature **455**:804–807.

20. **Vaishnava S**, **Behrendt CL**, **Ismail AS**, **Eckmann L**, **Hooper LV**. 2008. Paneth cells directly sense gut commensals and maintain homeostasis at the intestinal

host-microbial interface. Proc Natl Acad Sci U S A **105**:20858–20863.

21. **Cash HL**, **Whitham CV**, **Behrendt CL**, **Hooper LV**. 2006. Symbiotic bacteria direct expression of an intestinal bactericidal lectin. Science **313**:1126–1130.

22. **Ruiz-Garbajosa P**, **del Campo R**, **Coque TM**, **Asensio A**, **Bonten M**, **Willems R**, **Baquero F**, **Canton R**. 2009. Longer Intestinal Persistence of *Enterococcus faecalis* Compared to *Enterococcus faecium* Clones in Intensive-Care-Unit Patients. J Clin Microbiol **47**:345–351.

23. **Guiton PS**, **Hannan TJ**, **Ford B**, **Caparon MG**, **Hultgren SJ**. 2013. *Enterococcus faecalis* Overcomes Foreign Body-Mediated Inflammation To Establish Urinary Tract Infections. Infect Immun **81**:329–339.

24. **Nigo M**, **Munita JM**, **Arias CA**, **Murray BE**. 2014. What's New in the Treatment of Enterococcal Endocarditis? Curr Infect Dis Rep **16**:431.

25. **Jett BD**, **Huycke MM**, **Gilmore MS**. 1994. Virulence of enterococci. Clin Microbiol Rev **7**:462–478.

26. **Sillanpaa J**. 2004. A family of putative MSCRAMMs from *Enterococcus faecalis*. Microbiology **150**:2069–2078.

27. **Ton-That H**, **Schneewind O**. 2004. Assembly of pili in Gram-positive bacteria. Trends Microbiol **12**:228–234.

28. **Telford JL**, **Barocchi MA**, **Margarit I**, **Rappuoli R**, **Grandi G**. 2006. Pili in Gram-positive pathogens. Nat Rev Microbiol **4**:509–519.

29. **Nallapareddy SR**, **Singh KV**, **Sillanpää J**, **Garsin DA**, **Höök M**, **Erlandsen SL**, **Murray BE**. 2006. Endocarditis and biofilm-associated pili of *Enterococcus faecalis*. J Clin Invest **116**:2799–2807.

30. **Tendolkar PM**, **Baghdayan AS**, **Shankar N**. 2006. Putative surface proteins encoded within a novel transferable locus confer a high-biofilm phenotype to *Enterococcus faecalis*. J Bact **188**:2063–2072.

31. **Nallapareddy SR**, **Sillanpaa J**, **Mitchell J**, **Singh KV**, **Chowdhury SA**, **Weinstock GM**, **Sullam PM**, **Murray BE**. 2011. Conservation of Ebp-Type Pilus Genes among Enterococci and Demonstration of Their Role in Adherence of *Enterococcus faecalis* to Human Platelets. Infect Immun **79**:2911–2920.

32. **Sillanpää J**, **Chang C**, **Singh K**, **Montealegre MC**, **Nallapareddy SR**, **Harvey BR**, **Ton-That H**, **Murray BE**. 2013. Contribution of Individual Ebp Pilus Subunits of *Enterococcus faecalis* OG1RF to Pilus Biogenesis, Biofilm Formation and Urinary Tract Infection. PLoS One **8**:e68813.

33. **Nielsen HV**, **Flores-Mireles AL**, **Kau AL**, **Kline KA**, **Pinkner JS**, **Neiers F**, **Normark S**, **Henriques-Normark B**, **Caparon MG**, **Hultgren SJ**. 2013. Pilin and Sortase Residues Critical for Endocarditis- and Biofilm-Associated Pilus Biogenesis in *Enterococcus faecalis*. J Bacteriol **195**:4484–4495.

34. **Nallapareddy SR**, **Singh KV**, **Sillanpaa J**, **Zhao M**, **Murray BE**. 2011. Relative Contributions of Ebp Pili and the Collagen Adhesin Ace to Host Extracellular Matrix Protein Adherence and Experimental Urinary Tract Infection by *Enterococcus faecalis* OG1RF. Infect Immun **79**:2901–2910.

35. **Nallapareddy SR**, **Murray BE**. 2008. Role Played by Serum, a Biological Cue, in the Adherence of *Enterococcus faecalis* to Extracellular Matrix Proteins, Collagen, Fibrinogen, and Fibronectin. J Infect Dis **197**:1728–1736.

36. **Singh KV**, **Nallapareddy SR**, **Murray BE**. 2007. Importance of the *ebp* (Endocarditis- and Biofilm- Associated Pilus) Locus in the Pathogenesis of *Enterococcus faecalis* Ascending Urinary Tract Infection. J Infect Dis **195**:1671–1677.

37. **Nielsen HV**, **Guiton PS**, **Kline KA**, **Port GC**, **Pinkner JS**, **Neiers F**, **Normark S**, **Henriques-Normark B**, **Caparon MG**, **Hultgren SJ**. 2012. The Metal Ion-Dependent Adhesion Site Motif of the *Enterococcus faecalis* EbpA Pilin Mediates Pilus Function in Catheter-Associated Urinary Tract Infection. mBio **3**:e00177–12.

38. **Bourgogne A**, **Singh KV**, **Fox KA**, **Pflughoeft KJ**, **Murray BE**, **Garsin DA**. 2007. EbpR Is Important for Biofilm Formation by Activating Expression of the Endocarditis and Biofilm-Associated Pilus Operon (*ebpABC*) of *Enterococcus faecalis* OG1RF. J Bacteriol **189**:6490–6493.

39. **Gao P**, **Pinkston KL**, **Nallapareddy SR**, **van Hoof A**, **Murray BE**, **Harvey BR**. 2010. *Enterococcus faecalis rnjB* Is Required for Pilin Gene Expression and Biofilm Formation. J Bacteriol **192**:5489–5498.

40. **Bourgogne A**, **Thomson LC**, **Murray BE**. 2010. Bicarbonate enhances

expression of the endocarditis and biofilm associated pilus locus, *ebpR-ebpABC*, in *Enterococcus faecalis*. BMC Microbiol **10**:17.

41. **Hendrickx AP**, **van Wamel WJ**, **Posthuma G**, **Bonten MJ**, **Willems RJ**. 2007. Five Genes Encoding Surface-Exposed LPXTG Proteins Are Enriched in Hospital-Adapted *Enterococcus faecium* Clonal Complex 17 Isolates. J Bacteriol **189**:8321–8332.

42. **Sillanpaa J**, **Nallapareddy SR**, **Prakash VP**, **Qin X**, **Hook M**, **Weinstock GM**, **Murray BE**. 2008. Identification and phenotypic characterization of a second collagen adhesin, Scm, and genome-based identification and analysis of 13 other predicted MSCRAMMs, including four distinct pilus loci, in *Enterococcus faecium*. Microbiology **154**:3199–3211.

43. **Hendrickx A**, **Bonten MJ**, **van Luit Asbroek M**, **Schapendonk CM**, **Kragten AHM**, **Willems RJ**. 2008. Expression of two distinct types of pili by a hospital-acquired *Enterococcus faecium* isolate. Microbiology **154**:3212–3223.

44. **Qin X**, **Galloway Peña JR**, **Sillanpää J**, **Roh J**, **Nallapareddy SR**, **Chowdhury S**, **Bourgogne A**, **Choudhury T**, **Muzny DM**, **Buhay CJ**, **Ding Y**, **Dugan-Rocha S**, **Liu W**, **Kovar C**, **Sodergren E**, **Highlander S**, **Petrosino JF**, **Worley KC**, **Gibbs RA**, **Weinstock GM**, **Murray BE**. 2012. Complete genome sequence of *Enterococcus faecium* strain TX16 and comparative genomic analysis of *Enterococcus faecium* genomes. BMC Microbiol **12**:135.

45. **Hendrickx AP**, **Schapendonk CM**, **van Luit-Asbroek M**, **Bonten MJ**, **van Schaik W**, **Willems RJ**. 2010. Differential PilA pilus assembly by a hospital-acquired and a community-derived *Enterococcus faecium* isolate. Microbiology **156**:2649–2659.

46. **Kim DS**, **Singh KV**, **Nallapareddy SR**, **Qin X**, **Panesso D**, **Arias CA**, **Murray BE**. 2010. The *fms21 (pilA)-fms20* locus encoding one of four distinct pili of *Enterococcus faecium* is harboured on a large transferable plasmid associated with gut colonization and virulence. J Med Microbiol **59**:505–507.

47. **Sillanpää J**, **Nallapareddy SR**, **Singh KV**, **Prakash VP**, **Fothergill T**, **Ton-That H**, **Murray BE**. 2010. Characterization of the ebp_{fm} pilus-encoding operon of *Enterococcus faecium* and its role in biofilm formation and virulence in a murine model of urinary tract infection. Virulence **1**:236–246.

48. **Arias CA**, **Murray BE**. 2009. Antibiotic-resistant bugs in the 21st century-a clinical super-challenge. N Engl J Med **360**:439–443.

49. **Ruiz-Garbajosa P**, **Bonten MJM**, **Robinson DA**, **Top J**, **Nallapareddy SR**, **Torres C**, **Coque TM**, **Canton R**, **Baquero F**, **Murray BE**, **del Campo R**, **Willems RJL**. 2006. Multilocus Sequence Typing Scheme for *Enterococcus faecalis* Reveals Hospital-Adapted Genetic Complexes in a Background of High Rates of Recombination. J Clin Microbiol **44**:2220–2228.

50. **Homan WL**, **Tribe D**, **Poznanski S**, **Li M**, **Hogg G**, **Spalburg E**, **van Embden JDA**, **Willems RJL**. 2002. Multilocus Sequence Typing Scheme for *Enterococcus faecium*. J Clin Microbiol **40**:1963–1971.

51. **Palmer KL**, **Godfrey P**, **Griggs A**, **Kos VN**, **Zucker J**, **Desjardins C**, **Cerqueira G**, **Gevers D**, **Walker S**, **Wortman J**, **Feldgarden M**, **Haas B**, **Birren B**, **Gilmore MS**. 2011. Comparative Genomics of Enterococci: Variation in *Enterococcus faecalis*, Clade Structure in *E. faecium*, and Defining Characteristics of *E. gallinarum* and *E. casseliflavus*. mBio **3**:e00318–11–e00318–11.

52. **Top J**, **Willems RJ**, **Blok H**, **de Regt M**, **Jalink K**, **Troelstra A**, **Goorhuis B**, **Bonten M**. 2007. Ecological replacement of *Enterococcus faecalis* by multiresistant clonal complex 17 *Enterococcus faecium*. Clin Microbiol Infect **13**:316–319.

53. **Willems RJ**, **Top J**, **van Schaik W**, **Leavis H**, **Bonten M**, **Sirén J**, **Hanage WP**, **Corander J**. 2012. Restricted Gene Flow among Hospital Subpopulations of *Enterococcus faecium*. mBio **3**:e00151–12.

54. **Leavis HL**, **Bonten MJ**, **Willems RJ**. 2006. Identification of high-risk enterococcal clonal complexes: global dispersion and antibiotic resistance. Curr Opin Microbiol **9**:454–460.

55. **Leavis HL**, **Willems RJ**, **van Wamel WJ**, **Schuren FH**, **Caspers MP**, **Bonten MJ**. 2007. Insertion Sequence–Driven Diversification Creates a Globally Dispersed Emerging Multiresistant Subspecies of *E. faecium*. PLoS Pathog **3**:e7.

56. **van Schaik W**, **Top J**, **Riley DR**, **Boekhorst J**, **Vrijenhoek JE**, **Schapendonk CM**, **Hendrickx AP**, **Nijman IJ**, **Bonten MJ**, **Tettelin H**, **Willems RJ**. 2010. Pyrosequencing-based comparative genome analysis of the nosocomial pathogen

Enterococcus faecium and identification of a large transferable pathogenicity island. BMC Genomics **11**:239.

57. **Galloway-Peña J**, **Roh JH**, **Latorre M**, **Qin X**, **Murray BE**. 2012. Genomic and SNP Analyses Demonstrate a Distant Separation of the Hospital and Community-Associated Clades of *Enterococcus faecium*. PLoS One **7**:e30187.

58. **Galloway-Pena JR**, **Rice LB**, **Murray BE**. 2011. Analysis of PBP5 of Early U.S. Isolates of *Enterococcus faecium*: Sequence Variation Alone Does Not Explain Increasing Ampicillin Resistance over Time. Antimicrob Agents Chemother **55**:3272–3277.

59. **Lebreton F**, **van Schaik W**, **McGuire AM**, **Godfrey P**, **Griggs A**, **Mazumdar V**, **Corander J**, **Cheng L**, **Saif S**, **Young S**, **Zeng Q**, **Wortman J**, **Birren B**, **Willems RJ**, **Earl AM**, **Gilmore MS**. 2013. Emergence of Epidemic Multidrug-Resistant *Enterococcus faecium* from Animal and Commensal Strains. mBio e00534–13.

60. **de Been M**, **van Schaik W**, **Cheng L**, **Corander J**, **Willems RJ**. 2013. Recent Recombination Events in the Core Genome Are Associated with Adaptive Evolution in *Enterococcus faecium*. Genome Biol Evol **5**:1524–1535.

61. **Ghuysen JM**. 1994. Molecular structures of penicillin-binding proteins and β-lactamases. Trends Microbiol **2**:372–380.

62. **Scheffers DJ**, **Pinho MG**. 2005. Bacterial Cell Wall Synthesis: New Insights from Localization Studies. Microbiol Mol Biol Rev **69**:585–607.

63. **Rice LB**, **Carias LL**, **Rudin S**, **Hutton R**, **Marshall S**, **Hassan M**, **Josseaume N**, **Dubost L**, **Marie A**, **Arthur M**. 2009. Role of Class A Penicillin-Binding Proteins in the Expression of Beta-Lactam Resistance in *Enterococcus faecium*. J Bact **191**:3649–3656.

64. **Sauvage E**, **Kerff F**, **Fonz x000E9 E**, **Herman R**, **Schoot B**, **Marquette JP**, **Taburet Y**, **Prevost D**, **Dumas J**, **Leonard G**, **Stefanic P**, **Coyette J**, **Charlier P**. 2002. The 2.4-A crystal structure of the penicillin-resistant penicillin-binding protein $PBP5_{fm}$ from *Enterococcus faecium* in complex with benzylpenicillin. Cell MolLife Sci **59**:1223–1232.

65. **Williamson R**, **Le Bouguénec C**, **Gutmann L**, **T H**. 1985. One or Two Low Affinity Penicillin-binding Proteins May Be Responsible for the Range of Susceptibility of

Enterococcus faecium to Benzylpenicillin. J Gen Microbiol **131**:1933–1940.

66. **Canepari P**, **Lleó MDM**, **Fontana R**, **Satta G**. 1986. In *Streptococcus faecium* Penicillin-binding Protein 5 Alone Is Sufficient for Growth at Sub-maximal But Not at Maximal Rate. J Gen Microbiol **132**:2061–2061.

67. **Fontana R**, **Cerini R**, **Longoni P**, **Grossato A**, **Canepari P**. 1983. Identification of a streptococcal penicillin-binding protein that reacts very slowly with penicillin. J Bacteriol **155**:1343–1350.

68. **Pietta E**, **Montealegre MC**, **Roh JH**, **Cocconcelli PS**, **Murray BE**. 2014. *Enterococcus faecium* PBP5-S/R, the Missing Link between PBP5-S and PBP5-R. Antimicrob Agents Chemother **58**:6978–6981.

69. **Flores-Mireles AL**, **Pinkner JS**, **Caparon MG**, **Hultgren SJ**. 2014. EbpA vaccine antibodies block binding of *Enterococcus faecalis* to fibrinogen to prevent catheter-associated bladder infection in mice. Sci Transl Med **6**:254ra127.

70. **Pinkston KL**, **Singh KV**, **Gao P**, **Wilganowski N**, **Robinson H**, **Ghosh S**, **Azhdarinia A**, **Sevick-Muraca EM**, **Murray BE**, **Harvey BR**. 2014. Targeting Pili in Enterococcal Pathogenesis. Infect Immun **82**:1540–1547.

71. **Kozak M**. 1983. Comparison of initiation of protein synthesis in procaryotes, eucaryotes, and organelles. Microbiol Rev **47**:1–45.

72. **Laursen BS**, **Sorensen HP**, **Mortensen KK**, **Sperling-Petersen HU**. 2005. Initiation of Protein Synthesis in Bacteria. Microbiol Mol Biol Rev **69**:101–123.

73. **Binns N**, **Masters M**. 2002. Expression of the *Escherichia coli pcnB* gene is translationally limited using an inefficient start codon: a second chromosomal example of translation initiated at AUU. Mol Microbiol **44**:1287–1298.

74. **Sacerdot C**, **Fayat G**, **Dessen P**, **Springer M**, **Plumbridge JA**, **Grunberg-Manago M**, **Blanquet S**. 1982. Sequence of a 1.26-kb DNA fragment containing the structural gene for *E.coli* initiation factor IF3: presence of an AUU initiator codon. EMBO J **1**:311–315.

75. **Kristich CJ**, **Chandler JR**, **Dunny GM**. 2007. Development of a host-genotype-independent counterselectable marker and a high-frequency conjugative delivery system and their use in genetic analysis of *Enterococcus faecalis*. Plasmid **57**:131–144.

76. **Panesso D**, **Montealegre MC**, **Rincón S**, **Mojica MF**, **Rice LB**, **Singh KV**, **Murray BE**, **Arias CA**. 2011. The *hyl*$_{Efm}$ gene in pHylEfm of *Enterococcus faecium* is not required in pathogenesis of murine peritonitis. BMC Microbiol **11**:20.

77. **Murray BE**, **Singh KV**, **Ross RP**, **Heath JD**, **Dunny GM**, **Weinstock GM**. 1993. Generation of restriction map of *Enterococcus faecalis* OG1 and investigation of growth requirements and regions encoding biosynthetic function. J Bacteriol **175**:5216–5223.

78. **Leenhouts K**. 1996. A general system for generating unlabelled gene replacements in bacterial chromosomes. Mol Gen Genet **253**:217–24.

79. **Ramesh A**, **DebRoy S**, **Goodson JR**, **Fox KA**, **Faz H**, **Garsin DA**, **Winkler WC**. 2012. The Mechanism for RNA Recognition by ANTAR Regulators of Gene Expression. PLoS Genet **8**:e1002666.

80. **Hammerstrom TG**, **Roh JH**, **Nikonowicz EP**, **Koehler TM**. 2011. Bacillus anthracis virulence regulator AtxA: oligomeric state, function and CO2-signalling. Mol Microbiol **82**:634–647.

81. **Mohamed JA**, **Huang W**, **Nallapareddy SR**, **Teng F**, **Murray BE**. 2004. Influence of Origin of Isolates, Especially Endocarditis Isolates, and Various Genes on Biofilm Formation by *Enterococcus faecalis*. Infect Immun **72**:3658–3663.

82. **Meyerovich M**, **Mamou G**, **Ben-Yehuda S**. 2010. Visualizing high error levels during gene expression in living bacterial cells. Proc Natl Acad Sci USA **107**:11543–11548.

83. **Sacerdot C**, **Chiaruttini C**, **Engst K**, **Graffe M**, **Milet M**, **Mathy N**, **Dondon J**, **Springer M**. The role of the AUU initiation codon in the negative feedback regulation of the gene for translation initiation factor IF3 in *Escherichia coli*. Mol Microbiol **21**:331–346.

84. **O'Donnell SM**, **Janssen GR**. 2001. The Initiation Codon Affects Ribosome Binding and Translational Efficiency in *Escherichia coli* of cI mRNA with or without the 5' Untranslated Leader. J Bacteriol **183**:1277–1283.

85. **Myasnikov AG**, **Simonetti A**, **Marzi S**, **Klaholz BP**. 2009. Structure–function insights into prokaryotic and eukaryotic translation initiation. Curr Opin Struct Biol **19**:300–309.

86. **Whittaker CA**. 2002. Distribution and Evolution of von Willebrand/Integrin A Domains: Widely Dispersed Domains with Roles in Cell Adhesion and Elsewhere. Mol Biol Cell **13**:3369–3387.

87. **Konto-Ghiorghi Y**, **Mairey E**, **Mallet A**, **Duménil G**, **Caliot E**, **Trieu-Cuot P**, **Dramsi S**. 2009. Dual role for pilus in adherence to epithelial cells and biofilm formation in *Streptococcus agalactiae*. PLoS Pathog **5**:e1000422.

88. **Izoré T**, **Contreras-Martel C**, **Mortaji El L**, **Manzano C**, **Terrasse R**, **Vernet T**, **Di Guilmi AM**, **Dessen A**. 2010. Structural Basis of Host Cell Recognition by the Pilus Adhesin from *Streptococcus pneumoniae*. Structure **18**:106–115.

89. **Danne C**, **Dubrac S**, **Trieu-Cuot P**, **Dramsi S**. 2014. Single Cell Stochastic Regulation of Pilus Phase Variation by an Attenuation-like Mechanism. PLoS Pathog **10**:e1003860.

90. **Sillanpaa J**, **Prakash VP**, **Nallapareddy SR**, **Murray BE**. 2009. Distribution of Genes Encoding MSCRAMMs and Pili in Clinical and Natural Populations of *Enterococcus faecium*. J Clin Microbiol **47**:896–901.

91. **Almohamad S**, **Somarajan SR**, **Singh KV**, **Nallapareddy SR**, **Murray BE**. 2014. Influence of isolate origin and presence of various genes on biofilm formation by *Enterococcus faecium*. FEMS Microbiol Lett **353**:151–156.

92. **Nallapareddy SR**, **Singh KV**, **Murray BE**. 2006. Construction of Improved Temperature-Sensitive and Mobilizable Vectors and Their Use for Constructing Mutations in the Adhesin-Encoding acm Gene of Poorly Transformable Clinical *Enterococcus faecium* Strains. Appl Environ Microbiol **72**:334–345.

93. **Pace CN**, **Vajdos F**, **Fee L**, **Grimsley G**, **Gray T**. 1995. How to measure and predict the molar absorption coefficient of a protein. Protein Sci **4**:2411–2423.

94. **Singh KV**, **Nallapareddy SR**, **Sillanpää J**, **Murray BE**. 2010. Importance of the Collagen Adhesin Ace in Pathogenesis and Protection against *Enterococcus faecalis* Experimental Endocarditis. PLoS Pathog **6**:e1000716.

95. **Chang C**, **Mandlik A**, **Das A**, **Ton-That H**. 2011. Cell surface display of minor pilin adhesins in the form of a simple heterodimeric assembly in *Corynebacterium diphtheriae*. Mol Microbiol **79**:1236–1247.

96. **Montealegre MC**, **La Rosa SL**, **Roh JH**, **Harvey BR**, **Murray BE**. 2015. The

Enterococcus faecalis EbpA Pilus Protein: Attenuation of Expression, Biofilm Formation, and Adherence to Fibrinogen Start with the Rare Initiation Codon ATT. mBio **6**:e00467–15.

97. **Wolz C**, **McDevitt D**, **Foster TJ**, **Cheung AL**. 1996. Influence of *agr* on fibrinogen binding in *Staphylococcus aureus* Newman. Infect Immun **64**:3142–3147.

98. **Singh KV**, **Coque TM**, **Weinstock GM**, **Murray BE**. 1998. In vivo testing of an *Enterococcus faecalis efaA* mutant and use of *efaA* homologs for species identification. FEMS Immunol Med Microbiol **21**:323–331.

99. **Kemp KD**, **Singh KV**, **Nallapareddy SR**, **Murray BE**. 2007. Relative contributions of *Enterococcus faecalis* OG1RF sortase-encoding genes, *srtA* and *bps* (*srtC*), to biofilm formation and a murine model of urinary tract infection. Infect Immun **75**:5399–5404.

100. **Hendrickx APA**, **Willems RJL**, **Bonten MJM**, **van Schaik W**. 2009. LPxTG surface proteins of enterococci. Trends Microbiol **17**:423–430.

101. **Wu C**, **Mishra A**, **Yang J**, **Cisar JO**, **Das A**, **Ton-That H**. 2011. Dual Function of a Tip Fimbrillin of Actinomyces in Fimbrial Assembly and Receptor Binding. J Bacteriol **193**:3197–3206.

102. **Dramsi S**, **Caliot E**, **Bonne I**, **Guadagnini S**, **Prévost MC**, **Kojadinovic M**, **Lalioui L**, **Poyart C**, **Trieu-Cuot P**. 2006. Assembly and role of pili in group B streptococci. Mol Microbiol **60**:1401–1413.

103. **Swierczynski A**, **Ton-That H**. 2006. Type III Pilus of Corynebacteria: Pilus Length Is Determined by the Level of Its Major Pilin Subunit. J Bacteriol **188**:6318–6325.

104. **Zhao M**, **SillanpÃ Ã J**, **Nallapareddy SR**, **Murray BE**. 2009. Adherence to host extracellular matrix and serum components by *Enterococcus faecium* isolates of diverse origin. FEMS Microbiol Lett **301**:77–83.

105. **Mandlik A**, **Arrlene S**, **Das A**, **Ton-That H**. 2007. *Corynebacterium diphtheriae* employs specific minor pilins to target human pharyngeal epithelial cells. Mol Microbiol **64:**111-124.

106. **Leavis HL**, **Willems RJ**, **Top J**, **Bonten MJ**. 2006. High-Level Ciprofloxacin Resistance from Point Mutations in *gyrA* and *parC* Confined to Global Hospital-

Adapted Clonal Lineage CC17 of *Enterococcus faecium*. J Clin Microbiol **44**:1059–1064.

107. **Werner G**, **Fleige C**, **Geringer U**, **van Schaik W**, **Klare I**, **Witte W**. 2011. IS element IS16 as a molecular screening tool to identify hospital-associated strains of *Enterococcus faecium*. BMC Infect Dis **11**:80.

108. **Lund B**, **Edlund C**. 2003. Bloodstream Isolates of *Enterococcus faecium* Enriched with the Enterococcal Surface Protein Gene, esp, Show Increased Adhesion to Eukaryotic Cells. J Clin Microbiol **41**:5183–5185.

109. **Leendertse M**, **Heikens E**, **Wijnands LM**, **van Luit Asbroek M**, **Teske GJD**, **Roelofs JJTH**, **Bonten MJM**, **van der Poll T**, **Willems RJL**. 2009. Enterococcal Surface Protein Transiently Aggravates *Enterococcus faecium*–Induced Urinary Tract Infection in Mice. J Infect Dis **200**:1162–1165.

110. **Nallapareddy SR**, **Singh KV**, **Murray BE**. 2008. Contribution of the Collagen Adhesin Acm to Pathogenesis of *Enterococcus faecium* in Experimental Endocarditis. Infect Immun **76**:4120–4128.

111. **Weisser M**, **Oostdijk EA**, **Willems RJ**, **Bonten MJ**, **Frei R**, **Elzi L**, **Halter J**, **Widmer AF**, **Top J**. 2012. Dynamics of ampicillin-resistant *Enterococcus faecium* clones colonizing hospitalized patients: Data from a prospective observational study. BMC Infect Dis **12**:68.

112. **Murray BE**, **Singh KV**, **Heath JD**, **Sharma BR**, **Weinstock GM**. 1990. Comparison of genomic DNAs of different enterococcal isolates using restriction endonucleases with infrequent recognition sites. J Clin Microbiol **28**:2059–2063.

113. **Creti R**, **Koch S**, **Fabretti F**, **Baldassarri L**, **Huebner J**. 2006. Enterococcal colonization of the gastro-intestinal tract: role of biofilm and environmental oligosaccharides. BMC Microbiol **6**:60.

114. **Rice LB**, **Laktičová V**, **Carias LL**, **Rudin S**, **Hutton R**, **Marshall SH**. 2009. Transferable capacity for gastrointestinal colonization in *Enterococcus faecium* in a mouse model. J Infect Dis **199**:342–349.

115. **Carias LL**, **Rudin SD**, **Donskey CJ**, **Rice LB**. 1998. Genetic linkage and cotransfer of a novel, *vanB*-containing transposon (Tn5382) and a low-affinity penicillin-binding protein 5 gene in a clinical vancomycin-resistant *Enterococcus*

faecium isolate. J Bact **180**:4426–4434.

116. **Arias CA**, **Torres HA**, **Singh KV**, **Panesso D**, **Moore J**, **Wanger A**, **Murray BE**. 2007. Failure of Daptomycin Monotherapy for Endocarditis Caused by an *Enterococcus faecium* Strain with Vancomycin-Resistant and Vancomycin-Susceptible Subpopulations and Evidence of In Vivo Loss of the *vanA* Gene Cluster. Clin Infect Dis **45**:1343–1346.

117. **Arduino RC**, **Jacques-Palaz K**, **Murray BE**, **Rakita RM**. 1994. Resistance of *Enterococcus faecium* to neutrophil-mediated phagocytosis. Infect Immun **62**:5587–5594.

118. **Coque TM**, **Tomayko JF**, **Ricke SC**, **Okhyusen PC**, **Murray BE**. 1996. Vancomycin-resistant enterococci from nosocomial, community, and animal sources in the United States. Antimicrob Agents Chemother **40**:2605–2609.

119. **Dutka-Malen S**, **Evers S**, **Courvalin P**. 1995. Detection of glycopeptide resistance genotypes and identification to the species level of clinically relevant enterococci by PCR. J Clin Microbiol **33**:24–27.

120. **Nallapareddy SR**, **Weinstock GM**, **Murray BE**. 2003. Clinical isolates of *Enterococcus faecium* exhibit strain-specific collagen binding mediated by Acm, a new member of the MSCRAMM family. Mol Microbiol **47**:1733–1747.

121. **Zhang X**, **Top J**, **de Been M**, **Bierschenk D**, **Rogers M**, **Leendertse M**, **Bonten MJM**, **van der Poll T**, **Willems RJL**, **van Schaik W**. 2013. Identification of a Genetic Determinant in Clinical *Enterococcus faecium* Strains that Contributes to Intestinal Colonization During Antibiotic Treatment. J Infect Dis **207**:1633–1636.

122. **Lipsitch M**, **Dykes JK**, **Johnson SE**, **Ades EW**, **King J**, **Briles DE**, **Carlone GM**. 2000. Competition among *Streptococcus pneumoniae* for intranasal colonization in a mouse model. Vaccine **18**:2895–2901.

123. **La Rosa SL**, **Casey PG**, **Hill C**, **Diep DB**, **Nes IF**, **Brede DA**. 2013. In Vivo Assessment of Growth and Virulence Gene Expression during Commensal and Pathogenic Lifestyles of *luxABCDE*-Tagged *Enterococcus faecalis* Strains in Murine Gastrointestinal and Intravenous Infection Models. Appl Environ Microbiol **79**:3986–3997.

124. **Andersson DI**. 2006. The biological cost of mutational antibiotic resistance: any

practical conclusions? Curr Opin Microbiol **9**:461–465.

125. **Starikova I**, **Al-Haroni M**, **Werner G**, **Roberts AP**, **Sørum V**, **Nielsen KM**, **Johnsen PJ**. 2013. Fitness costs of various mobile genetic elements in *Enterococcus faecium* and *Enterococcus faecalis*. J Antimicrob Chemother **68**:2755–2765.

126. **Foucault M-L**, **Courvalin P**, **Grillot-Courvalin C**. 2009. Fitness cost of VanA-type vancomycin resistance in methicillin-resistant *Staphylococcus aureus*. Antimicrob Agents Chemother **53**:2354–2359.

127. **Moles L**, **Gómez M**, **Jiménez E**, **Fernández L**, **Bustos G**, **Chaves F**, **Canton R**, **Rodríguez JM**, **del Campo R**. 2015. Preterm infant gut colonization in the neonatal ICU and complete restoration 2 years later. Clin Microbiol Infect **21**:936.e1–936.e10.

128. **Shenoy ES**, **Paras ML**, **Noubary F**, **Walensky RP**, **Hooper DC**. 2014. Natural history of colonization with methicillin-resistant *Staphylococcus aureus* (MRSA) and vancomycin-resistant *Enterococcus* (VRE): a systematic review. BMC Infect Dis **14**:177.

129. **Galloway Peña JR**, **Nallapareddy SR**, **Arias CA**, **Eliopoulos GM**, **Murray BE**. 2009. Analysis of Clonality and Antibiotic Resistance among Early Clinical Isolates of *Enterococcus faecium* in the United States. J Infect Dis **200**:1566–1573.

130. **Grayson ML**, **Eliopoulos GM**, **Wennersten CB**, **Ruoff KL**, **De Girolami PC**, **Ferraro MJ**, **Moellering RC**. 1991. Increasing resistance to beta-lactam antibiotics among clinical isolates of *Enterococcus faecium*: a 22-year review at one institution. Antimicrob Agents Chemother **35**:2180–2184.

131. **Rice LB**, **Bellais S**, **Carias LL**, **Hutton-Thomas R**, **Bonomo RA**, **Caspers P**, **Page MGP**, **Gutmann L**. 2004. Impact of Specific *pbp5* Mutations on Expression of Beta-Lactam Resistance in *Enterococcus faecium*. Antimicrob Agents Chemother **48**:3028–3032.

132. **Rybkine T**, **Mainardi JL**, **Sougakoff W**, **Collatz E**, **Gutmann L**. 1998. Penicillin-binding protein 5 sequence alterations in clinical isolates of *Enterococcus faecium* with different levels of beta-lactam resistance. J Infect Dis **178**:159–163.

133. **Sifaoui F**, **Arthur M**, **Rice L**, **Gutmann L**. 2001. Role of Penicillin-Binding Protein

5 in Expression of Ampicillin Resistance and Peptidoglycan Structure in *Enterococcus faecium*. Antimicrob Agents Chemother **45**:2594–2597.

134. **Zorzi W**, **Zhou XY**, **Dardenne O**, **Lamotte J**, **Raze D**, **Pierre J**, **Gutmann L**, **Coyette J**. 1996. Structure of the low-affinity penicillin-binding protein 5 $PBP5_{fm}$ in wild-type and highly penicillin-resistant strains of *Enterococcus faecium*. J Bact **178**:4948–4957.

135. **Fontana R**, **Aldegheri M**, **Ligozzi M**, **Lopez H**, **Sucari A**, **Satta G**. 1994. Overproduction of a low-affinity penicillin-binding protein and high-level ampicillin resistance in *Enterococcus faecium*. Antimicrob Agents Chemother **38**:1980–1983.

136. **Klare I**, **Rodloff AC**, **Wagner J**, **Witte W**, **Hakenbeck R**. 1992. Overproduction of a penicillin-binding protein is not the only mechanism of penicillin resistance in *Enterococcus faecium*. Antimicrob Agents Chemother **36**:783–787.

137. **Mainardi JL**. 2000. Novel Mechanism of beta-lactam Resistance Due to Bypass of DD-Transpeptidation in *Enterococcus faecium*. J Biol Chem **275**:16490–16496.

138. **Miranda AG**, **Singh KV**, **Murray BE**. 1991. DNA fingerprinting of *Enterococcus faecium* by pulsed-field gel electrophoresis may be a useful epidemiologic tool. J Clin Microbiol **29**:2752–2757.

139. **Davlieva M**, **Shi Y**, **Leonard PG**, **Johnson TA**, **Zianni MR**, **Arias CA**, **Ladbury JE**, **Shamoo Y**. 2015. A variable DNA recognition site organization establishes the LiaR-mediated cell envelope stress response of enterococci to daptomycin. Nucleic Acids Res **43**:4758.

140. **Singh KV**, **La Rosa SL**, **Somarajan SR**, **Roh JH**, **Murray BE**. The Fibronectin-Binding Protein EfbA Contributes to Pathogenesis and Protects against Infective Endocarditis Caused by *Enterococcus faecalis*. Infect Immun **83**:4487–4494.

141. **Ligozzi M**, **Pittaluga F**, **Fontana R**. 1993. Identification of a genetic element (*psr*) which negatively controls expression of *Enterococcus hirae* penicillin-binding protein 5. J Bacteriol **175**:2046–2051.

142. **Rice LB**, **Carias LL**, **Hutton-Thomas R**, **Sifaoui F**, **Gutmann L**, **Rudin SD**. 2001. Penicillin-Binding Protein 5 and Expression of Ampicillin Resistance in *Enterococcus faecium*. Antimicrob Agents Chemother **45**:1480–1486.

143. **Massidda O**, **Kariyama R**, **Daneo-Moore L**, **Shockman GD**. 1996. Evidence that the PBP5 synthesis repressor (*psr*) of *Enterococcus hirae* is also involved in the regulation of cell wall composition and other cell wall-related properties. J Bact **178**:5272–5278.

144. **Eberhardt C**, **Kuerschner L**, **Weiss DS**. 2003. Probing the Catalytic Activity of a Cell Division-Specific Transpeptidase In Vivo with B-Lactams. J Bacteriol **185**:3726–3734.

145. **Shultzaberger RK**, **Bucheimer RE**, **Rudd KE**, **Schneider TD**. 2001. Anatomy of *Escherichia coli* ribosome binding sites. J Mol Biol **313**:215–228.

146. **Osterman IA**, **Evfratov SA**, **Sergiev PV**, **Dontsova OA**. 2013. Comparison of mRNA features affecting translation initiation and reinitiation. Nucleic Acids Res **41**:474.

147. **Montealegre MC**, **Singh KV**, **Murray BE**. Gastrointestinal Tract Colonization Dynamics by Different *Enterococcus faecium* Clades. J Infect Dis.

148. **Whitman MS**, **Pitsakis PG**, **DeJesus E**, **Osborne AJ**, **Levison ME**, **Johnson CC**. 1996. Gastrointestinal tract colonization with vancomycin-resistant *Enterococcus faecium* in an animal model. Antimicrob Agents Chemother **40**:1526–1530.

149. **Rice LB**, **Hutton Thomas R**, **Laktičová V**, **Helfand MS**, **Donskey CJ**. 2004. Beta-lactam antibiotics and gastrointestinal colonization with vancomycin-resistant enterococci. J Infect Dis **189**:1113–1118.

150. **Rice LB**, **Laktičová V**, **Helfand MS**, **Hutton Thomas R**. 2004. In Vitro Antienterococcal Activity Explains Associations between Exposures to Antimicrobial Agents and Risk of Colonization by Multiresistant Enterococci. J Infect Dis **190**:2162–2166.

151. **Pultz NJ**, **Stiefel U**, **Subramanyan S**, **Helfand MS**, **Donskey CJ**. 2005. Mechanisms by which anaerobic microbiota inhibit the establishment in mice of intestinal colonization by vancomycin-resistant *Enterococcus*. J Infect Dis **191**:949–956.

152. **Gilmore MS**, **Rauch M**, **Ramsey MM**, **Himes PR**, **Varahan S**, **Manson JM**, **Lebreton F**, **Hancock LE**. 2015. Pheromone killing of multidrug-resistant

Enterococcus faecalis V583 by native commensal strains. Proc Natl Acad Sci USA **112**:7273–7278.

153. **Kommineni S**, **Bretl DJ**, **Lam V**, **Chakraborty R**, **Hayward M**, **Simpson P**, **Cao Y**, **Bousounis P**, **Kristich CJ**, **Salzman NH**. 2015. Bacteriocin production augments niche competition by enterococci in the mammalian gastrointestinal tract. Nature **526**:719–722.

154. **Caballero S**, **Carter R**, **Ke X**, **Sušac B**, **Leiner IM**, **Kim GJ**, **Miller L**, **Ling L**, **Manova K**, **G PE**. 2015. Distinct but Spatially Overlapping Intestinal Niches for Vancomycin-Resistant *Enterococcus faecium* and Carbapenem-Resistant *Klebsiella pneumoniae*. PLoS Pathog **11**:e1005132.

155. **Dancer SJ**. 2001. The problem with cephalosporins. J Antimicrob Chemother **48**:463–478.

156. **Suppola JP**, **Volin L**, **Valtonen VV**, **Vaara M**. 1996. Overgrowth of *Enterococcus faecium* in the feces of patients with hematologic malignancies. Clin Infect Dis **23**:694–697.

157. **Zhang X**, **Paganelli FL**, **Bierschenk D**, **Kuipers A**, **Bonten MJM**, **Willems RJL**, **van Schaik W**. 2012. Genome-Wide Identification of Ampicillin Resistance Determinants in *Enterococcus faecium*. PLoS Genet **8**:e1002804.

VITA

Maria Camila Montealegre was born in Ibague, Colombia on March 28, 1984, the daughter of Melva Ortiz Santos and Gustavo Montealegre Lynett. She attended Los Andes University in Bogota, Colombia and earned a Bachelor of Science with a major in microbiology in 2006. She also received the degree of Master in Biological Sciences from the same University in 2007. For the next year, she worked as a research assistant at the Laboratory of Molecular Diagnostics at Los Andes University, and for the following 3 years she was a research associate at the International Center for Medical Research and Training in Cali, Colombia. In September of 2011 she joined Ph.D. program at The University of Texas Graduate School of Biomedical Sciences at Houston and in May 2012 she officially joined the Microbiology and Molecular Genetics Program and the laboratory of Dr. Barbara E. Murray.